MIRIAM SAYURI NAGASHIMA HOHMANN

PERSPECTIVAS DO USO DE EXTRATO DE *Hypericum perforatum* E DOS FLAVONOIDES VITEXINA E QUERCETINA NO TRATAMENTO DE INTOXICAÇÕES POR ACETAMINOFENO E DICLOFENACO E FIBROSE PULMONAR IDIOPÁTICA

Londrina
2017

MIRIAM SAYURI NAGASHIMA HOHMANN

PERSPECTIVAS DO USO DE EXTRATO DE *Hypericum perforatum* E DOS FLAVONOIDES VITEXINA E QUERCETINA NO TRATAMENTO DE INTOXICAÇÕES POR ACETAMINOFENO E DICLOFENACO E FIBROSE PULMONAR IDIOPÁTICA

Tese apresentada à banca do Programa de Pós-Graduação em Ciências da Saúde da Universidade Estadual de Londrina como requisito para obtenção do título de Doutora em Ciências da Saúde.

Orientador: Prof. Dr. Waldiceu Aparecido Verri Junior

Londrina
2017

Ficha de identificação da obra elaborada pelo autor, através do Programa de Geração Automática do Sistema de Bibliotecas da UEL

Hohmann, Miriam Sayuri Nagashima.
Perspectivas do uso do extrato de Hypericum perforatum e dos flavonoides vitexina e quercetina no tratamento de intoxicações por acetaminofeno e diclofenaco e fibrose pulmonar idiopática / Miriam Sayuri Nagashima Hohmann. - Londrina, 2017.
128 f. : il.

Orientador: Waldiceu Aparecido Verri Júnior.
Tese (Doutorado em Ciências da Saúde) - Universidade Estadual de Londrina, Centro de Ciências da Saúde, Programa de Pós-Graduação em Ciências da Saúde, 2017.
Inclui bibliografia.

1. Plantas medicinais - Uso terapêutico - Tese. 2. Fígado - Doenças - Tese. 3. Rins - Doenças - Tese. 4. Flavonóides - Tese. I. Verri Júnior, Waldiceu Aparecido. II. Universidade Estadual de Londrina. Centro de Ciências da Saúde. Programa de Pós-Graduação em Ciências da Saúde. III. Título.

MIRIAM SAYURI NAGASHIMA HOHMANN

PERSPECTIVAS DO USO DE EXTRATO DE *Hypericum perforatum* E DOS FLAVONOIDES VITEXINA E QUERCETINA NO TRATAMENTO DE INTOXICAÇÕES POR ACETAMINOFENO E DICLOFENACO E FIBROSE PULMONAR IDIOPÁTICA

Tese apresentada à banca do Programa de Pós-Graduação em Ciências da Saúde da Universidade Estadual de Londrina como requisito para obtenção do título de Doutora em Ciências da Saúde.

BANCA EXAMINADORA

_____

Orientador: Prof. Dr. Waldiceu Aparecido Verri Junior
Universidade Estadual de Londrina – UEL

_____

Prof. Dr. Fábio Henrique Kwasniewski
Universidade Estadual de Londrina – UEL

_____

Profa. Dra Glaura Scantamburlo Alves Fernandes
Universidade Estadual de Londrina – UEL

_____

Profa. Dra. Ilce Mara Colus
Universidade Estadual de Londrina – UEL

_____

Prof. Dr. Wander Rogério Pavanelli
Universidade Estadual de Londrina – UEL

Londrina, 05 de abril de 2017.

AGRADECIMENTOS

Agradeço primeiramente à minha família que sempre me apoiou e incentivou meus esforços em busca dos meus objetivos. Muito obrigada pela força, carinho e orgulho que sentem por mim. Sou muito grata à formação que vocês me deram. Se hoje cheguei até aqui, é graças a vocês!

Ao Matheus, meu amor e melhor amigo, muito obrigada pelo apoio, incentivo e palavras de carinho. Obrigada por SEMPRE estar ao meu lado. Agradeço, também, pela sua imensa compreensão e paciência. Agradeço também à família Tófoli, que são pessoas maravilhosas que sempre me incentivaram.

Ao meu orientador Prof. Dr. Waldiceu Aparecido Verri Junior, agradeço imensamente pela orientação, incentivo, paciência e conhecimentos científicos. Obrigada pela oportunidade de trabalhar e aprender em seu laboratório e não medir esforços para nos apoiar.

Guardo um agradecimento especial para o Dr. Cory Hogaboam e sua equipe do Cedars Sinai Medical Center, que me receberam e braços abertos e me deram um grande voto de confiança antes mesmo de me conhecerem pessoalmente. Não tenho palavras suficientes para agradecer ao Dr. David Habiel por tudo que me ensinou, pela paciência, dedicação e boa vontade em compartilhar comigo um pouco de seu imenso conhecimento científico.

Agradeço todos amigos e colegas do Laboratório de Dor, Inflamação, Neuropatia e Câncer da Universidade Estadual de Londrina. Obrigada pela agradável convivência, amizade e auxílio, direta ou indiretamente, neste trabalho.

Agradeço à minha amiga Talita Perdigão Domiciano pela amizade, companheirismo e parceria de todas as horas.

Agradeço também à minha amiga Tanyalak Parimon pela amizade e parceria nos treinos de Crossfit e compras no Whole Foods.

Agradeço à disponibilidade e dedicação da banca examinadora, por contribuírem com valioso conhecimento para a finalização deste trabalho.

À Coordenação de Aperfeiçoamento de Pessoal de Nível Superior (Capes), Fundação Araucária, ao Departamento de Ciência e Tecnologia da Secretaria de Ciência, Tecnologia e Insumos Estratégicos (Decit/SCTIE) e Ministério da Saúde (MS) (Decit/ SCTIE/MS) por intermédio do Conselho Nacional de Pesquisa (CNPq) pelo auxílio financeiro.

HOHMANN, Miriam Sayuri Nagashima. **Perspectivas do uso do extrato de *Hypericum perforatum* e dos flavonoides vitexina e quercetina no tratamento de intoxicações por acetaminofeno e diclofenaco e fibrose pulmonar idiopática**. 2017. 128 f. Tese (Doutorado em Ciências da Saúde) – Universidade Estadual de Londrina, Londrina, 2017.

RESUMO

Apesar de existirem terapias para tratar inúmeras doenças em que a exacerbação do processo inflamatório ou reparo tecidual têm papel central, ainda há necessidade de buscar novas abordagens terapêuticas. Os tratamentos atuais ainda não são eficazes em curar ou parar a progressão de algumas doenças e condições. Na hepatotoxicidade por acetaminofeno (N-acetil-p-aminofenol; APAP), por exemplo, há apenas um tratamento e este é mais eficaz quando administrado precocemente. Após o início da lesão hepatocelular, a eficácia é substancialmente diminuída e o risco de insuficiência hepática aguda é alto. Na nefrotoxicidade induzida por anti-inflamatórios não-esteroides (AINES) como o diclofenaco, ainda não há tratamentos específicos. As terapias atuais, em sua maioria, são controversas ou direcionadas ao tratamento das complicações da falência renal. Na fibrose pulmonar idiopática (FPI), as terapias aprovadas são eficazes apenas em desacelerarem a progressão da doença, mas não impedir sua progressão ou diminuir a mortalidade. A persistência de fibroblastos senescentes resistentes à apoptose nos focos de fibrose pulmonar contribui para a progressão da fibrose, assim abordagens terapêuticas focadas na modulação deste fenótipo podem contribuir com os tratamentos atualmente utilizados e parar a progressão da doença. Nesse contexto, nós avaliamos o efeito do extrato de *Hypericum perforatum* (*H. perforatum*) e da vitexina na letalidade, lesão hepática e renal, estresse oxidativo e inflamação induzidos por APAP e diclofenaco em camundongos swiss machos. Além disso, investigamos se a quercetina restaura a susceptibilidade de fibroblastos senescentes isolados do pulmão de pacientes com FPI estável ou de progressão rápida a estímulos pró-apoptóticos e os mecanismos envolvidos neste efeito. A análise por HPLC demonstrou a presença de rutina, quercetina, hipericina, pseudohipericina e hiperforina em extrato de *H. perforatum*. O APAP (0,15; 0,5; 1,5 e 3,0 g/kg, via oral; p.o.) induziu letalidade dose-dependente. A dose letal sub-máxima de APAP (1,5 g/kg, p.o.) foi escolhida para os demais experimentos deste estudo. O tratamento com o extrato de *H. perforatum* (30, 100 e 300 mg/kg, intra-peritoneal, i.p.) 30 min antes do estímulo reduziu, de forma dose-dependente, a letalidade induzida por APAP. O aumento induzido por APAP nas concentrações plasmáticas de aspartato aminotransferase (AST) e alanina aminotransferase (ALT), e na atividade da mieloperoxidase hepática, nos níveis de IL-1β, TNF-α e IFN-γ, bem como na depleção da glutationa reduzida (GSH) e da capacidade de sequestrar o radical cátion 2,2′ -azinobis-(3-etilbenzotiazolina-6-sulfonato) ($ABTS^{\cdot+}$) foram inibidos pelo tratamento com *H. perforatum* (300 mg/kg). Para avaliar o efeito protetor da vitexina na nefrotoxicidade induzida por diclofenaco, os camundongos foram tratados com vitexina (1, 3 ou 10 mg/kg, i.p.) 30 min antes da administração de diclofenaco (200 mg/kg, p.o.). Somente a dose de 10 mg/kg (i.p.) de vitexina inibiu o aumento nos níveis séricos de ureia e creatinina. A vitexin (10 mg/kg, i.p.) inibiu a proteinúria, depleção da capacidade antioxidante [redução dos níveis de GSH, do poder de

reduzir o ferro (FRAP) e da capacidade de sequestrar o radical cátion $ABTS^{\cdot+}$] e o aumento nos níveis de ânion superóxido e peroxidação lipídica no rim e sangue. A vitexin (10 mg/kg, i.p.) também inibiu o aumento de IL-1β, TNF-α, IL-6 e IFN-γ, ativação do fator nuclear-kappa B (NF-κB) e redução dos níveis de IL-10 no rim e sangue induzidos pelo diclofenaco. No estudo da quercetina em fibroblastos senescentes, observamos que fibroblastos de pacientes com FPI apresentam fenótipo senescente, i.e. replicação celular diminuída, expressão de β-galactosidase associada à senescência e expressão aumentada dos genes da p16 e p21. Fibroblastos controle e de pacientes com FPI (estável ou de progressão rápida) foram submetidas a passagens em série até a senescência de toda a cultura. Os fibroblastos senescentes de pacientes com FPI exibiram resistência à apoptose induzida por mediadores indutores de apoptose [ligante de Fas (FasL) e ligante indutor de apoptose relacionado ao fator de necrose tumoral (TRAIL)], diminuição na expressão dos receptores do FasL (Fas) e do TRAIL (DR4 e DR5), da caveolina-1, bem como, aumento na ativação de AKT comparado aos de pacientes controle. O tratamento apenas com quercetina (50 ou 100 μM) não induziu apoptose em fibroblastos senescentes controle ou de FPI, no entanto restaurou a susceptibilidade à apoptose induzida por FasL e TRAIL. Além disso, a quercetina (50 μM) aumentou a expressão de Fas e caveolina-1, bem como diminuiu a ativação de AKT. Em conjunto os resultados deste trabalho demonstram o efeito protetor do extrato de *H. perforatum* e da vitexina na hepatotoxicidade e nefrotoxicidade induzidas pelo APAP e diclofenaco, respectivamente, e este efeito parece estar relacionado com a inibição da inflamação e estresse oxidativo. Além disso, demonstram que quercetina restaura a susceptibilidade à apoptose mediada pelo FasL e TRAIL em fibroblastos senescentes de pacientes com FPI e este efeito pode ser atribuído à regulação da expressão de caveolina-1 e Fas e modulação da ativação de AKT. Assim, este trabalho aponta a necessidade de mais estudos para investigar o potencial terapêutico do *H. perforatum*, da vitexina e quercetina nos modelos estudados e em outras condições que a inflamação, o estresse oxidativo e a perda da susceptibilidade à apoptose têm papel importante.

Palavras-chave: *Hypericum perforatum*. Vitexina. Quercetina. Hepatoxicidade. Nefrotoxicidade. Inflamação. Estresse oxidativo. Fibrose pulmonar idiopática. Senescência. Apoptose.

HOHMANN, Miriam Sayuri Nagashima. **Perspectives on the use of *Hypericum perforatum* extract and the flavonoids vitexin and quercetin in the treatment of acetaminophen and diclofenac-induced toxicity and idiopathic pulmonary fibrosis.** 2017. 128 p. Thesis (Doctorate degree in Health Sciences) – Universidade Estadual de Londrina, Londrina, 2017.

ABSTRACT

Although there are therapies currently available to treat numerous diseases in which the exacerbation of the inflammatory process or wound healing plays a central role, there is still a need for new therapeutic approaches. Therapies available are not effective in curing or stopping the progression of some diseases and conditions. In acetaminophen (N-acetyl-p-aminophenol; APAP)-induced hepatotoxicity, for example, there is only one treatment option, which is most effective when administered shortly after intoxication. After the onset of hepatocellular injury, efficacy is substantially decreased and the risk of acute liver failure is high. In cases of acute renal failure induced by drugs, for example diclofenac, specific and targeted therapies are still not available. Moreover, therapies currently used are controversial or directed at the management of the complications of renal failure. In idiopathic pulmonary fibrosis (IPF), the therapies that are approved to treat this disease are effective only at slowing the progression of the disease, but not halting its progression or reducing mortality. Studies show that the persistence of apoptosis resistant senescent fibroblasts within the fibrotic foci contributes to the progression of fibrosis. Therefore, therapies focused on the modulation of this phenotype may contribute to the currently used therapeutic approach and halt the progression of the disease. In this context, we assessed the effect of *Hypericum perforatum* (*H. perforatum*) extract and vitexin on the lethality, hepatic and renal injury, inflammation, and oxidative stress induced by APAP and diclofenac, respectively in male swiss mice. Additionally, we investigated whether quercetin could restore the susceptibility of senescent fibroblasts isolated from the lungs of patients with IPF (stable or rapidly progressing disease) to pro-apoptotic stimuli and the mechanisms involved. HPLC analysis demonstrated the presence of rutin, quercetin, hypericin, pseudohypericin, and hyperforin in *H. perforatum* extract. APAP (0.15, 0.5, 1.5, and 3.0 g/kg, per oral; p.o.) induced dose-dependent mortality. The sub-maximal lethal dose of APAP (1.5 g/kg, per oral; p.o.) was chosen for the experiments in the study. Treatment with *H. perforatum* (30, 100, and 300mg/kg, intra-peritoneal; i.p.) 30 min before stimulus dose-dependently reduced APAP-induced lethality. APAP-induced increase in aspartate aminotransferase (AST) and alanine aminotransferase (ALT) in the plasma and myeloperoxidase activity and IL-1β, TNF-α, and IFN-γ concentrations in the liver, as well as decreased reduced glutathione (GSH) concentrations and capacity to reduce 2,2′-azinobis-(3-ethylbenzothiazoline-6-sulfonate radical cation; $ABTS^{\cdot+}$) were inhibited by *H. perforatum* (300mg/kg) treatment. To assess the protective effect of vitexin in diclofenac-induced nephrotoxicity, mice were treated with vitexin (1, 3 or 10 mg/kg, i.p.) 30 min before the administration of diclofenac (200 mg/kg, p.o.). Only the dose of 10 mg/kg (i.p.) of vitexin inhibited the increase in ureia and creatinine levels in the serum. Vitexin (10 mg/kg, i.p.) inhibited proteinuria, the depletion in antioxidant capacity [reduction in GSH levels, ferric-reducing antioxidant power (FRAP), and free radical scavenging ability (ABTS)], and increase in the levels of superoxide anion and

lipid peroxidation in the kidney and blood. Vitexin (10 mg/kg, i.p.) also inhibited diclofenac-induced increase in IL-1β, TNF-α, IL-6 e IFN-γ levels, activation of nuclear factor-kappa B (NF-κB), the reduction in IL-10 levels in the kidney and blood. In the investigation using senescent lung fibroblasts, we observed that fibroblasts from patients with IPF exhibit senescent phenotype, i.e. decreased cell replication, senescence associated β-galactosidase expression, and increased p16 and p21 gene expression. Control and IPF (stable or rapidly progressing disease) were submitted to serial passages until all fibroblasts became senescent. Senescent fibroblasts from patients with IPF exhibited resistance to apoptosis induced by pro-apoptotic mediators [Fas ligand (FasL) and tumor necrosis factor-related apoptosis inducing ligand (TRAIL)], decreased FasL (Fas) receptor, TRAIL receptors (DR4 and DR5), and caveolin-1 expression, as well as increased AKT activation compared to those from control patients. Treatment with quercetin alone (50 or 100 μM) did not induce apoptosis in control or FPI fibroblasts, however, it restored the susceptibility to apoptosis induced by FasL and TRAIL. In addition, quercetin (50 μM) increased the expression of Fas and caveolin-1, as well as decreased AKT activation. Collectively, these results demonstrate the protective effect of *H. perforatum* extract and vitexin on the lethality and hepatic and kidney injury induced by APAP and diclofenac, respectively. Moreover, this effect seems to be related to the inhibition of inflammation and oxidative stress. Additionally, the data demonstrates that quercetin can restore the susceptibility to apoptosis mediated by FasL and TRAIL in senescent fibroblasts from patients with IPF. The mechanisms involved in this effect are increased caveolin-1 and Fas expression and regulation of AKT activation. In conclusion, this study elucidates the need for further investigations on the therapeutic potential of *H. perforatum*, vitexin, and quercetin in the models studied and other conditions that inflammation, oxidative stress, and loss of susceptibility to apoptosis play an important role.

Keywords: *Hypericum perforatum.* Vitexin. Quercetin. Hepatoxicity. Nephrotoxicity. Inflammation. Oxidative stress. Idiopathic pulmonary fibrosis. Senescence. Apoptosis.

LISTA DE ILUSTRAÇÕES

Figura 1 – Fases da hepatotoxicidade induzida pelo o acetaminofeno (APAP) 15
Figura 2 – *Hypericum perforatum* L 20
Figura 3 – Papel das células senescentes nas doenças pulmonares crônicas 28

LISTA DE TABELAS

Tabela 1 – Principais grupos e respectivas compostos encontrados no extrato de *Hypericum perforatum* e algumas de suas atividades biológicas 20

LISTA DE ABREVIATURAS E SIGLAS

ABTS	2,2'-azino-bis(3-etilbenzotiazolina-6-sulfonato)
$ABTS^{\cdot+}$	Radical cátion ABTS
AINES	Anti-inflamatórios não-esteroides
AKT	Proteína quinase B
ALT	Alanina aminotransferase
APAP	N-acetil-p-aminofenol ou acetaminofeno
AST	Aspartato aminotransferase
CLAE	Cromatografia líquida de alta eficiência
CYP	Citocromo P450
CYP2E1	Citocromo 2E1
COPD	Doença pulmonar obstrutiva crônica
COX	Ciclo-oxigenase
DAMPs	Padrões moleculares associados ao dano
DR	Receptor de TRAIL
DTNB	Ácido 5,5-ditiobis(2-nitrobenzóico)
EDTA	Ácido etilenodiamino tetra-acético
ERNs	Espécies reativas de nitrogênio
EROs	Espécies reativas de oxigênio
FasL	Ligante Fas
FGF	Fator de crescimento de fibroblasto
FPI	Fibrose Pulmonar Idiopática
FRAP	Poder antioxidante de reduzir o ferro
GSH	Glutationa reduzida
HMGB1	Proteína de alta mobilidade box 1
HO-1	Hemeoxigenase 1
HTAB	Brometo de hexadeciltrimetilamônio
IFN-γ	Interferon gamma
IKK	IκB kinase
IL	Interleucina
iNOS	Óxido nítrico sintase induzível
i.p.	Intraperitoneal
JNK	quinase C-jun-N-terminal

LDH	Lactato desidrogenase
LPS	Lipopolissacarídeo
MDA	Malonodialdeido
MEC	Matriz Extracelular
MPO	Mieloperoxidase
NAC	N-acetil-cisteína
NADPH	Nicotinamida adenina dinucleotídeo fosfato
NAPQI	N-acetil-p-benzoquinona imina
NBT	Nitroazul de tetrazólio
NF-κB	Fator nuclear-kappa B
NO	Óxido nítrico
NOX	NADPH oxidase
Nrf2	Fator nuclear eritróide 2 relacionado ao fator 2
PCRq	PCR quantitativo
PDGF	Fator de crescimento derivado de plaquetas
PDTC	Pirrolidina ditiocarbamato de amônio
PGs	Prostaglandinas
PI3k	Fosfatidilinositol 3-quinases
p.o.	Via oral
PTEN	Fosfatase homóloga à tensina deletada no cromossomo 10
SASP	Fenótipo secretor associado a senescência
TBARS	Substâncias reativas ao ácido tiobarbitúrico
TGF	Fator de transformação do crescimento
TNF	Fator de necrose tumoral
TRAIL	Ligante Indutor de Apoptose Relacionado ao TNF
VEGF	Fator de crescimento endotelial vascular

SUMÁRIO

1. INTRODUÇÃO 13
1.1 Hepatotoxicidade 14
1.2 Amplificação da Lesão Hepática Induzida pelo APAP 16
1.3 Abordagens Terapêuticas para a Hepatotoxicidade Induzida pelo APAP 19
1.4 Lesão Renal Induzida por Anti-Inflamatórios Não-Esteroides e Diclofenaco 23
1.5 Mecanismos Envolvidos na Lesão Renal Aguda Induzida pelo Diclofenaco 24
1.6 Abordagens Terapêuticas para a Toxicidade e Lesão Renal Induzidas por Medicamentos 25
1.7 Fibrose 26
1.8 Fibrose Pulmonar Idiopática (FPI) 27
1.9 Senescência na FPI 27
1.10 Senescência e Resistência à Apoptose 29
1.11 Abordagens Terapêuticas para a FPI 30

2. OBJETIVOS 32

3. MATERIAIS E MÉTODOS 33
3.1 ARTIGO 1 e 2 33
3.2 ARTIGO 3 37

4. RESULTADOS E DISCUSSÃO 42
4.1 ARTIGO 1 42
4.2 ARTIGO 2 48
4.3 ARTIGO 3 72

5. CONSIDERAÇÕES FINAIS 111

6. REFERÊNCIAS 115

7. ANEXOS 127

1. INTRODUÇÃO

A inflamação é uma resposta adaptativa desencadeada por estímulos nocivos, como infecção ou injúria tecidual. Embora a resposta inflamatória seja parte integrante dos mecanismos de defesa do hospedeiro, sua exacerbação pode causar danos aos tecidos (1). Uma resposta inflamatória bem sucedida resulta na eliminação do agente infeccioso ou lesivo, seguida de uma fase de resolução e reparo tecidual (1). Porém, a persistência ou exposição repetida a um agente nocivo não permite a resolução da inflamação, criando um ambiente pró-fibrogênico (2). Em conjunto, estas condições favorecem a desregulação do processo de reparo e desenvolvimento de doenças fibróticas (3, 4).

Apesar de existirem terapias para tratar inúmeras doenças em que a exacerbação do processo inflamatório ou reparo tecidual têm papel central, ainda persiste a necessidade de buscar novas abordagens terapêuticas. Os tratamentos atuais ainda não são eficazes em curar ou parar a progressão de algumas doenças (5, 6). Além disso, muitos tratamentos apresentam diversas reações adversas que dificultam o seu uso e adesão (7). Assim, cada vez mais tem aumentado o interesse em avaliar o potencial terapêutico de produtos naturais (extratos e compostos isolados). Neste trabalho foi avaliado o efeito do extrato de *Hypericum perforatum* (*H. perforatum*) e o flavonoide vitexina na lesão hepática e renal induzida pelo acetaminofeno e diclofenaco, respectivamente. Além disso, foi avaliado o efeito da quercetina em fibroblastos pulmonares senescentes de pacientes com fibrose pulmonar idiopática; sendo que neste estudo foi focado no efeito da quercetina na resistência à apoptose apresentada por fibroblastos, um aspecto essencial da progressão da fibrose na FPI.

Considerando que estes estudos abordam aspectos diferentes da inflamação, a introdução desta tese foi subdividida em três seções. Em cada seção foi abordada a bibliografia relevante para os temas sob estudo.

Artigo científico 1: "*Hypericum perforatum* reduces paracetamol-induced hepatotoxicity and lethality in mice by modulating inflammation and oxidative stress"

1.1 Hepatotoxicidade por Acetaminofeno

O acetaminofeno (N-acetil-p-aminofenol; APAP), também conhecido como paracetamol, é amplamente utilizado por seus efeitos analgésicos e antipiréticos. Apesar do APAP ser considerado um medicamento seguro em doses terapêuticas, i.e. doses ≤ 4 g/dia para adultos e 80 mg/kg para crianças, a ingestão de doses elevadas pode causar intoxicações potencialmente fatais (8, 9). Tentativas de suicídio são uma causa frequente da exposição aguda a doses altas deste medicamento. Além disso, a ingestão não intencional de doses altas do APAP devido ao uso concomitante de medicamentos que possuem o APAP em sua composição farmacêutica, por exemplo medicamentos para dores musculares, gripe, resfriados e enxaqueca, tem sido cada vez mais frequente (8, 10).

A intoxicação por APAP pode acometer os rins, o fígado, coração e sistema nervoso central, no entanto a morte por intoxicação aguda da droga é secundária, principalmente, à disfunção hepática e falência hepática aguda (11), sendo estas caracterizadas pela necrose hepática centrolobular (12). Atualmente, a hepatotoxicidade por APAP é uma das causas mais comuns de falência hepática aguda em muitos países desenvolvidos (10, 13). Apesar de ainda não existirem dados precisos das principais causas de falência hepática aguda no Brasil, estudos demonstram que o número de casos de intoxicação por APAP vem aumentando nos últimos anos (14, 15). De acordo com o Centro de Informação Toxicológica (CIT) do Rio Grande do Sul, nos últimos anos, os analgésicos/antipiréticos têm sido uma das principais classes de agentes envolvidas nas exposições a agentes tóxicos, sendo que, dentre os medicamentos desta classe, o APAP foi responsável por mais de 60% dos casos (15). Em Santa Catarina (CIT/SC), a intoxicação por APAP correspondeu a 6,5% dos casos atendidos no período de 2003 a 2010 e 55% dos casos de intoxicação por analgésicos/antipiréticos (16). Assim, é possível que a falência hepática aguda decorrente da hepatotoxicidade por APAP também seja elevado no Brasil.

O passo inicial para a lesão hepática é a metabolização do APAP e a formação do metabólito altamente reativo, N-acetil-p-benzoquinona imina (NAPQI) (12). Em doses terapêuticas, mais de 90% do APAP sofre glicuronidação ou sulfatação e é eliminado pela via renal ou biliar. Apenas uma porcentagem pequena é metabolizada pelo citocromo P450 (CYP), principalmente pelo citocromo 2E1 (CYP2E1), produzindo a NAPQI (17). Este metabólito é quase que imediatamente detoxificado pela conjugação com a glutationa reduzida (GSH) hepática. No entanto, na intoxicação por APAP, há saturação das vias de

glicuronidação e sulfatação, resultando em excesso de formação de NAPQI, que, por sua vez, depleta os níveis de GSH (18). Assim, a NAPQI se torna disponível para ligar-se com proteínas celulares (19), principalmente proteínas mitocondriais (20) (Figura 1).

A ligação covalente do NAPQI com proteínas da mitocôndria não é diretamente responsável pela morte celular. Eventos celulares subsequentes são responsáveis pela injúria e morte hepatocelular (20, 21). A ligação do NAPQI com proteínas da mitocôndria inibe a cadeia respiratória e desencadeia a formação de peroxinitrito e o estresse oxidativo (22, 23). O estresse oxidativo mitocondrial ativa a quinase c-jun-N-terminal (JNK) 1/2 via diferentes MAP quinases redox-sensíveis (24, 25). A subsequente translocação da JNK fosforilada para a mitocôndria amplifica o estresse oxidativo, o que resulta na abertura dos poros de transição de permeabilidade mitocondrial e no colapso do potencial de membrana (26). Além disso, a formação de poros na membrana da mitocôndria permite a translocação de proteínas mitocondriais como o citocromo c, fator indutor de apoptose e a endonuclease G para o núcleo que, por sua vez, causam a fragmentação do DNA (27, 28) (Figura 1).

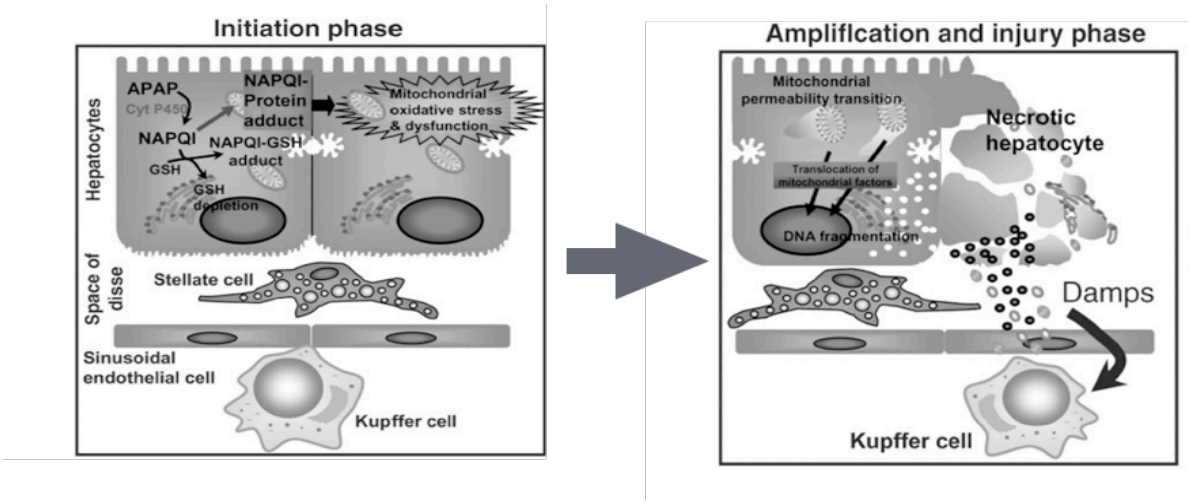

Fonte: Adaptado de Jaeschke et al. (2012) (20).

Figura 1. Fases da hepatotoxicidade induzida pelo o acetaminofeno (APAP). Após a ingestão de dose elevada de APAP, o APAP é transformado em seu metabolito reativo N-acetil-p-benzoquinona-imina (NAPQI) pelo citocromo P450 (CYP450) (citocromo 2E1). O excesso de NAPQI formado esgota a reserve hepática de glutationa (GSH) e favorece a ligação covalente do NAPQI com proteínas da mitocôndria. Essa ligação inibe a cadeia respiratória e desencadeia a formação de peroxinitrito e o estresse oxidativo, iniciando o processo de injúria. Na fase de amplificação, estas alterações mitocondriais resultam na ativação de c-jun-N-quinase terminal (JNK) 1/2, seguido da abertura dos poros de transição de permeabilidade mitocondrial e translocação de proteínas mitocondriais, tais como fator indutor da apoptose e endonuclease G, para o núcleo, produzindo a fragmentação do DNA e

necrose celular. Os componentes celulares liberados durante a necrose, incluindo fragmentos de DNA nuclear, peptídeos e a proteína de alta mobilidade box 1 (HMGB1), podem atuar como padrões moleculares associados a dano (DAMPs) e ativar células endoteliais e do sistema imune, por exemplo células de Kupffer (macrófagos residentes do fígado) e neutrófilos, amplificando a injúria hepática.

[Amplification and injury phase: fase da amplificação e injúria; APAP: acetaminofeno; Cyt P450: citocromo P450; DAMPS: padrões moleculares associados a danos; DNA fragmentation: fragmentação do DNA; GSH: glutationa reduzida; GSH depletion: depleção de GSH; hepatocytes: hepatócitos; initiation phase: fase inicial; Kupffer cell: célula de Kupffer; mitochondrial oxidative stress & dysfunction: estresse oxidativo e disfunção mitocondrial; mitochondrial permeability transition: transição de permeabilidade mitocondrial; NAPQI: N-acetil-p-benzoquinona-imina; NAPQI-GSH adduct: aduto NAPQI-GSH; NAPQI-protein adduct: aduto de proteína-NAPQI; necrotic hepatocytes: hepatócitos necróticos; sinusoidal endothelial cell: célula endotelial sinusoidal; space of disse: espaço de disse; stellate cells: células de Ito; translocation of mitochondrial factors: translocação de proteínas da mitocôndria].

1.2 Amplificação da Lesão Hepática Induzida pelo APAP

Apesar da necrose celular possuir papel central na hepatotoxicidade por APAP, esta é autolimitada e não explica a extensão da necrose hepática comumente observada. Estudos mostram que os componentes celulares liberados por células necróticas podem atuar como padrões moleculares associados a dano (DAMPs) e ativar células endoteliais e do sistema imune (por exemplo, células de Kupffer (macrófagos residentes do fígado) e neutrófilos) (29) (Figura 1). Quando ativadas, estas células são fonte de mediadores inflamatórios como citocinas, espécies reativas e enzimas lisossomais que em conjunto sustentam o processo inflamatório e estresse oxidativo (30-32). Estudos têm demonstrado que a inflamação e o estresse oxidativo desempenham papel importante na amplificação da lesão hepática por APAP (31, 33-35). Nesse contexto, nesta próxima sessão foram abordados os mecanismos secundários à necrose celular que são importantes para a amplificação da lesão hepática induzida pelo APAP.

1.2.1 Participação dos neutrófilos na amplificação da lesão hepática induzida pelo APAP

Há evidências de que a interação entre as células parenquimais e não parenquimais possui papel importante na amplificação da hepatoxicidade por APAP. Os neutrófilos são as primeiras células imunes a responder à necrose celular durante a hepatotoxicidade por APAP (35). DAMPS (por exemplo HMGB1, proteínas S-100, proteínas do choque térmico, entre outros) e citocinas liberados durante a lesão e necrose recrutam neutrófilos para a vasculatura e tecido hepático (29, 35). Apesar da presença de neutrófilos no local da lesão ser essencial para a eliminação de restos celulares e retorno à homeostase, o seu recrutamento pode agravar a inflamação e lesão hepática induzida pelo APAP (35-37). Neutrófilos ativados são fonte de proteases e espécies reativas e o seu extravasamento dos sinusóides e aderência aos hepatócitos (38) permite que oxidantes como o peróxido de hidrogênio e ácido hipocloroso induzam a morte a morte de hepatócitos e (35, 39, 40).

1.2.2 Participação de citocinas na amplificação da lesão hepática induzida pelo APAP

A hepatotoxicidade por APAP é acompanhada do aumento nos níveis séricos e hepáticos de citocinas inflamatórias como a interleucina (IL)-1α, IL-1β, fator de necrose tumoral (TNF)-α, IL-6, entre outras (31, 41). No fígado, as citocinas são produzidas principalmente pelas células de Kupffer e são potentes propagadores da hepatotoxicidade induzida pelo APAP (42). As citocinas podem ativar outras células não-parenquimais, e sustentar a inflamação (33, 37). A IL-1β e o TNF-α, por exemplo, ativam e recrutam neutrófilos para vasculatura e tecido hepático (33, 41). O TNF-α também estimula a produção de outras citocinas e liberação de espécies reativas de oxigênio (EROs) por células de Kupffer e neutrófilos infiltrados (43). Além disso, o TNF-α por si só é capaz de gerar efeitos citotóxicos e induzir apoptose e necrose (44). Corroborando o papel destas citocinas na amplificação das lesões secundárias ao APAP, a neutralização da IL-1β e o TNF-α com anticorpos específicos reduz a lesão do fígado e outras manifestações da intoxicação por APAP (33).

O aumento de interferon gama (IFN-γ) também está associado às lesões hepáticas induzidas pelo APAP. Foi demonstrado que o IFN-γ possui papel importante no recrutamento de leucócitos e aumento da expressão de outras citocinas, como a IL-1α, IL-1β, IL-6 e o TNF-α, quimiocinas (por exemplo, proteína quimioatraente de monócito-1 e proteínas inflamatórias de macrófagos-1α e -2), moléculas de adesão (molécula de adesão intercelular-1 e molécula de adesão celular-vascular-1) e óxido nítrico sintase induzível (iNOS) na hepatoxicidade por APAP; e uso de anticorpos anti-IFN-γ reduz a inflamação, necrose hepática, bem como a letalidade induzida pelo APAP (45). Em conjunto, estes estudos elucidam o papel central das citocinas na lesão hepática induzida pelo APAP.

1.2.3 Participação do estresse oxidativo na amplificação da lesão hepática induzida pelo APAP

O estresse oxidativo é outro mecanismo implicado na propagação da lesão hepática induzida pelo APAP (46). O estresse oxidativo pode resultar do excesso de produção de espécies reativas ou da depleção das defesas antioxidantes; e na hepatotoxicidade por APAP ambos são observados (47, 48).

Após a exposição a doses tóxicas do APAP, aumento nos níveis hepáticos de EROs e espécies reativas de nitrogênio (ERNs) é rapidamente detectado. Este aumento está atribuído a diversas fontes, leucócitos ativados (neutrófilos e células de Kupffer) (37, 49, 50), mitocôndrias disfuncionais e até mesmo o CYP450 durante a formação da NAPQI (51).

As espécies reativas podem iniciar a peroxidação de membranas fosfolipídicas, oxidação de proteínas e alterações no DNA. Nesse sentido, estas são consideradas potentes mediadores da lesão tecidual (46). O aumento nos níveis do NO, por exemplo, se correlaciona positivamente com os níveis do marcador de lesão hepática alanina aminotransferase (ALT) (32). Além disso, o peroxinitrito, um produto da reação entre o ânion superóxido e NO, é um potente agente oxidante capaz de promover a nitração de resíduos de tirosina em proteínas e o aumento dos seus níveis se correlaciona com a toxicidade induzida pelo APAP (34).

Em condições normais, as espécies reativas como o peróxido de hidrogênio, peroxinitrito e ácido hipocloroso são detoxificados pela GSH/GSH peroxidase (52), no entanto, na hepatotoxicidade por APAP este importante mecanismo de defesa encontra-se comprometido (34). Além da GSH, a atividade de outros antioxidantes como a superóxido dismutase, catalase, GSH peroxidase e GSH redutase também está diminuída após administração de APAP (53). Os antioxidantes são essenciais para a detoxificação de espécies reativas e manutenção da homeostase redox (54), assim, a depleção dos antioxidantes hepáticos contribui significativamente para o acúmulo de espécies reativas e estresse oxidativo observado na hepatotoxicidade por APAP (46).

Além da ação direta nos danos teciduais, o estresse oxidativo também pode amplificar a lesão hepática de maneira indireta, por exemplo pela produção de citocinas (55). Diversos fatores de transcrição sensíveis às espécies reativas podem induzir a transcrição de genes de citocinas como a IL-1, IL-6, TNF-α e moléculas de adesão. O fator nuclear-kappa B (NF-κB) é um dos fatores de transcrição mais importantes que respondem diretamente ao estresse oxidativo. As espécies reativas podem regular a atividade de quinases responsáveis pela ativação da via de sinalização do NF-κB. Vários antioxidantes capazes de detoxificar as espécies reativas podem inibir a ativação do NF-κB, sugerindo que

as espécies reativas possuem papel central nesta via de sinalização (55, 56). Além disso, existe evidência que citocinas como o TNF-α e IL-1β podem ativar nicotinamida adenina dinucleotídeo fosfato (NADPH) oxidase e induzir a produção de EROs e estas, por sua vez, induzirem a ativação de NF-κB e, assim, aumentar a produção de citocinas (57). Assim, as citocinas também têm papel importante na manutenção do próprio estresse oxidativo.

1.3 Abordagens Terapêuticas para a Hepatotoxicidade Induzida pelo APAP

Atualmente, único antídoto clinicamente aprovado para a toxicidade induzida por APAP é a N-acetilcisteína (NAC). A NAC é um precursor para a síntese de GSH e atua aumentando a eliminação do metabólito reativo NAPQI durante a fase de metabolismo (58). O seu uso é mais eficaz dentro de 8 horas da sobredosagem. Embora a NAC seja benéfica mesmo após 24 horas, a eficácia é substancialmente diminuída e o risco de insuficiência hepática aguda é alto (6, 58). Desta forma, tratamentos que modulem os mecanismos responsáveis pela propagação da lesão hepática iniciada pelo APAP poderiam contribuir com terapias existentes.

1.3.1 *Hypericum perforatum (H. perforatum)*

O *Hypericum perforatum* L. (Hypericaceae), popularmente conhecido como Erva de São João, é uma planta herbácea perene amplamente utilizada na medicina popular e fitoterápica (Figura 2) (59). Os extratos das partes aéreas da planta contêm 6 grandes grupos: naftodiantronas, floroglucinóis, flavonoides, biflavonas, fenilpropanos e proantocianidinas e cada um possui seus compostos específicos, que são responsáveis pelos inúmeros efeitos biológicos descritos (Tabela 1) (60).

Fonte: Karioti e Bilia, 2010 (61).

Figura 2. *Hypericum perforatum* L.

Tabela 1. Principais grupos e respectivas compostos encontrados no extrato de *Hypericum perforatum* e algumas de suas atividades biológicas

Grupos	Compostos	Atividades Biológicas
Naftodiantronas	Hipericina	Inibição da liberação de ácido araquidônico, leucotrieno B_4 e NO e IL-1α) de leucócitos (63)
	Pseudo-hipericina (62)	Inibição da produção de prostaglandinas E_2, NO e citocinas (IL-1β, TNF-α e IL-6) em macrófagos (64)
Floroglucinóis	Hiperforina	Inibição da produção de prostaglandina E_2 em macrófagos (64) e da atividade da 5-lipoxigenase (65)
	Adhiperforina (60)	Redução de edema (66)
Flavonoides	Kaempferol,	Aumenta a atividade de glutationa e das enzimas glutationa peroxidase e redutase

		e superóxido dismutase (69) e produção de TNF-α e IL-6 e ativação de NF-κB (70)
	Luteolina	Inibição da expressão de TNF-α, IL-1β, IL-6, dos receptors toll like 2 e 4, metalloproteinase-2 e -9 e atividade de NF-κB (71)
	Miricetina	Inibição da expressão de TNF-α, IL-1β, IL-6, ativação de NF-κB e produção de EROs e aumento da expressão de glutationa peroxidase e superóxido dismutase (72)
	Quercetina	Inibição da produção de prostaglandinas E_2, NO e citocinas (IL-1β, TNF-α e IL-6) e macrófagos (64)
	Hiperosídeo	Efeito 'scavanger' de EROs e aumento da atividade de enzimas antioxidants (73) e inibição da produção de TNF-α, IL-6 e NO e ativação de NF-κB (74)
	Rutina	Inibição do recrutamento de neutrófilos (75) e da produção de NO e TNF-α, da atividade da mieloperoxidase (MPO) em neutrófilos (76)
	Quercitrina	Inibiçao da atividade da MPO, e peroxidação lipídica (77, 78) e produção de TNF-α, IL-6 e EROs
	Isoquercitrina (60, 67, 68)	Inibição da produção de TNF-α, IL-1β e IL-6, expressão de iNOS e da vias de NF-κB e MAP quinase (79)
Biflavonas	3',8''-biapigenina	Não conhecidas
	Amentoflavona	Inibição da produção de prostaglandinas E_2, NO e citocinas (IL-1β, TNF-α e IL-6) e macrófagos (64)
	6',8''-diquercetina (80, 81)	Não conhecidas

Fenilpropanos	Ácido clorogênico (60)	Inibição da produção de prostaglandinas E_2, NO e citocinas (IL-1β, TNF-α e IL-6) e macrófagos (64)
Proantocianidinas	Procianidinas (82)	Inibição da ativação de NF-κB e produção de EROs (83)

Atualmente, o *H. perforatum* é uma das plantas medicinais mais consumidas mundialmente por seus efeitos antidepressivos e antissépticos (84), porém o seu potente efeito anti-inflamatório também é relevante. O extrato de *H. perforatum* inibe o recrutamento e ativação de leucócitos, principalmente neutrófilos, *in vivo* (85). Este efeito pode ser atribuído à atividade inibitória do extrato na expressão de moléculas de adesão e produção das citocinas pró-inflamatórias IL-1β, TNF-α e IL-6 (74, 85, 86). Além disso, a hiperforina (65), bem como extrato hidroalcoólico de *H. perforatum* (87), inibe a 5-lipoxigenase, uma enzima com papel importante na letalidade e hepatotoxicidade induzidas pelo APAP (88).

Além do efeito anti-inflamatório direto, o extrato de *H. perforatum* também modula a resposta inflamatória pela sua ação antioxidante (89). O extrato de *H. perforatum* possui atividade 'scavenger' de espécies reativas (90) e a inibição de espécies reativas como EROs previne a infiltração de neutrófilos para o sítio de inflamação (91, 92). A capacidade do extrato de *H. Perforatum de* neutralizar radicais livres está diretamente relacionada à presença de flavonoides (93, 94), que são conhecidos por seus efeitos antioxidantes (95). Além da atividade anti-inflamatória atribuída ao seu efeito antioxidante, o *H. perforatum* também protege os tecidos contra danos oxidativos. Em modelo de isquemia e reperfusão do tecido intestinal, o *H. perforatum* inibiu a peroxidação lipídica, oxidação do DNA e danos secundários ao estresse nitrosativo (expressão de nitrotirosina nos tecidos) (89). Achados semelhantes foram reportados em outros modelos experimentais (96).

Considerando o potencial anti-inflamatório e antioxidante do *H. perforatum,* o seu extrato apresenta-se como um tratamento interessante para inibir os mecanismos que amplificam a lesão hepática iniciada pelo APAP.

Artigo científico 2: "Vitexin inhibits diclofenac-induced acute kidney injury by targeting NF-κB activation, inflammatory cytokines, and oxidative stress in mice"

1.4 Lesão Renal Induzida por Anti-inflamatórios Não-Esteroides (AINES) e Diclofenaco

Os anti-inflamatórios não-esteroides (AINES) são uma das classes de medicamentos mais utilizados mundialmente por seus efeitos anti-inflamatórias, analgésicas e antipiréticas (97, 98). O efeito terapêutico dos AINES está relacionado, principalmente, à inibição da ciclo-oxigenase-1 (COX-1) e -2 (COX-2), que modulam a síntese dos mediadores da inflamação prostaglandinas (PGs) e tromboxano (98). A COX-1 é a forma constitutiva da COX, encontrada em plaquetas, células endoteliais, estômago e rins, onde está envolvida na produção de prostaglandinas responsáveis pela proteção da parede do estômago (PGE_2), agregação plaquetária (tromboxano A_2) e manutenção da função renal (PGI_2) (99). Por outro lado, a COX-2 é a forma induzida da COX e é expressa em locais de inflamação e infecção. Porém, estudos demonstram que a COX-2 também pode ser encontrada no cérebro, rim e intestino, mesmo na ausência da inflamação, e sua expressão está relacionada à homeostase destes tecidos (99, 100). Nesse sentido, a inibição da COX-1 e/ou COX-2 por AINES é responsável pelos inúmeros efeitos adversos dos AINES (98, 101).

O diclofenaco é o AINE mais frequentemente prescrito para o tratamento de inúmeras condições dolorosas, como cólicas renais, gota aguda, dismenorreia, enxaqueca e febre e doenças osteomusculares, articulares, periarticulares e do tecido mole (98, 102-104). Assim como os demais AINES, o seu uso está relacionado à toxicidade e efeitos adversos gastrointestinais, do sistema nervosos central, hematológicos e hepáticos (105, 106). Além disso, o uso do diclofenaco está relacionado a efeitos adversos renais. Estudos demonstram que o diclofenaco pode causar toxicidade e alterações transitórias, como redução da função renal, proteinúria e aumento de ureia e creatinina no sangue. Porém, o diclofenaco também pode causar alterações renais mais graves, como a nefrite intersticial, síndrome nefrótica e insuficiência renal aguda (107-110). Estudos reportam que pacientes fazendo o uso do diclofenaco apresentam aumento de 77% no risco de desenvolver a lesão renal aguda (111) e o manejo inadequado deste quadro pode acelerar o desenvolvimento da insuficiência renal crônica. Um único episódio de lesão renal aguda aumenta em 1,9 vezes o risco de desenvolvimento da insuficiência renal crônica, quando comparado com pacientes que não apresentaram um episódio de lesão renal (112). Assim, fica evidente a relevância e o impacto da toxicidade e efeitos adversos renais do diclofenaco na saúde pública (111, 113).

1.5 Mecanismos Envolvidos na Lesão Renal Aguda Induzida pelo Diclofenaco

As duas principais causas de insuficiência renal aguda induzida pelo diclofenaco e outros AINES são a redução da perfusão renal (causa pré-renal) e lesão do parênquima renal (causa renal ou intrínseca) e ambas estão associadas à redução dos níveis de PGs (111, 114). As PGs, especificamente a PGE_2 e a PGI_2, são responsáveis pela manutenção da perfusão renal e taxa de filtração glomerular (115); e a inibição da síntese destas moléculas pode causar alterações da função renal, a diminuição da pressão hidrostática glomerular e, consequentemente, disfunção renal (106, 114).

Outro fator que parece estar diretamente relacionado à nefroxicidade e lesão renal induzida pelo diclofenaco, é o seu acúmulo nos rins (116). Quando comparado a outros órgãos, as concentrações do diclofenaco e seus resíduos encontram-se significativamente elevadas (116). Diferentes mecanismos de lesão renal induzida pelo diclofenaco foram demonstrados em estudos *in vitro* e *in vivo.* Ng et al. (2006) demonstraram que a disfunção mitocondrial é um evento inicial da lesão renal induzida pelo diclofenaco (107). O diclofenaco reduz a produção de NADPH e, consequentemente, a síntese de ATP na mitocôndria (107, 117). Além disso, o diclofenaco aumenta os níveis de EROs e peroxidação lipídica, o que resulta em fragmentação do DNA e apoptose das células renais (108). Corroborando o papel do estresse oxidativo na lesão renal, o estímulo com dose tóxica de diclofenaco induz depleção das defesas antioxidantes e o tratamento com moléculas antioxidantes inibem a apoptose e lesão renal (118).

Além do estresse oxidativo, a inflamação também possui papel importante nas lesões renais e na nefrotoxicidade induzida pelo diclofenaco (118, 119). A intoxicação com diclofenaco induz a produção das citocinas inflamatórias IL-1β, IL-6, IFN-γ e TNF-α no rim de camundongos (118). Estudos demonstram que as citocinas podem mediar a iniciação e propagação da inflamação no rim (120). A IL-6, por exemplo, ativa a resposta inflamatória na nefrotoxicidade e lesão renal induzida pela isquemia (121, 122). Por outro lado, o TNF-α medeia a apoptose e lesão tecidual (123). Na lesão renal aguda induzida por cisplatina ou endotoxina, a inibição da produção ou ação do TNF-α protege o rim contra a nefrotoxicidade. Além disso, níveis mais elevados de citocinas no sangue está relacionado ao risco aumentado de morte em pacientes diagnosticados com insuficiência renal aguda (124).

Na última década, estudos têm demonstrando o papel do fator de transcrição NF-κB na fisiopatologia das lesões renais. Na nefropatia diabética e doença glomerular em humanos (125-127) e lesão renal aguda induzida pelo diclofenaco ou ácido fólico em camundongos (118, 128), o aumento da ativação de NF-κB é observada. Corroborando o papel da ativação do NF-κB na lesão renal induzida pelo diclofenaco, o tratamento com a vinpocetina [um inibidor da IKK (IκB kinase)] [19] ou PDTC (pirrolidina ditiocarbamato de

amônio, uma molécula inibidora do NF-κB) [Borghi et al. em preparação] reduz a lesão renal, bem como o estresse oxidativo, produção de citocinas e ativação de NF-κB renal induzidos pelo diclofenaco.

1.6 Abordagens Terapêuticas para a Toxicidade e Lesão Renal Induzidas por Medicamentos

Atualmente não existe uma terapia específica preconizada para o tratamento da toxicidade e lesão renal induzidas por medicamentos. Em sua maioria, as terapias são direcionadas ao tratamento das complicações decorrentes do comprometimento da função renal e têm como objetivo a recuperação da mesma (101). No passado, o efeito do tratamento com corticoides na recuperação da função renal decorrente da lesão renal aguda induzida por medicamentos já foi investigada. Apesar de alguns estudos terem observado que a terapia com o corticoide acelera e promove a recuperação completa da função renal (129-131), outros não confirmaram estes resultados (132-134). Nesse sentido, o uso do corticoide para o tratamento da lesão renal induzida por medicamentos ainda é controverso. Assim, fica evidente a necessidade de estudos buscado abordagens terapêuticas para a toxicidade e lesão renal induzidas por medicamentos, principalmente o diclofenaco, que é um dos medicamentos mais utilizados mundialmente.

1.6.1 Vitexina

A vitexina (apigenina-8-C-D-glucopiranosideo) é um flavonoide encontrado em plantas medicinais e consumidas na dieta (95), como *Vigna radiata* L. (Broto de feijão mungo) (135), *Crataegus spp*. (Biancospino, espinheira branca ou Crataegus) (136), *Passiflora spp.* (Flor do maracujá) (137), *Mimosa pudica* L. (138) e *Phyllostachys nigra.* A vitexina possui diversos efeitos biológicos (139-141), dentre eles, o seu efeito antioxidante se destaca. Estudos *in vitro* demonstram que a vitexina possui um IC_{50} de 84 µg/mL e 16 µg/mL para capacidade de sequestrar o radical DPPH (142) e ABTS (143), respectivamente. Além disso, a vitexina também possui a capacidade de sequestrar o ânion superóxido (142, 144) e reduzir a peroxidação lipídica induzida pelo Fe(II) (IC_{50} de 2313 µM) (145). *In vivo*, a vitexina aumenta a expressão de enzimas antioxidantes e capacidade antioxidante total em tecidos como o fígado, rim e a pele, bem como inibe o dano oxidativo (peroxidação lipídica) (141, 146, 147). O seu efeito inibitório no estresse oxidativo confere proteção na lesão induzida por isquemia e reperfusão no miocárdio e cardiotoxicidade induzida pela doxirubicina em ratos e reduz a

dor inflamatória em camundongos (141, 148).

Além do seu potente efeito antioxidante, a vitexina também modula a inflamação (139, 149). O efeito anti-inflamatório da vitexina parece estar relacionado principalmente à modulação da produção de citocinas. Em macrófagos RAW 264.7 estimulados com lipopolissacarídeo (LPS), a vitexina inibe a produção de IL-1β, NO, PGE_2, bem como aumenta a IL-10 (150). *In vivo*, a vitexina inibe da produção de TNF-α , IL-1β , IL-6 e IL-33 induzida pela carragenina e este efeito contribui para a redução da dor inflamatória induzido por este estímulo em camundongos (147).

Considerando o efeito antioxidante e anti-inflamatório da vitexina, esta apresenta-se como uma droga candidata interessante para o tratamento da nefrotoxicidade induzida por medicamentos como o diclofenaco.

Artigo 3: "Quercetin Enhances Ligand-Induced Apoptosis in Senescent Idiopathic Pulmonary Fibrosis Fibroblasts"

1.7 Fibrose

Durante o processo inflamatório, a injúria tecidual também inicia uma série de eventos para reparar a integridade estrutural e funcional do tecido danificado (151). O processo de reparo tipicamente envolve duas fases distintas, a regeneração, na qual as células lesadas são substituídas pelo mesmo tipo celular, e a cicatrização, também conhecida como fibroplasia ou fibrose, na qual ocorre deposição de elementos da matriz extracelular (MEC) e substituição do tecido parenquimatoso por tecido conjuntivo (151).

Embora a cicatrização seja essencial para a manutenção da integridade funcional dos órgãos e sistemas, a exposição crônica a um agente lesivo pode desregular o processo de reparo. Apesar de possuir manifestações etiológicas e clínicas distintas, a maioria das doenças fibróticas crônicas têm em comum a persistência do dano tecidual e a desregulação do processo de reparo (4, 152, 153).

O contínuo estímulo lesivo sustenta a produção de fatores de crescimento, enzimas proteolíticas, fatores angiogênicos e citocinas fibrogênicas, que estimulam a deposição exagerada de elementos do tecido conjuntivo e remodelam e destroem a arquitetura do tecido (151, 154). Em algumas doenças, por exemplo a fibrose pulmonar idiopática, cirrose hepática e fibrose cardiovascular, a remodelação extensa de tecidos e fibrose podem levar à falência de órgãos e morte (4, 153, 155).

1.8 Fibrose Pulmonar Idiopática (FPI)

A fibrose pulmonar idiopática (FPI) é a forma mais comum e letal de pneumonia intersticial idiopática. Esta doença acomete principalmente pessoas na sexta e sétima décadas de vida e do sexo masculino (156, 157). A sobrevida média após o diagnóstico é de 3-5 anos e a progressão clínica da doença é imprevisível, variando de um declínio lento durante vários anos (FPI estável) para uma deterioração rápida (FPI de progressão rápida) e morte em alguns meses (158, 159). Os fatores desencadeadores da doença ainda são desconhecidos, mas o fumo, a exposição ambiental e ocupacional, infecções virais, refluxo ácido gástrico e predisposição genética têm sido relatados como fatores de risco para FPI (160-162).

A patologia da FPI é caracterizada por repetidas micro lesões às células epiteliais alveolares e mecanismo de reparo desregulado, deposição excessiva de MEC, perda da arquitetura parenquimatosa e comprometimento dos alvéolos e da função pulmonar (155, 163, 164). Na FPI, os fibroblastos exibem proliferação desregulada e diferenciam-se em miofibroblastos, os quais produzem componentes da MEC excessivamente e conferem rigidez ao tecido. O acúmulo destas células forma focos fibroblásticos, que são o local de remodelação tecidual ativa (165).

1.9 Senescência na FPI

Apesar da FPI ser uma doença que tem como fenômeno central a proliferação de fibroblastos, cada vez mais surgem evidências que há um aumento de senescência de fibroblastos (166), particularmente dentro dos focos de fibrose em biópsias pulmonares de FPI (167). A senescência celular é um estado de parada permanente do ciclo celular, associada a alterações fenotípicas, que tem um papel importante na manutenção da homeostase fisiológica, por exemplo supressão de tumores, cicatrização de feridas e proteção contra a fibrose tecidual em condições fisiológicas (168). No entanto, estudos vêm demonstrando que as células senescentes podem ter efeitos prejudiciais *in vivo* e causar, ou contribuir, para a remodelação de tecidos, envelhecimentos do organismo e doenças relacionadas à idade, como a FPI e doença pulmonar obstrutiva crônica (COPD) (162, 168-170) (Figura 3). Recentemente foi demonstrado que os focos fibroblásticos de FPI são predominantemente compostos de fibroblastos senescentes. Além disso, miofibroblastos senescentes são detectados nos pulmões de camundongos envelhecidos e o acúmulo destas células impede a resolução de fibrose pulmonar induzida por bleomicina (167).

As células senescentes secretam diversos mediadores como citocinas pró-inflamatórias, quimiocinas, fatores de crescimento e proteases de matriz extracelular, que juntos constituem o fenótipo secretor associado a senescência (SASP). O SASP, associado aos altos níveis de EROs em células senescentes, pode cronicamente sustentar a inflamação e o dano tecidual, o que explica a correlação entre o acúmulo destas células, a remodelação tecidual contínua e a fibrose progressiva (171-173). Assim, intervenções terapêuticas que têm como alvo a redução do número de células senescentes são estratégias promissoras para modular a progressão da FPI e outras doenças relacionadas à idade.

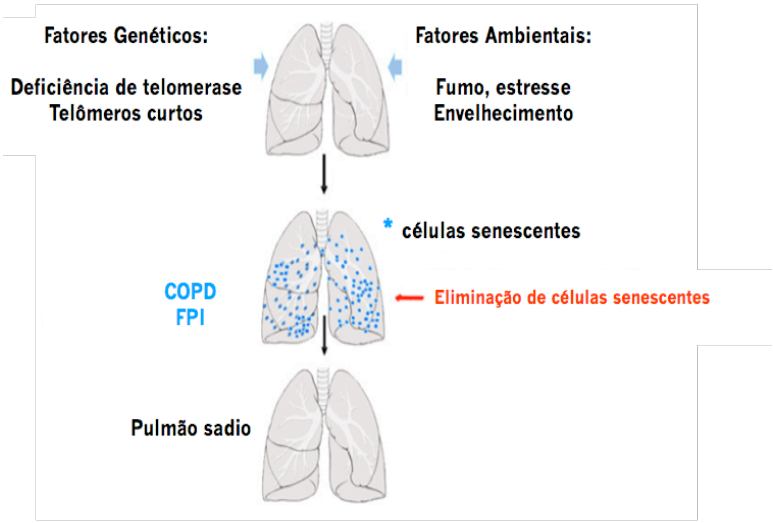

Fonte: Adaptado de Adnot et al. (2015) (171).

Figura 3. Papel das células senescentes nas doenças pulmonares crônicas. A senescência celular pode ser desencadeada por fatores genéticos (por exemplo, a disfunção de telômeros ou deficiência da telomerase, enzima responsável por adicionar sequências específicas e repetitivas de DNA à extremidade 3' dos cromossomos aos telômeros), ou ambientais (por exemplo, idade avançada ou exposição a estímulos lesivos como o estresse oxidativo e fumo). As células senescentes podem ter efeitos prejudiciais *in vivo.* Elas secretam citocinas pró-inflamatórias, quimiocinas, espécies reativas de oxigênio (EROs), fatores de crescimento e proteases de matriz extracelular, que juntos constituem o fenótipo secretor associado a senescência (SASP). Este fenótipo sustenta cronicamente a inflamação e o dano tecidual, favorecendo a remodelação tecidual contínua e/ou a fibrose progressiva observada em doenças pulmonares como a doença pulmonar obstrutiva crônica (COPD) e

fibrose pulmonar idiopática (FPI). Intervenções terapêuticas capazes de reduzir o número de células senescentes são estratégias promissoras para modular a progressão da doença pulmonares relacionadas à idade (171, 172).

1.10 Senescência e Resistência à Apoptose

Além do SASP, o aumento da resistência à apoptose é uma característica inerente às células senescentes (174, 175). Os mecanismos pelos quais as células senescentes resistem à apoptose ainda não são totalmente compreendidos. Porém, em algumas células, isso foi atribuído a alterações na expressão de proteínas que regulam a morte celular por apoptose (176, 177). Uma análise da expressão de genes envolvidos na regulação da morte celular revelou que em adipócitos senescentes a expressão de reguladores negativos da apoptose e genes anti-apoptóticos está aumentada e vias anti-apoptóticos e pró-sobrevivência ativadas (178).

Na FPI diversos mecanismos de resistência à apoptose foram descritos, porém, em sua maioria em fibroblastos proliferantes. A proteína quinase B (AKT), por exemplo, é um componente central da via Fosfatidilinositol 3-quinases (PI3K)/AKT “pró-sobrevivência” e a ativação aumentada de AKT promove a resistência à apoptose (179, 180). Na FPI, a ativação exacerbada da via PI3K/AKT está atribuído à baixa expressão de caveolina-1 em fibroblastos. Baixa expressão de caveolina-1, por sua vez, resulta em baixa atividade de fosfatase homóloga à tensina deletada no cromossomo 10 (PTEN) na membrana, o que favorece a ativação sustentada da via PI3K/AKT (181).

A caveolina-1 é o componente principal das estruturas de membrana celular denominada caveolas, e a baixa expressão de caveolina-1 resulta em baixa expressão de Fas, receptor do ligante Fas [FasL; um ligante da família do TNF, que possui potente capacidade de induzir apoptose em diversos tipos de células (182)], na membrana das células (180, 183). A expressão diminuída de receptores de proteínas pró-apoptóticos tem papel central na perda da susceptibilidade à apoptose em diversos tipos celulares (180, 184-186). Em fibroblastos de FPI, a expressão de Fas está diminuída quando comparada a expressão em fibroblastos normais/controle, e a baixa expressão deste receptor foi implicada na redução da susceptibilidade à apoptose (180, 185).

No âmbito da senescência, Hecker et al. (2015) demonstraram que perda da homeostase redox, caracterizada pela expressão elevada de NADPH oxidase (NOX) 4, níveis aumentados de EROs e a redução da capacidade de induzir a defesa antioxidante Nrf2 (fator nuclear eritróide 2 relacionado ao fator 2), favorece a resistência à apoptose em miofibroblastos senescentes e o acúmulo destas células em focos de fibrose pulmonar em

camundongos envelhecidos (167). A modulação gênica e farmacológica da NOX4 em camundongos envelhecidos com fibrose pulmonar induzida por bleomicina estabelecida restaurou a susceptibilidade à apoptose em miofibroblastos senescentes no pulmão e a resolução da fibroses pulmonar (167).

Diversos mecanismos de resistência à apoptose em fibroblastos de FPI foram descritos, no entanto, em sua maioria, estes mecanismos foram observados em células proliferantes. Assim, pouco se sabe ainda a respeito dos mecanismos responsáveis pela resistência à apoptose em fibroblastos e miofibroblastos senescentes na FPI e como modulá-los. Portanto, estudos que buscam elucidar estes mecanismos podem contribuir para o conhecimento dos mecanismos fisiopatológicos da doença e também o desenvolvimento de novas estratégias terapêuticas para a FPI.

1.11 Abordagens Terapêuticas para a FPI

O desenvolvimento de novos fármacos para a FPI tem focado principalmente na fibrogênese e fibroproliferação. Atualmente, apenas duas drogas foram aprovadas pela Agência Nacional de Vigilância Sanitária (ANVISA) no Brasil (187) e outras agências, como a Food and Drug Administration nos EUA (188, 189), para o tratamento da FPI: a Ofev® (nintedanibe) e Esbriet® (pirfinidona).

A pirfinidona é uma molécula pleiotrópica que apresenta atividade antifibrótica, anti-inflamatória e antioxidante (190). Por outro lado, o nintedanibe, que foi originalmente desenvolvido como um fármaco anticâncer, é um inibidor de tirosina quinases que inibe os receptores do fator de crescimento endotelial vascular (VEGF) 1-3, receptores do fator de crescimento derivado de plaquetas (PDGF) α e β e receptores do fator de crescimento de fibroblasto (FGF) 1-3 (191). O efeito anti-fibrótico da pirfinidona e do nintedanib está relacionado, mas não limitado, à diminuição da deposição de MEC e inibição do aumento e a ação de citocinas inflamatórias e dos mediadores pró-fibróticos fator de transformação do crescimento (TGF)-β, PDGF, FGF, entre outros (192-196). Embora a perfinidona e o nintendanib sejam eficazes em desacelerem a progressão da doença, estes medicamentos não curam, nem reduzem a mortalidade da doença (5). Assim, ainda é necessário novas terapias capazes de parar a progressão da FPI e diminuir a mortalidade da doença.

1.11.1 Quercetina

A quercetina, que pertencente à classe dos flavonols, é o flavonoide encontrado em maior quantidade nos alimentos, principalmente frutas e verduras (197). Diversas atividades

biológicas foram demonstrados para a quercetina, como anti-inflamatório, antioxidante, anti-hipertensivo, antiaterogênico, anticâncer, antiviral, antimicrobiana, entre outros (198-200). Além disso, a quercetina também atua na indução de apoptose e inibição de várias enzimas envolvidas na proliferação e via de transdução de sinal (201). Em células altamente resistentes à apoptose, como células de câncer, a quercetina não só demonstrou efeito pro-apoptótico (202), por mecanismos como aumento da relação Bax/Bcl-2 (203), liberação de citocromo-c da mitocôndria e ativação de caspase-3 e caspase-9 (204), como também aumentou a susceptibilidade à estímulos pro-apoptóticos (205, 206).

Recentemente Zhu et al. (2015) demonstraram que a quercetina induz apoptose de células endoteliais da veia umbilical humana senescentes e de células senescentes em tecido adiposo inguinal de camundongos envelhecidos. Os autores descreveram essa atividade como “senolítica”, visto que a quercetina induzia morte de maneira seletiva em células senescentes *in vitro* e *in vivo*. Considerando estes efeitos da quercetina, a mesma apresenta-se como uma molécula promissora para investigar seu efeito e mecanismos reguladores em fibroblastos senescentes de FPI.

2. OBJETIVOS

2.1 Objetivos gerais

Demonstrar o efeito e mecanismos de ação do extrato de *H. Perforatum* e dos flavonoides vitexina e quercetina no tratamento de intoxicações por acetaminofeno e diclofenaco e fibrose pulmonar idiopática.

2.2 Objetivos específicos para demonstrar o efeito terapêutico e mecanismos de ação do extrato de *H. perforatum* na hepatotoxicidade induzida pelo APAP em camundongos:

2.2.1 Avaliar o efeito do extrato de *H. perforatum* sobre a letalidade, lesão hepática, o aumento dos níveis das citocinas IL-1β, TNF-α e IFN-γ, recrutamento de neutrófilos e depleção da capacidade antioxidante no fígado induzidos pelo APAP;

2.3 Objetivos específicos para demonstrar o efeito terapêutico e mecanismos de ação da vitexina na lesão renal induzida pelo diclofenaco em camundongos:

2.3.1 Avaliar o efeito da vitexina sobre a lesão renal, o estresse oxidativo, aumento dos níveis das citocinas IL-1β, TNF-α, IL-6, IFN-γ e IL-10 e ativação do fator de transcrição NF-κB no rim e/ou no sangue induzidos pelo diclofenaco;

2.4 Objetivos específicos para demonstrar o efeito e mecanismos de ação da quercetina sobre a resistência à apoptose em fibroblastos pulmonares senescentes de pacientes com FPI:

- Avaliar a susceptibilidade de fibroblastos senescentes de pacientes controle e com FPI (doença estável e progressão rápida) à apoptose e os possíveis mecanismos relacionados à resistência à apoptose;

- Avaliar o efeito da quercetina na apoptose e sobre a susceptibilidade à apoptose, bem como os mecanismos de ação envolvidos, em fibroblastos senescentes de pacientes controle e com FPI (doença estável e progressão rápida).

3. MATERIAS E MÉTODOS

3.1 Protocolos experimentais e ensaios laboratoriais utilizados nos artigos científicos 1 "*Hypericum perforatum* reduces paracetamol-induced hepatotoxicity and lethality in mice by modulating inflammation and oxidative stress" e 2 "Vitexin inhibits diclofenac-induced acute kidney injury by targeting NF-κB activation, inflammatory cytokines, and oxidative stress in mice"

3.1.1 Animais Experimentais

Foram utilizados camundongos machos Swiss pesando 20-25g. Os animais eram provenientes do Biotério Central da Universidade Estadual de Londrina e mantidos no Biotério do Departamento de Ciências Patológicas da Universidade Estadual de Londrina pelo menos 72 horas antes dos experimentos. Os animais foram mantidos em ciclo de claro/escuro (12/12 h), com livre acesso a água e ração e controle de temperatura. Os estudos foram aprovados pelo do Comitê de Ética em Experimentação Animal da Universidade Estadual de Londrina [Número do processo CEUA UEL: 13280.2011.64 (Anexo 1) e 12742.2016.32 (Anexo 2)] e seguiram suas normas. Animais morimbundos ou que apresentassem sofrimento extremo foram submetidos à eutanásia.

3.1.2 Cromatografia líquida de alta eficiência (CLAE)

O extrato de *H. Perforatum* disponível comercialmente (Iperisan®, Fazenda Marjan, Santo Amaro-SP, Brasil) foi caracterizado por CLAE (Shimadzu) equipado com um detector fotodiodo (SPD-M10Avp), sistema de entrega de multisolventes (LC-10Avp), sistema de controle do forno (CTO-10ASvp) e controle de software Software Classe VP 6.14. A cromatografia foi realizada em coluna analítica de fase reversa Spherisob® (C-18 ODS) (250 × 4,6 mm i.d., tamanho de partícula 5μm) (Waters). Os solventes de grau CLAE foram fornecidos por Panreac® e a água foi purificada usando Sistemas de filtro Milli-Q-plus (Millipore). Para execuções da CLAE um gradiente de água acidificado (ácido fórmico 2%) (solvente A) e acetonitril (ácido fórmico 2%), (solvente B) a uma vazão de 1 mL/min (volume = 20 μL) foi utilizado. Gradiente da CLAE: 0 min, 0% de B; 5 min, 0% de B; 20 min, 2,5% de B; 30 min, 5% de B; 50 min, 15% de B; 60 min, 25% de B; 65 min, 30% de B; 70 min, 45% B; 75 min, 50% de B; 80 min, 70% de B; 85 min, 90% de B; 90 min, 100% de B; 95 min, 100% de B; 110 min, 0% de B. A detecção UV foi realizada a 200-400 nm e ajustado para 280 e 340 nm. Espectros UV foram registados para cada pico principal nos cromatogramas. A quercetina-3-O-rutinosida (rutina, Sigma), quercetina (Sigma) e hipericina (Sigma) foram

utilizadas como padrões. Espectros de massa de alta resolução (HR-MS) foram registados por infusão de soluções 0,1 mg/mL (MeCN-H_2O 7:3 v/v) em uma vazão de 0,1 mL/h em espectrômetros ultrO-TOF e de micro-TOF (Bruker Daltonics, EUA) e uma fonte de ionização por electrospray (ESI) em modo negativo (mz = $[M - H]^-$).

3.1.3 Protocolo experimental

No estudo da avaliação do efeito protetor do *H. perforatum* na hepatotoxicidade induzido por APAP, foi realizado um estudo de dose-resposta para determinar a dose letal submáxima do APAP. Foi administrado pela via oral (p.o.) as doses de 0,15; 0,5; 1,5 e 3,0 g/kg de APAP (200 mg/mL) ou o veículo (salina) e a letalidade foi avaliada a cada 6 horas durante 72 horas. A dose de 1,5 g/kg de APAP foi selecionada para os demais experimentos deste estudo. Em seguida foi avaliado o efeito do extrato de *H. perforatum* na letalidade, lesão hepática, recrutamento de neutrófilos, produção de citocinas e estresse oxidativo induzidos pelo APAP. Os animais foram tratados pela via intraperitoneal (i.p.) com 30, 100 e 300 mg/kg de extrato de *H. perforatum* ou veículo (tween 20%) 30 min antes da administração do APAP (1,5 g/kg, p.o.) ou salina e a letalidade foi avaliada conforme descrito. Para a avalição dos demais parâmetros, os animais foram submetidos à eutanásia 4 horas após a administração do APAP e amostras de plasma e tecido hepático foram coletados conforme descrito anteriormente (88).

Para avaliar o efeito protetor da vitexina na nefrotoxicidade induzida por diclofenaco, os camundongos foram tratados com vitexina (1, 3 ou 10 mg/kg, i.p.) 30 min antes da administração de diclofenaco (200 mg/kg, p.o.) e após 24 horas amostras de urina foram coletadas e em seguida os animais foram submetidos à eutanásia e amostras de sangue e rim foram coletados para a avaliação dos níveis séricos da ueia e creatinina, da proteinúria, do estresse oxidativo, produção de citocinas e ativação de NF- κB (118).

3.1.4 Avaliação da lesão hepática

A determinação dos níveis plasmáticos dos marcadores de lesão hepática aspartato aminotrasferase (AST), alanina aminotransferase (ALT) foi realizada utilizando kits comerciais da Labtest Diagnóstico S.A. (Brasil) (88, 118).

3.1.5 Avaliação da lesão renal

A determinação dos níveis séricos dos marcadores de lesão renal ureia e creatinina foi realizada utilizando kits comerciais da Labtest Diagnóstico S.A. (Brasil). A proteinúria foi avaliada pelo método de Lowry, conforme descrito anteriormente (88, 118).

3.1.6 Dosagem de citocinas

As citocinas, IL-1β, TNF-α, IL-6, IL-10 e IFN-γ foram quantificadas no soro, tecido hepático ou renal por ELISA utilizando kits comerciais da eBioscience (EUA) e os resultados expressos em pg/mg de tecido ou mL de soro (88, 118).

3.1.7 Determinação da atividade da mieloperoxidase (MPO)

O recrutamento de neutrófilos para o fígado foi avaliado de maneira indireta pela determinação da atividade da MPO. O tecido hepático foi homogeneizado em tampão fosfato 0,05M pH 6,0 adicionado de HTAB (brometo de hexadecil trimetil amônio) e centrifugado por 2 minutos a 14000rpm. Alíquotas do sobrenadante foram pipetadas em uma microplaca de ELISA, seguido da adição de 200μL de tampão fosfato (pH 6,0) contendo orto-dianisidina e peróxido de hidrogênio. As amostras foram incubadas a temperatura ambiente por 15 min, seguida da leitura da absorbância a 450nm. Simultaneamente, uma curva padrão de neutrófilos foi avaliada para cálculo da quantidade de neutrófilos/mg de tecido (207, 208).

3.1.8 Quantificação de GSH

As amostras de tecido hepático ou renal foram homogeneizadas em EDTA (Ácido etilenodiamino tetra-acético) 0,02M gelado. Em seguida foi adicionado ácido tricloroacético 50% e as amostras foram homogeneizadas em vórtex, incubadas por 15 min e centrifugadas (4.000 rpm, 15 min). O sobrenadante ou soro foram pipetados em uma microplaca de ELISA e Tris-HCl 0,4M (pH 8,9) e DTNB (ácido 5,5-ditiobis(2-nitrobenzóico)) foram adicionados. Após 5 min de incubação a temperatura ambiente e a absorbância foi determinada em espectrofotômetro a 412 nm. Uma curva padrão de concentrações conhecidas de GSH foi utilizada para a determinação da concentração de GSH nas amostras (209). Simultaneamente foram determinados os níveis de proteína nas amostras conforme descrito anteriormente (210). Os resultados foram expressos μmol de GSH/mg de proteína ou mL de soro.

3.1.9 Determinação da capacidade antioxidante

A capacidade antioxidante foi avaliada pelo ensaio do poder antioxidante de reduzir o ferro (FRAP) e da capacidade de sequestrar o radical cátion 2,2′ -azinobis-(3-etilbenzotiazolina-6-sulfonato) ($ABTS^{\cdot+}$); ABTS] (88, 118, 211). As amostras de tecido hepático ou renal foram primeiramente homogeneizadas em KCl 1.15% gelado e centrifugadas a 1.500 rpm por 10 min a 4^{o}C. Para o ensaio do FRAP, o sobrenadante ou soro foram pipetadas em uma microplaca de ELISA contendo água deionizada e o reagente de FRAP foi adicionado. As amostras foram incubadas a 37°C for 30 min e a absorbância determinada a 595 nm. Para o ensaio do ABTS, o sobrenadante ou soro foram pipetadas em uma microplaca de ELISA contendo água deionizada e o reagente ABTS contendo radical cátion $ABTS^{\cdot+}$ (7 mM) em tampão fosfato (pH 7,4). Após 6 min de incubação a temperatura ambiente a absorbância das amostras foram determinados a 734 nm. Uma curva padrão de concentrações conhecidas de Trolox foi utilizada para a determinação da capacidade antioxidante das amostras equivalente ao Trolox. Os resultados foram expressos em nmol equivalente de Trolox/mg de tecido ou mL de soro (118).

3.1.10 Determinação da redução do nitroazul de tetrazólio (NBT)

As amostras de rim foram primeiramente homogeneizadas em KCl 1.15% gelado e alíquotas de 50 µL do homogenato ou do soro foram pipetadas em microplaca de ELISA. Em seguida foi adicionado 100 µL da solução de NBT (1 mg/mL) e as amostras incubadas a 37°C por 5 min. O sobrenadante foi removido e o precipitado contendo formazan foi solubilizado com 120 µL de KOH (2M) e 140 µL de dimetil sulfóxido. As absorbâncias foram medidas a 600 nm. A concentração de proteínas na amostra foi utilizado para a normalização dos dados e os resultados foram expressos como redução de NBT (densidade óptica [OD]/mg de proteína ou mL de soro) (118).

3.1.11 Determinação da peroxidação lipídica

Os níveis de substâncias reativas ao ácido tiobarbitúrico (TBARS), principalmente o malonodialdeido (MDA), foram quantificados por espectrofotometria utilizando um método adaptado previamente descrito (118, 212). O homogenato de tecido renal ou soro reagem com o ácido tiobarbitúrico, formando complexos MDA-(ácido tiobarbitúrico)$_2$. As proteínas foram precipitadas pelo ácido tricloroacético e as amostras foram incubadas por 15 min a 95-100^{o}C e em seguida transferidas para banho de gelo. O MDA, um produto intermediário da peroxidação lipídica, foi determinada pela diferença das absorbâncias a 535 e 572 nm. Os resultados foram expressos em TBARS (ΔOD A535-A572 /mg de proteína ou mL de soro) (118).

3.1.12 Determinação da ativação de NF-κB

Para a determinação da ativação de NF-κB o tecido renal foi homogeneizado em tampão de lise gelado (Cell Signaling Technology, USA), homogenato centrifugado (16,100 g x 10 min a 4°C) e o sobrenadante foi utilizado para quantificar os níveis de NF-κB p65 total e fosforilada por ELISA utilizando os kits PathScan #7836 e #7834, respectivamente (Cell Signaling Technology, USA). Os resultados foram expressos como ativação de NF-κB (razão p-NF-κB:total-NF-κB /mg de tecido) (118).

3.1.13 Análise estatística

As análises estatísticas foram realizadas utilizando o GraphPad Prism 5 (GraphPad Software, La Jolla, CA). Os resultados expressos como média ± EPM e foram consideradas significativas as diferenças onde $P<0,05$. As taxas de sobrevida forma estimadas pelo método de Kaplan-Meier e a análise estatística realizada pelo teste de Log-Rank. As diferenças estatísticas entre dois ou mais grupos foram comparadas por ANOVA de uma via, seguido do pós-teste de comparações múltiplas de Bonferroni ou Tukey. Os experimentos foram realizados duas vezes e os dados representativos foram utilizados.

3.2 Protocolos experimentais e ensaios laboratoriais utilizados no artigo científico 3 "Quercetin enhances ligand-induced apoptosis in senescent idiopathic pulmonary fibrosis fibroblasts"

3.2.1 Obtenção de cultura primária de fibroblastos pulmonares

Os fibroblastos pulmonares foram isoladas de biópsias pulmonares de pacientes normais (controle), i.e. não diagnosticados com alguma doença pulmonar fibrótica, ou de pacientes com FPI clinicamente classificados como tendo a doença estável ou de progressão rápida. Para isolar as células os tecidos de pulmão foram finamente cortadas e os pedaços foram dispersos em frascos de cultura celular de 150 cm^2 contendo meio de cultura completo DMEM (Lonza) contendo 15% de soro fetal bovino (Cell Generation), 100 UI de penicilina e 100 µg/mL de estreptomicina (Lonza), 292 µg/mL de L-Glutamina (Lonza) e 100 µg/mL de Primocin (Invivogen). As células foram submetidas a cinco passagens em série para se obter populações puras de fibroblastos de pulmão. Os fibroblastos foram cultivados em meio de cultura completo a 37°C em incubadora de CO_2 a 10%. O uso destas

células foi aprovado pelo comitê de revisão institucional (IRB) do Cedars Sinai Medical Center (Los Angeles, CA) (Número de aprovação: Pro34067).

3.2.2 Obtenção de fibroblastos senescentes

Fibroblastos pulmonares proliferantes isolados de pacientes controle e com FPI foram submetidas a passagem em série até que as células adquirissem o fenótipo de senescência (morfologia achatada, parada irreversível da proliferação celular, alteração de padrão de expressão gênica (expressão aumentada dos genes CDKN1A , CDKN2A , IL6 e IL8) e aumento na atividade da beta-galactosidase associada à senescência (β-galactosidase staining Kit, BioVision) (213).

3.2.3 Avaliação da susceptibilidade de fibroblastos pulmonares senescentes à apoptose

Fibroblastos pulmonares senescentes de pacientes controle e com FPI (doença estável ou de progressão rápida) (5 x 10^4 células/poço) foram tratados com duas concentrações de FasL recombinante humana (rh) (75 ou 150 ng/mL) + anticorpo monoclonal anti-poli-histidina ou TRAILrh (100 ou 200 ng/mL) + anticorpo monoclonal anti-poli-histidina (R&D Systems) ou veículo (0,05% de DMSO em meio de cultura DMEM) durante 24 h. A apoptose dos fibroblastos foi avaliada pela análise de imagens obtidas em microscópio de contraste de fase (IncuCyte ZOOM® Live Cell Imaging; Essen Bioscience) e medição da atividade da caspase-3, viabilidade celular e a liberação de lactato desidrogenase (LDH) conforme descrito na seção de métodos deste projeto.

3.2.4 Avaliação do efeito pró-apoptótico da quercetina em fibroblastos pulmonares senescentes

Fibroblastos pulmonares senescentes de pacientes controle e com FPI (doença estável ou de progressão rápida) (5 x 10^4 células/poço) foram tratados com duas concentrações de quercetina (50 ou 100 μM) (Sigma Aldrich) ou veículo (0,05% DMSO em meio de cultura DMEM) durante 24 h e a apoptose foi avaliada conforme descrito anteriormente e detalhado na seção de métodos deste projeto (178).

3.2.5 Avaliação do efeito da quercetina na susceptibilidade de fibroblastos pulmonares senescentes à apoptose

Fibroblastos pulmonares senescentes de pacientes controle e com FPI (doença

estável ou de progressão rápida) (5 x 10^4 células/poço) foram tratados com quercetina (50 μM) ou veículo e as doses mais baixas de FasLrh (75 ng/mL) + anticorpo monoclonal anti-poli-histidina ou TRAILrh (100 ng/mL) + anticorpo monoclonal anti-poli-histidina durante 24 h e a apoptose foi avaliada conforme descrito anteriormente e detalhado na seção de métodos deste projeto.

3.2.6 Atividade da caspase-3

A atividade da caspase-3 foi quantificada utilizando o kit comercial Caspase-3 Fluorometric Assay Kit (BioVision). Primeiramente o sobrenadante foi removido e os poços contendo os fibroblastos foram lavados com PBS. As células foram lisadas com tampão de lise durante 30 min em gelo. Em seguida, o tampão de reação 2x contendo 10 mM DTT e 50 μM de substrato DEVD-AFC foram adicionados as amostras lisadas e a placa foi incubada a 37°C durante 1 h. As amostras foram lidas num fluorômetro equipado com um filtro de excitação a 400 nm e filtro de emissão a 505 nm e os resultados foram expressos como unidades de fluorescência relativas normalizado para a β-actina.

3.2.7 Viabilidade celular

Para avaliar a viabilidade celular, primeiramente o sobrenadante foi removido e os poços contendo os fibroblastos foram lavados duas vezes com PBS. Em seguida foi adicionada a solução tetraZ fornecida no TetraZ Cell Counting Kit (Biolegend) e a placa foi incubada durante 2 horas a 37°C e 10% de CO_2. As absorbâncias das amostras foram determinadas por espectrofotometria a 450 nm e estas foram consideradas diretamente proporcionais ao número de células viáveis.

3.2.8 Liberação de LDH

A liberação de LDH pelas células apoptóticas foi avaliada utilizando o sobrenadante dos fibroblastos e seguindo as instruções do fabricante (Pierce LDH Citotoxicity Assay Kit, Life Technologies). Resumidamente, o sobrenadante dos fibroblastos foi transferido para uma nova placa de 96 poços contendo o Reaction Mixture do kit. As amostras foram incubadas à temperatura ambiente durante 30 min e em seguida foi adicionada a STOP Solution do kit para parar a reação. A absorbância das amostras a 490 nm e 680 nm foi medida por espectrofotometria e a diferença A490 nm - A680 nm foi considerada diretamente proporcional à atividade do LDH.

3.2.9 PCR quantitativo (PCRq) em tempo real

O RNA total foi extraído utilizando o TRIzol (Thermo Fischer Scientific), conforme as orientações do fabricante. O grau de pureza do RNA foi estimado pela razão entre as absorbâncias medidas a 260 e 280 nm, que deve ser entre 1,8 e 2,0. A transcrição reversa do RNA total em DNAc e o PCR foram realizadas utilizando GoTaq® 2 step RT-qPCR System (Promega) seguindo as instruções do fabricante. A expressão de genes de interesse foi quantificada por PCRq em tempo real (VIIa ™ 7 Real-Time PCR System, Life Technologies) utilizando primers específicos (Integrated DNA Technologies) listados na tabela abaixo. A expressão do RNAm de 18S foi utilizado como o gene de referência para normalizar a expressão dos genes avaliados em cultura de fibroblastos. A expressão relativa foi medida usando o método comparativo $2^{-(\Delta\Delta Cq)}$.

Humanos:

Genes	**Sequência**
18S	F: 5'-AACCCGTTGAACCCCATT-3' R: 5'-CCATCCAATGCGTAGTAGCG-3'
CAV1	F: 5'-CAGGGAAACCTCCTCACAG-3' R: 5'-TGTAGAGATGTCCCTCCGA-3'
DR4	F: 5'-CAGAACGTCCTGGAGCCTGTAAC-3' R: 5'-ATGTCCATTGCCTGATTCTTT GTG-3'
DR5	F: 5'-GCGAAGAAGATTCTCCTGAGATGTG-3' R: 5'-ACATTGTCCTCAGCCCCAGGTCG -3'
FAS	F: 5'-GGTTCTTACGTCTGTTGCT-3' R: 5'-CATGTTCACATCTGGAGGAC-3'
HO1	F: 5'-GCCAGGTGCTCAAAAAGATT3' R: 5'-CCTGCAACTCCTCAAAAGAGC3'
IL6	F: 5'-ATGTAGCCGCACACAGA-3' R: 5'-ATTTGCCGAAGAGCCCCTCAG-3'
IL8	F: 5'-AGAGTCATTGAGAGTGGACC-3' R: 5'-ACTTCTCCACAACCCTCTG-3'
NOX4	F: 5'-GGAGAGCCAGATGAACAGG-3' R: 5'-CTCAGTCTTTGACCCTCGG3-'
NRF2	F: 5'-gagagcccagtcttcattgc-3' R: 5'-TTGGCTTCTGGACTTGGAAC-3'

Genes	**Primers TaqMan e ID dos probes**
CDKN1A	Hs00355782_m1
CDKN2A	Hs00923894_m1

3.2.10 Western blot

Os fibroblastos foram lisados em tampão de lise (Cell Signaling Technology) contendo inibidor de protease (Roche). Quantidades iguais de proteínas totais foram transferidas para géis Bolt® 4-12 % Bis-Tris (Thermo Fisher Scientific). As amostras foram transferidas para uma membrana de nitrocelulose e incubadas com anticorpos para as seguintes proteínas: p-AKT (Ser473) e AKT (PAN) (Cell Signaling Technology), Caveolina-1 (Thermo Fisher Scientific) e β-actina (Santa Cruz Biotechnology).

3.2.11 Níveis de peróxido de hidrogênio

Os níveis de peróxido de hidrogênio foram medido utilizando kit comercial Amplex® Red Hydrogen Peroxide/Peroxidase Assay Kit (Thermo Fischer Scientific).

3.2.12 Análise estatística

As análises estatísticas foram realizadas utilizando o GraphPad Prism 6 (GraphPad Software, La Jolla, CA). Os resultados foram expressos como média ± EPM e foram consideradas significativas as diferenças onde $P<0,05$. As diferenças estatísticas entre dois grupos foram comparadas pelo teste *t* de Student. As diferenças entre dois ou mais grupos foram comparadas por ANOVA de uma via, seguido do pós-teste de comparações múltiplas de Tukey.

4. RESULTADOS E DISCUSSÃO

4.1 Artigo científico 1: "*Hypericum perforatum* reduces paracetamol-induced hepatotoxicity and lethality in mice by modulating inflammation and oxidative stress". Este artigo foi publicado no periódico Phytotherapy Research em 2015.

PHYTOTHERAPY RESEARCH
Phytother. Res. **29**: 1097–1101 (2015)
Published online 8 April 2015 in Wiley Online Library
(wileyonlinelibrary.com) **DOI**: 10.1002/ptr.5350

SHORT COMMUNICATION

Hypericum perforatum Reduces Paracetamol-Induced Hepatotoxicity and Lethality in Mice by Modulating Inflammation and Oxidative Stress

Miriam S. N. Hohmann,[1] Renato D. R. Cardoso,[1] Victor Fattori,[1] Nilton S. Arakawa,[2] José C. Tomaz,[3] Norberto P. Lopes,[3] Rubia Casagrande[2] and Waldiceu A. Verri Jr.[1]*

[1]Department of Pathology, Biological Science Centre, State University of Londrina, Londrina, PR, Brazil
[2]Department of Pharmaceutical Sciences, Health Sciences Centre, State University of Londrina, Londrina, PR, Brazil
[3]Núcleo de Pesquisa em Produtos Naturais e Sintéticos, Departamento de Química e Física, Faculdade de Ciências Farmacêuticas de Ribeirão Preto, Universidade de São Paulo, Av. do café, s/n, Campus universitário, Monte Alegre14040-903, Ribeirão Preto, SP, Brazil

***Hypericum perforatum* is a medicinal plant with anti-inflammatory and antioxidant properties, which is commercially available for therapeutic use in Brazil. Herein the effect of *H. perforatum* extract on paracetamol (acetaminophen)-induced hepatotoxicity, lethality, inflammation, and oxidative stress in male swiss mice were investigated. HPLC analysis demonstrated the presence of rutin, quercetin, hypericin, pseudohypericin, and hyperforin in *H. perforatum* extract. Paracetamol (0.15–3.0 g/kg, p.o.) induced dose-dependent mortality. The sub-maximal lethal dose of paracetamol (1.5 g/kg, p.o.) was chosen for the experiments in the study. *H. perforatum* (30–300 mg/kg, i.p.) dose-dependently reduced paracetamol-induced lethality. Paracetamol-induced increase in plasma aspartate aminotransferase (AST) and alanine aminotransferase (ALT) concentrations, and hepatic myeloperoxidase activity, IL-1β, TNF-α, and IFN-γ concentrations as well as decreased reduced glutathione (GSH) concentrations and capacity to reduce 2,2′-azinobis-(3-ethylbenzothiazoline-6-sulfonate radical cation; $ABTS^{\cdot+}$) were inhibited by *H. perforatum* (300 mg/kg, i.p.) treatment. Therefore, *H. perforatum* protects mice against paracetamol-induced lethality and liver damage. This effect seems to be related to the reduction of paracetamol-induced cytokine production, neutrophil recruitment, and oxidative stress. Copyright © 2015 John Wiley & Sons, Ltd.**

Keywords: Hypericum perforatum; paracetamol hepatotoxicity; cytokines; oxidative stress.

INTRODUCTION

Paracetamol, also known as acetaminophen, is a widely used analgesic and antipyretic drug that is safe at therapeutic doses. However, when taken in overdose, severe hepatotoxicity, acute liver failure, and death can occur. In fact, paracetamol overdose is considered the most common cause of acute liver failure in many Western countries. Paracetamol metabolism results in production of *N*-acetyl-*p*-benzoquinone imine (NAPQI) that binds to mitochondrial proteins followed by mitochondrial oxidative stress and dysfunction, DNA fragmentation, and necrotic death of hepatocytes (Kaplowitz, 2004). Cytokine production plays an important role in amplifying paracetamol-induced hepatoxicity (Ishida *et al.,* 2002) by recruiting and activating macrophages and neutrophils in the liver (Liu *et al.,* 2006). Activated neutrophils and macrophages produce inflammatory and oxidative molecules including cytokines, leukotrienes, and reactive oxygen species, which increase inflammation and oxidative stress, resulting in further liver injury (Liu *et al.,* 2006; Hohmann *et al.,* 2013).

* Correspondence to: Waldiceu A. Verri Jr., Department of Pathology, Biological Science Centre, State University of Londrina, Rodovia Celso Garcia Cid Pr 445,Km 380. Cx. Postal 10.011, Londrina, PR 86057-970, Brazil.
E-mail: waldiceujr@yahoo.com.br

Hypericum perforatum L. (*Hypericaceae*) is popularly known as St. John's Wort. *H. perforatum* extract (HPE) has been widely used in popular medicine and phytotherapy because of antiseptic and antidepressant effects, but significant anti-inflammatory and antioxidant activities are also relevant properties. HPE reduced periodontitis-induced neutrophil recruitment and activation, expression of cytokines and adhesion molecules (Paterniti *et al.,* 2010), and reduced hepatic ischemia/reperfusion injury-induced oxidative stress (Bayramoglu *et al.,* 2014). Moreover, hyperforin, which is present in HPE, inhibited 5-lipoxygenase (Feisst *et al.,* 2009), an enzyme involved in paracetamol-induced hepatotoxicity and lethality (Hohmann *et al.,* 2013).

Taking into account the above mentioned evidence, the effect of HPE on paracetamol-induced lethality, hepatotoxicity, cytokine production, neutrophil recruitment, and antioxidant depletion was investigated.

MATERIALS AND METHODS

Animals. Male Swiss mice (20–25 g), from the Universidade Estadual de Londrina, Londrina, Paraná, Brazil, were used in this study. Mice were housed in standard clear plastic cages with free access to food

Received 06 March 2015
Revised 17 March 2015
Accepted 18 March 2015

and water, a light/dark cycle of 12:12 h, and kept at 21°C. Animals were handled humanely, and all procedures concerning animal care and use were approved by the Research and Ethics Committee of Universidade Estadual de Londrina (process number 13280.2011.64).

High-performance liquid chromatography (HPLC) characterization of HPE. Commercially obtained HPE (Iperisan®, Marjan Farm, Santo Amaro-SP, Brazil) was analyzed by HPLC (Shimadzu) equipped with a photodiode array detector (SPD-M10Avp), multisolvent delivery system (LC-10Avp), oven control system (CTO-10ASvp) and controlled software Class VP 6.14 software. Chromatography was performed on an analytical reverse phase column Spherisob® (C-18 ODS) (250 × 4.6 mm i.d.; particle size 5 μm) (Waters). The HPLC grade solvents were supplied by Panreac®, and water was purified using Milli-Q-plus filter systems (Millipore). For HPLC runs, a gradient of acidified H_2O (2% formic acid) (solvent A) and acetonitrile (2% formic acid) (solvent B) was used at a flow rate of 1 mL/min, and the volume injected was 20 μL. HPLC gradient: 0 min, 0% B; 5 min, 0% B; 20 min, 2.5% B; 30 min, 5% B; 50 min, 15% B; 60 min, 25% B; 65 min, 30% B; 70 min, 45% B; 75 min, 50% B; 80 min, 70% B; 85 min, 90% B; 90 min, 100% B; 95 min, 100% B; 110 min, 0% B. UV detection was performed at 200–400 nm (scan) and set to 280 and 340 nm. UV spectra were recorded for each main peak in the chromatograms. Quercetin-3-*O*-rutinoside (rutin, Sigma), quercetin (Sigma), and hypericin (Sigma) were used as references. High-resolution mass spectra (HR-MS) were recorded by direct infusion of 0.1 mg/mL solutions (MeCN-H2O 7:3 *v/v*) using a syringe pump at a flow rate of 0.1 mL/h on a ultrO-TOF and micro-TOF spectrometer (Bruker Daltonics, USA) with an electrospray ionization (ESI) source operating in the negative mode ($mz = [M - H]^-$).

General experimental procedures. A dose–response study was conducted to determine the sub-maximal lethal dose of paracetamol. For this, mice received p.o. administration of 0.15, 0.5, 1.5, and 3 g/kg of paracetamol suspended in saline (200 mg/mL) or equal volume of saline, and mice lethality was observed every 6 h, during 72 h. Any animal that showed extreme distress or became moribund during survival studies was sacrificed. The effect of HPE treatment on paracetamol-induced lethality, liver injury, inflammation, and oxidative stress was assessed. Mice were treated with 30, 100, and 300 mg/kg of HPE or vehicle (tween 20%) (i.p.) 30 min before administrating paracetamol (1.5 g/kg, p.o.) or saline, and lethality was evaluated as mentioned previously. For the subsequent experiments, mice were sacrificed 4 h after paracetamol overdose, and blood and liver samples were collected and processed as previously described (Hohmann *et al.,* 2013). Liver damage was assessed by determining the plasma concentrations of aspartate aminotransferase (AST) and alanine aminotransferase (ALT) using commercial diagnostic kits (Labtest Diagnóstico S.A., Brazil) according to the manufacturer's instructions. Cytokine (IL-1β, TNF-α, and IFN-γ) concentrations in the liver were quantified by ELISA using eBioscience kits according to the manufacturer's instructions. Neutrophil recruitment to the liver was assessed by determining myeloperoxidase (MPO) activity, a commonly used indirect marker of neutrophil recruitment to tissues, and oxidative stress by the reduced glutathione (GSH) concentrations in the liver and antioxidant capacity of the hepatic tissue (capacity to reduce 2,2′-azinobis-(3-ethylbenzothiazoline-6-sulfonate radical cation; $ABTS^{\cdot+}$) (Hohmann *et al.,* 2013).

Statistical analysis. The results are expressed as mean ± S.E.M. Survival rates were estimated by the Kaplan–Meier method, and statistical analysis was carried out by the logrank test to test for equality of the survival curves. Statistical differences were compared by one-way ANOVA followed by Bonferroni's multiple comparison test. All statistical analyses were performed using Graph Pad Prism 5 (La Jolla, CA). The level of significance was set at $p < 0.05$. Studies were conducted twice and representative data are shown.

RESULTS AND DISCUSSION

HPE presents quercetin, hypericin, pseudohypericin, hyperforin, and rutin

Rutin, quercetin, and hypericin as reference compounds were identified in the ethanolic HPE. The individual compounds were identified by HPLC-PDA and comparison of UV data (λ_{max}) of reported value; as the extract indicated other main compounds, the HR-ESI-MS were recorded indicating the presence of pseudohypericin and hyperforin, *m/z* $[M - H]^-$: 301.0355, 503.0810, 519.0713, 535.3781, and 609.1453 for quercetin, hypericin, pseudohypericin, hyperforin, and rutin, respectively.

Paracetamol induces dose-dependent lethality in mice

A dose–response study with paracetamol was conducted as previously described in the general experimental procedures section. Saline and 0.15 g/kg of paracetamol did not induce death in any of the animals (Fig. 1A). The administration of 0.5 g/kg of paracetamol induced 10% lethality at 6 h and 40% at 12 h, which was maintained until the end of the experiment. The administration of 1.5 g/kg induced 65% lethality at 12 h, which was also maintained. Last, the dose of 3 g/kg induced 85% and 100% mortality within 6 and 12 h, respectively. Therefore, 1.5 g/kg of paracetamol was selected to induce lethality and hepatotoxicity in this study considering it presented sub-maximal lethality adequate to evaluate both increase and decrease in lethality by HPE. Nevertheless, the dose chosen in our study (Fig. 1A) is higher than previous studies which have used 500–750 mg/kg of paracetamol (Ishida *et al.,* 2002; Liu *et al.,* 2006). Plausible explanations for this dose difference include that in the present study mice were not fasted prior to paracetamol administration and paracetamol was administrated p.o., and in other studies mice were fasted and paracetamol was administrated i.p. Furthermore, the paracetamol dose necessary to induce hepatotoxicity and lethality varies among mice strains (Hohmann *et al.,* 2013).

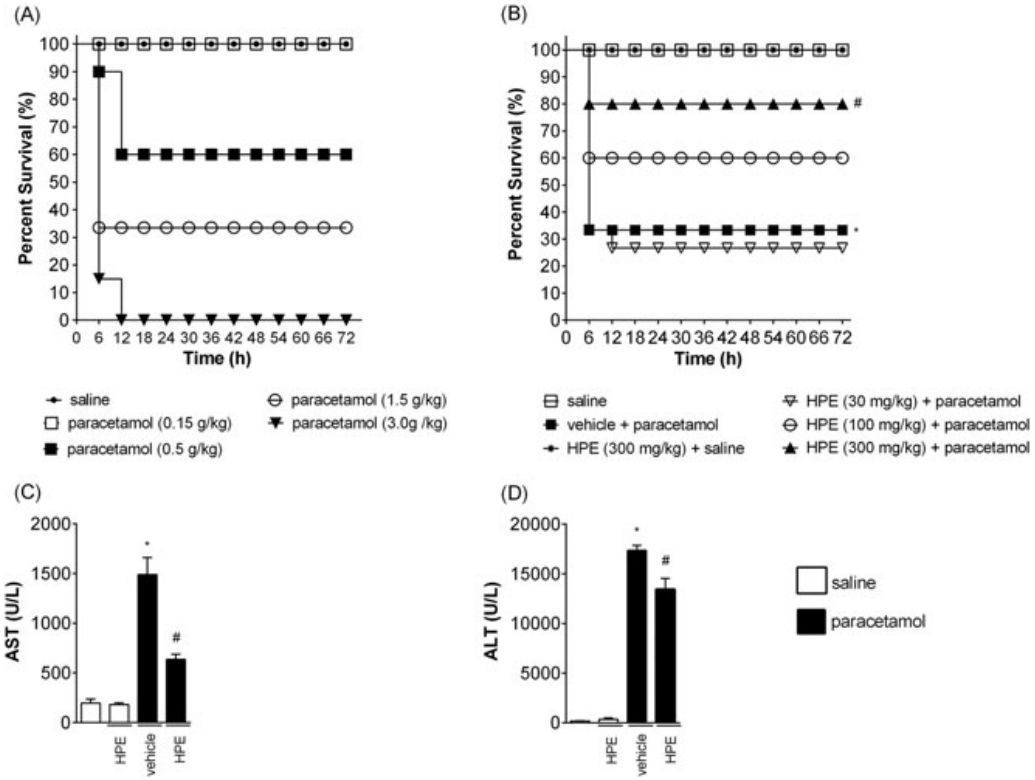

Figure 1. Paracetamol-induced dose-dependent lethality and the effect of *Hypericum perforatum* extract (HPE) on the lethality and liver injury induced by paracetamol in mice. (A) Mice received paracetamol (0.15–3.0 g/kg, p.o.) or saline and lethality was monitored during 72 h. (B) Mice were treated with HPE (30–300 mg/kg, i.p.) or vehicle (Tween 20%) 30 min before paracetamol (1.5 g/kg, p.o.) or saline and lethality was monitored. *n* was 10 for saline groups and 20 for all other groups, $*p < 0.05$ versus saline and $\#p < 0.05$ versus vehicle + paracetamol. Kaplan–Meier method, followed by the log-rank test. (A and B). Mice were treated with HPE (300 mg/kg, i.p.) 30 min before paracetamol (1.5 g/kg, p.o.) or saline and after 4-h plasma concentrations of (C) aspartate aminotransferase (AST) and (D) alanine aminotransferase (ALT) were determined. Values are mean + S.E.M., $n = 5$ per experimental group, representative of two separate experiments. $*p < 0.0001$ compared to saline, $\#p < 0.01$ compared to vehicle + paracetamol. One-way ANOVA followed by Bonferroni's test.

HPE reduces paracetamol-induced lethality and liver damage

Mice were treated with 30, 100, and 300 mg/kg of HPE (i.p.) or vehicle (tween 20%) 30 min before paracetamol (1.5 g/kg, p.o.) or saline administration. Saline and the highest dose of HPE alone did not induce death in any of the animals (Fig. 1B). Paracetamol induced 65% lethality at 12 h in mice treated only with vehicle (tween 20%), which was maintained until the end of the experiment, and 70% and 80% lethality at 6 and 12 h, respectively, in mice treated with the lowest dose of HPE (30 mg/kg) tested. There was no significant difference in lethality between these two groups. Paracetamol induced 40% and 20% lethality at 6 h in mice treated with 100 mg/kg and 300 mg/kg of HPE, respectively, which remained until the end of experiment. Considering the inhibition of paracetamol-induced lethality was greater with 300 mg/kg than 100 mg/kg of HPE, the dose of 300 mg/kg of HPE was chosen for the following experiments investigating its mechanisms of hepatic protection.

Saline and HPE alone did not alter AST and ALT plasma concentrations (Fig. 1C and D). Paracetamol induced significant increase in plasma concentrations of AST and ALT in mice, which was reduced by treatment with HPE, demonstrating that HPE protects against paracetamol-induced liver damage.

Paracetamol hepatotoxicity is dependent on the metabolization of paracetamol into the reactive metabolite NAPQI by cytochrome P-450 (CYP) enzymes, primarily CYP2E1 (Kaplowitz, 2004). In this sense, inhibition of CYP2E1 activity would result in reduced NAPQI formation and consequently reduced liver injury. However, treatment with a higher dose (435 mg/kg, daily, during 4 days) of HPE than in the present study did not affect CYP2E1 activity in Swiss mice. Moreover, HPE treatment for even longer periods (>21 days) can induce, but not inhibit, CYP2E1 activity (Bray *et al.,* 2002). Therefore, it is unlikely that the hepatic protection by HPE depends on reduced paracetamol metabolization by CYP2E1.

HPE reduces paracetamol-induced inflammation and antioxidant depletion in the liver

Treatment with saline or HPE alone did not alter the parameters assessed in the liver of mice (Fig. 2). Paracetamol induced significant increase in IL-1β, TNF-α, and IFN-γ concentrations and MPO activity in the liver of mice, which were reduced by treatment with HPE compared to vehicle (tween 20%) (Fig. 2A–D). This is in agreement with other studies demonstrating that HPE reduces cytokine production and leukocyte recruitment during other inflammatory conditions (Paterniti *et al.,* 2010). The reduction of paracetamol-induced increase of MPO activity by HPE treatment (Fig. 2D) lines up well with the reduction of IL-1β, TNF-α, and IFN-γ concentrations in the liver (Fig. 2A–C) since these

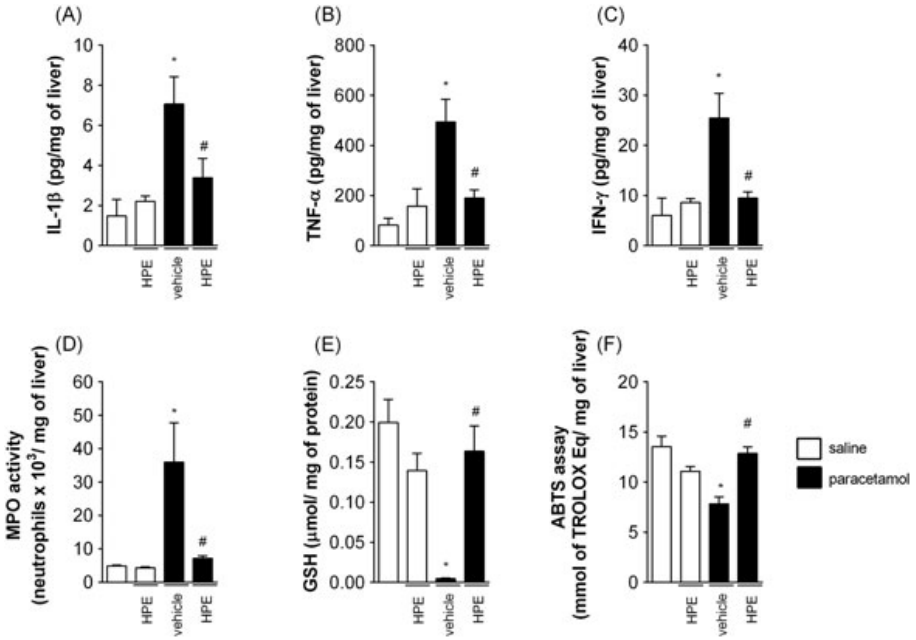

Figure 2. Effect of *Hypericum perforatum* extract (HPE) on the inflammation and antioxidant depletion induced by paracetamol. Mice were treated with HPE (300 mg/kg, i.p.) or vehicle (Tween 20%) 30 min before paracetamol (1.5 g/kg, p.o.) or saline was administered. After 4 h, liver (A) IL-1β, (B) TNF-α, and (C) IFN-γ concentrations, (D) myeloperoxidase activity, (E) reduced glutathione (GSH) concentrations, and (F) capacity of reducing 2,2′-azinobis (3-ethylbenzothiazoline 6-sulfonate; $ABTS^{\cdot+}$) were determined. Values are mean + S.E.M., $n = 5$ per experimental group, representative of two separate experiments. $*p < 0.01$ compared to saline. $\#p < 0.01$ compared to vehicle + paracetamol. One-way ANOVA followed by Bonferroni's test.

cytokines mediate neutrophil recruitment and activation (Ishida *et al.,* 2002). Additionally, the increase in cytokine (IL-1β, TNF-α, IFN-γ, among others) concentrations in the liver and excessive neutrophil recruitment has been implicated in amplifying paracetamol-induced liver damage (Ishida *et al.*, 2002; Liu *et al.*, 2006). Therefore, the reduction of paracetamol-induced increase in AST and ALT plasma concentrations by HPE treatment (Fig. 1C and D) can be attributed to reduced cytokine production and neutrophil recruitment to the liver.

Paracetamol reduced GSH concentrations (Fig. 2E) and antioxidant capacity (Fig. 2F) in the liver of mice, which was inhibited by treatment with HPE. Paracetamol induces liver antioxidant and GSH depletion in an antioxidant sensible manner. Thus, HPE inhibition of paracetamol-induced hepatic depletion of GSH and antioxidant capacity is an important protective mechanism. Some of the molecules present in the HPE, for example the flavonoids rutin and quercetin, can scavenge free radicals, and thus preserve tissue GSH and other antioxidants (De Paola *et al.,* 2005). Accordingly, previous studies have also evidenced the restoration of depleted GSH concentrations and antioxidant capacity in tissues by HPE (Singh *et al.,* 2002; Bayramoglu *et al.,* 2014). It is noteworthy that GSH is not only responsible for cellular defense against oxidative stress, but also the detoxification of NAPQI (Kaplowitz, 2004); thus it is possible that the HPE attenuation of GSH depletion in the liver contributed to further reduction of NAPQI accumulation and its hepatic damage (Kaplowitz, 2004).

In conclusion, HPE inhibits paracetamol-induced lethality and hepatotoxicity. The mechanisms involved in the effect of HPE include inhibition of paracetamol-induced cytokine production, neutrophil recruitment, and depletion of GSH and antioxidant capacity in the liver.

Acknowledgements

This work was supported by Brazilian grants from CNPq, CAPES, MCTI/SETI/Fundação Araucária, and Parana State Government.

Conflict of Interest

The authors have declared that there is no conflict of interest.

REFERENCES

Bayramoglu G, Bayramoglu A, Engur S, Senturk H, Ozturk N, Colak S. 2014. The hepatoprotective effects of *Hypericum perforatum* L. on hepatic ischemia/reperfusion injury in rats. *Cytotechology* **66**: 443–448.

Bray BJ, Perry NB, Menkes DB, Rosengren RJ. 2002. St. John's wort extract induces CYP3A and CYP2E1 in the Swiss Webster mouse. *Toxicol Sci* **66**: 27–33.

De Paola R, Muià C, Mazzon E, *et al*. 2005. Effects of *Hypericum perforatum* extract in a rat model of ischemia and reperfusion injury. *Shock* **24**: 255–263.

Feisst C, Pergola C, Rakonjac M, *et al*. 2009. Hyperforin is a novel type of 5-lipoxygenase inhibitor with high efficacy in vivo. *Cell Mol Life Sci* **66**: 2759–2771.

Hohmann MS, Cardoso RD, Pinho-Ribeiro FA, *et al*. 2013. 5-Lipoxygenase deficiency reduces acetaminophen-induced hepatotoxicity and lethality. *BioMed Res Int* **2013**: 627046.

Ishida Y, Kondo T, Ohshima T, Fujiwara H, Iwakura Y, Mukaida N. 2002. A pivotal involvement of IFN-γ in the pathogenesis of acetaminophen-induced acute liver injury. *FASEB J* **16**: 1227–1236.

Kaplowitz N. 2004. Acetaminophen hepatoxicity: what do we know, what don't we know, and what do we do next? *Hepatology* **40**: 23–26.

Liu XZ, Han D, Gunawan B, Kaplowitz N. 2006. Neutrophil depletion protects against murine acetaminophen hepatotoxicity. *Hepatology* **43**: 1220–1230.

Paterniti I, Briguglio E, Mazzon E, *et al*. 2010. Effects of *Hypericum perforatum*, in a rodent model of periodontitis. *BMC Complement Altern Med* **10**: 73.

Singh A, Naidu PS, Gupta S, Kulkarni SK. 2002. Effect of natural and synthetic antioxidants in a mouse model of chronic fatigue syndrome. *J Med Food* **5**: 211–220.

4.2 Artigo científico 2: “Vitexin inhibits diclofenac-induced acute kidney injury by targeting NF-κB activation, inflammatory cytokines, and oxidative stress in mice”. Este artigo será submetido ao periódico científico The Journal of Nutritional Biochemistry.

Normas do periódico: http://www.jnutbio.com/content/authorinfo

Vitexin inhibits diclofenac-induced acute kidney injury by targeting NF-κB activation, inflammatory cytokines, and oxidative stress in mice

Miriam S. N. Hohmann,[a] Victor Fattori,[a] Rubia Casagrande,[b] Waldiceu A. Verri, Jr., [a,*]

[a]Departament of Pathology - Centre of Biological Sciences, Rodovia Celso Garcia Cid Km 480 PR 445, CEP: 86.057-970, Postal Address 10.011, Londrina, Paraná, Brazil. Email: hohmann.miriam@gmail.com; vfattori@outlook.com

[b]Departament of Pharmaceutical Sciences, Centre of Health Sciences, Hospital Universitário, Universidade Estadual de Londrina, Av. Robert Koch, 60 - Operária, Londrina - PR, 86038-350, Londrina, Brazil. Email: rubiacasa@yahoo.com.br

*Corresponding author: Prof. Dr. Waldiceu A. Verri Jr. Present address: Department of Pathology, Universidade Estadual de Londrina, Rodovia Celso Garcia Cid Km 480 PR 445, CEP: 86.057-970, Postal Address 10.011, Londrina, Paraná, Brazil. Phone: + 55 43 3371 4979. Fax: + 55 43 3371 4387. E-mail: waverri@uel.br or waldiceujr@yahoo.com.br

Running title: Vitexin inhibits diclofenac-induced acute kidney injury

Financial support: Coordenação de Aperfeiçoamento de Pessoal de Nível Superior (CAPES), MCTI/SETI/Fundação Araucária and Parana State Government, Conselho Nacional de Desenvolvimento Científico e Tenológica (CNPq).

Keywords: acute kidney injury, non-steroidal anti-inflammatory drugs, chronic kidney disease, renal failure, flavones, nuclear factor-kappa B

Abstract

Acute Kidney Injury (AKI) is a serious and frequent clinical complication that can lead to sudden loss of renal function. Important causes of AKI are nephrotoxicity and drug adverse effects. Diclofenac, which is one of the most frequently used non-steroidal anti-inflammatory drug (NSAID) worldwide, is known to cause AKI in humans and animals. Herein, we investigated the protective effect and mechanisms of action of the flavonoid vitexin on AKI induced by diclofenac in mice. Mice were treated with vitexin (1, 3, or 10 mg/kg, i.p.) 30 min before diclofenac (200 mg/kg, p.o.) administration and, 24 hours after the stimulus, kidney damage, oxidative stress, cytokine production, and nuclear factor-kappa B (NF-κB) activation were assessed. Treatment with vitexin inhibited the increase in blood urea and creatinine levels and proteinuria induced by diclofenac. Vitexin also inhibited diclofenac-induced depletion in antioxidant defenses [reduced glutathione (GSH), ferric-reducing antioxidant power (FRAP), and free radical scavenging ability (ABTS)] and increase in superoxide anion and lipid peroxidation levels in the renal tissue and blood. Lastly, vitexin inhibited diclofenac-induced IL-1β, TNF-α, IL-6, and IFN-γ production, NF-κB activation, and the decrease in IL-10 levels in the kidney and blood. Collectively, these data show that vitexin has protective effects in diclofenac-induced AKI and the mechanisms associated with these effects are reduction of oxidative stress and modulation of cytokine production and NF-κB activation.

Keywords: acute kidney injury, non-steroidal anti-inflammatory drugs, chronic kidney disease, renal failure, flavones, nuclear factor-kappa B

1. Introduction

Acute Kidney Injury (AKI) is a serious and frequent clinical complication that can lead to sudden loss of renal function. It is associated with a very high risk for the development of chronic kidney disease (CKD) and high mortality rate (1-3). An important cause of AKI is nephrotoxicity. Compared to other organs, the kidneys are more susceptible to both chemical toxicity and drug adverse effects (3, 4).

Diclofenac (2-[(2,6-dichlorophenyl)amino]phenylacetate), which is one of the most frequently used non-steroidal anti-inflammatory drug (NSAID), is prescribed to millions of patients worldwide for the control of pain and inflammation associated with arthritis and other conditions, such as osteoarthritis, rheumatoid arthritis, and ankylosing spondylitis (5, 6). Although its toxicity is commonly associated with the gastrointestinal tract and with idiosyncratic hepatic injury (7, 8), there is a direct link between diclofenac and acute renal failure (9-11). In fact, a meta-analysis study assessing the individual effect of NSAIDs reveals that patients treated with diclofenac present a relative risk of 1.77 fold for the development of AKI, that is 77% increase in risk to develop AKI (12). This is important considering that NSAIDs intoxication has a direct impact on public health costs due to increased morbidity and mortality (12, 13). Moreover, if not properly managed, the complications of AKI can lead to incomplete renal recovery or can accelerate the progression to CKD (12). The two main types of acute renal failure induced by diclofenac and other NSAIDs are hemodynamic-mediated nephritis and acute interstitial nephritis, both associated with low levels of prostaglandins (PGs) (12, 14). PGs, mainly PGE_2 and prostacyclin (PGI_2), maintain normal renal blood flow and glomerular filtration rate (GFR) and the inhibition of their synthesis (15), secondary to cyclooxygenase-1 (COX-1) and -2 (COX-2) inhibition by diclofenac (16), leads to abnormal renal function, decline in glomerular hydraulic pressure, and ultimately renal dysfunction (8, 14).

Diclofenac and its residues are found to be more concentrated in the kidneys than in other organs and this seems to be directly responsible for diclofenac toxicity and kidney failure (17). Studies show that diclofenac targets kidney mitochondria, decreasing the rate of ATP biosynthesis (9, 18). Diclofenac also increases the production of reactive oxygen species (ROS) in the kidney, which induces oxidative stress and DNA fragmentation, ultimately translating into apoptotic cell death of kidney cells (10, 19). Moreover, diclofenac increases nuclear factor-kappa B (NF-κB) activation and thereby upregulates proinflammatory cytokines in the kidney. Accordingly, the inhibition of NF-κB activation reduces AKI (19).

Vitexin (apigenin-8-C-D-glucopyranoside) is a naturally-derived flavonoid compound (20)

that is found in several plants consumed for medicinal or dietary purpose, for example, *Vigna radiata* L. (Mung Bean) (21), *Crataegus spp*. (hawthorn) (22), *Passiflora spp.* (passion flower) (23), *Mimosa pudica* L. (24), and *Phyllostachys nigra.* Studies have shown that vitexin possesses several biological effects (25-27). Among them, its potent antioxidant effect stands out. Vitexin increases the expression of antioxidant enzymes and enhances overall antioxidant capacity in tissues such as the liver and kidney, in addition to reducing oxidative-mediated cell damage (i.e. lipid peroxidation) (27, 28). Its ability to modulate oxidative stress provides significant protection in myocardial ischemia/reperfusion and drug-induced cardiotoxicity in rats (27, 29). Moreover, vitexin also possesses anti-inflammatory effect (25, 30) and inhibits inflammatory pain in mice by targeting the production of pro-inflammatory cytokines (31).

Considering the aforementioned evidence for vitexin, it is conceivable that vitexin may have a protective effect in diclofenac-mediated nephrotoxicity. Therefore, the present study aimed to investigate the potential protective effect of vitexin in diclofenac-induced AKI in mice and to elucidate the underlying mechanisms, focusing on oxidative stress, inflammatory cytokines, and NF-κB activation, which are central mechanisms of AKI.

2. Materials and methods

2.1 Animals

The experiments were performed on male Swiss mice, weighing between 20-25g from Universidade Estadual de Londrina. Mice were housed in standard clear plastic cages with free access to water and food, light/dark cycle of 12/12 h and controlled temperature. Mice were maintained in the vivarium of the Department of Pathology, Universidade Estadual de Londrina for at least two days before the experiments. Mice were used only once and were acclimatized to the testing room at least 1 hour before the experiments, which was conducted during the light cycle. To collect blood samples, mice were first anesthetized by isoflurane 3% (Abbot, Abbott Park, IL, USA) inhalation. For euthanasia, mice were anesthetized by isoflurane 3% (Abbot, Abbott Park, IL, USA) inhalation overdose and terminally euthanized by cervical dislocation followed by decapitation. Animals were handled humanely and all efforts were made to minimize the number of animals used and their suffering. All procedures concerning animal care and use were approved by the Research and Ethics Committee of Universidade Estadual de Londrina (protocol number 12742.2016.32).

2.2 Experimental design

In the first set of experiments, mice (n = 6 per group) were treated with vitexin (1, 3, or 10 mg/kg, 100 µL, intraperitoneal, i.p.) (Sigma-Aldrich) or vehicle (sterile saline, 100 µL, per

oral, p.o.) 30 min prior to the administration of toxic dose of diclofenac (Neutaren®; Novartis Biociências S. A.) (200 mg/kg, 100 µL, per oral, p.o.). After 24 hours, blood levels of urea and creatinine were measured to determine the best dose vitexin for the following experiments in this study. The dose of 10 mg/kg of vitexin was selected for the assessment of proteinuria, oxidative stress [quantification of reduced glutathione (GSH), ferric-reducing antioxidant power (FRAP), free radical scavenging ability (ABTS), nitroblue tetrazolium (NBT) reduction, and lipid peroxidation], cytokine production (ELISA), and NF-κB activation (ELISA) in the blood and/or kidney tissue (19). The doses of diclofenac and vitexin, as well as the time of sample harvesting and analyses, were based on previous studies (10, 19, 31). All the analyses performed in renal tissue were performed using the entire organ.

2.3 Renal function tests

Blood samples were collected by cardiac puncture 24 hours after diclofenac administration. The serum was separated by centrifugation (200 x *g*, 10 min, 4°C). Serum samples were processed according to the manufacturer's instructions (Labtest Diagnóstico S.A., Lagoa Santa, MG, Brazil) to evaluate urea and creatinine levels as indicators of nephrotoxicity. Results are presented as mg/dL of plasma urea or creatinine. Urine was collected 24 hours after diclofenac administration by applying gentle pressure over the bladder. Total protein content in the urine was quantified using Lowry's method (32).

2.4 Reduced glutathione (GSH) assay

The levels of GSH in renal tissue samples were determined using a spectrophotometric method. Kidneys were collected 24 hours after the diclofenac administration and processed following a previously described protocol (32). The results are presented as nmols of GSH/mg of protein (Sigma Chemical Co., USA).

2.5 Ferric-reducing antioxidant power (FRAP) and free-radical scavenging ability (ABTS) assays

The kidney and serum samples were collected 24 hours after diclofenac administration. Kidney samples were homogenized with 500 µL of 1.15% KCl and centrifuged (200 x *g*, 10 min, 4°C). The ability of the samples to resist oxidative damage was determined as FRAP and ABTS (33). For FRAP assay, 15 µL of tissue supernatant or serum was mixed with 45 µL of deionized water and 200 µL of freshly prepared FRAP reagent (Sigma Chemical Co., USA). The reaction mixture was incubated at 37°C for 30 min, and the absorbance was measured at 595 nm. For ABTS assay, ABTS solution (Sigma Chemical Co., USA) was diluted with phosphate buffer saline at pH 7.4 to an absorbance of 0.80 at 730 nm. Then, 200 µL of diluted ABTS solution was mixed with 15 µL of tissue supernatant or

serum. After 6 min, the absorbance was measured at 730 nm. The results were equated against a Trolox standard curve (Sigma Chemical Co., USA). The protein levels in the samples were used for data normalization, and the results are expressed as nmol of Trolox equivalent/mg of protein or mL of serum.

2.6 Nitroblue tetrazolium (NBT) reduction assay

For NBT (Amresco, USA) reduction assay, kidney tissue and serum samples were collected 24 hours after diclofenac administration as described previously (34). Briefly, the kidney was homogenized with 500 µL of 1.15% KCl, and aliquots of 50 µL of tissue homogenate or serum were transferred to a 96-well plate, followed by the addition of 100 µL of NBT solution (1 mg/mL), and maintained at 37°C for 5 min. The supernatant was removed, and the precipitated formazan was solubilized by adding 120 µL of 2 M KOH (Sigma Chemical Co., USA) and 140 µL of dimethyl sulfoxide (DMSO, Sigma Chemical Co., USA). The optical density was measured at 600 nm using a microplate spectrophotometer reader (Multiskan GO Microplate Spectrophotometer, Thermo Scientific, Finland). The protein levels in the samples were used for data normalization and the results are presented as NBT reduction (optical density [OD]/mg of protein or mL of serum).

2.7 Lipid peroxidation assay

The levels of thiobarbituric acid (TBA)-reactive substances (TBARS), primarily malondialdehyde (MDA), were quantified spectrophotometrically using an adapted method as previously described (35). Tissue homogenate or serum reacted with TBA to form MDA-$(TBA)_2$ complexes, and the proteins were precipitated with trichloroacetic acid. Samples were incubated for 15 min in a boiling water bath and transferred to an ice bath. MDA, an intermediate product of lipid peroxidation, was determined by the difference between absorbance at 535 and 572 nm using a microplate spectrophotometer reader (Multiskan GO Microplate Spectrophotometer, Thermo Scientific, Finland). The results are presented as lipid peroxidation (ΔOD A535-A572 /mg of protein or mL of serum).

2.8 Cytokine production

For cytokine production assessment, samples of the kidney and serum were collected 24 hours after diclofenac administration. The kidney tissue samples were homogenized in 500 µL of the appropriate buffer containing protease inhibitors. Cytokine levels were determined by an enzyme-linked immunosorbent assay (ELISA) using eBioscience kits (eBioscience, USA) accordingly with manufacturer instructions. The results were expressed as pg of cytokine/mg of tissue or mL of serum.

2.9 NF-κB activation

The determination of NF-κB activation in renal tissue was performed accordingly with manufacturer instructions. The kidney was collected 24 hours after diclofenac administration and homogenized in ice-cold lysis buffer (Cell Signaling Technology, Beverly, MA, USA). The homogenates were centrifuged (16,100 *g* x 10 min at 4°C) and the supernatants used to assess the levels of total NF-κB p65 subunit and phosphorylated NF-κB p65 subunit by ELISA using PathScan kits #7836 and #7834, respectively (Cell Signaling Technology, USA). The results are presented as the sample ratio (phospho-p65:total-p65/mg of tissue) measured at 450 nm.

2.10 Statistical analysis

Results are presented as mean ± standard error means (SEM) of measurements made on six mice in each group per experiment. Results are representative of two independent experiments. Data were analyzed using one-way ANOVA followed by Tukey's post hoc using the statistical software GraphPad Prism 6 (Graphpad Software Inc., La Jolla, CA, USA). Statistical differences were considered significant when $P < 0.05$.

3. Results

3.1 Vitexin inhibits diclofenac-induced increase of serum urea and creatinine and proteinuria

Firstly, the dose of vitexin capable of reducing diclofenac-induced AKI was assessed (Fig.1). Mice were treated with vitexin (1, 3, or 10 mg/kg, i.p.) 30 min before the administration of diclofenac (200 mg/kg, p.o.) (19, 31). Blood samples were collected 24 hours after the stimulus for the determination of urea and creatinine serum levels. Diclofenac increased urea and creatinine levels, which were inhibited by 10 mg/kg of vitexin, but not by the doses of 1 or 3 mg/kg (Fig. 1A and B). Thus, the dose of 10 mg/kg of vitexin was selected for the following experiments of this study. Next, the effect of vitexin on proteinuria was assessed. Urine was collected 24 hours after the stimulus. Diclofenac-induced increase in proteinuria was inhibited by vitexin (10 mg/kg) (Fig. 1C).

3.2 Vitexin inhibits diclofenac-induced oxidative stress

In the next set of experiments, the effect of vitexin on diclofenac-induced oxidative stress in the kidney (Fig. 2) and blood (Fig. 3) was evaluated. Mice were treated with vitexin (10 mg/kg, i.p.) 30 min before the stimulus with diclofenac (200 mg/kg, p.o.) and, after 24 hours, kidney and blood samples were collected for the determination of the antioxidant

capacity, superoxide anion production (NBT reduction), and lipid peroxidation. Diclofenac significantly reduced antioxidant defenses in renal tissue, as observed by reductions in GSH levels, FRAP, and ABTS (Fig. 2A-C). Additionally, superoxide anion (Fig. 2D) and lipid peroxidation (Fig. 2E) levels were increased in diclofenac-stimulated mice. Treatment with vitexin (10 mg/kg) inhibited diclofenac-induced depletion of antioxidant defenses (Fig. 2A-C) and increase in superoxide anion (Fig. 2D) and lipid peroxidation (Fig. 2E) levels in the kidney. In the blood, diclofenac also reduced FRAP and ABTS (Fig. 3A and B, respectively) and increased superoxide anion production (Fig. 3C) and lipid peroxidation (Fig. 3D), which were inhibited by vitexin (10 mg/kg) (Fig. 3A-D).

3.3 Vitexin modulates diclofenac-induced cytokine production

We next investigated the effect of vitexin on diclofenac-induced increase in cytokine production. Mice were treated with vitexin (10 mg/kg, i.p.) 30 min before the stimulus with diclofenac (200 mg/kg, p.o.) and, after 24 hours, kidney and blood cytokine levels were determined (Fig. 4). Diclofenac increased IL-1β, TNF-α, IL-6, and IFN-γ (Fig. 4A-D) and reduced IL-10 (Fig. 4E) levels in the kidney. Treatment with vitexin, on the other hand, inhibited diclofenac-induced increase in IL-1β, TNF-α, IL-6, and IFN-γ levels (Fig. 4A-D). Further, vitexin inhibited the decrease in IL-10 levels induced by diclofenac (Fig. 4E). Similarly, diclofenac-induced increase in IL-6 levels in the blood was reduced by vitexin (Fig. 4F).

3.4 Vitexin inhibits diclofenac-induced NF-κB activation in the kidney

Considering the inhibitory effect of vitexin on diclofenac-induced cytokine production, its effect on NF-κB activation was investigated. Mice were treated with vitexin (10 mg/kg, i.p.) 30 min before the stimulus with diclofenac (200 mg/kg, p.o.) and kidney sample was collected and NF-κB activation was determined by ELISA (phosphorylated-p65/total-p65 ratio). Diclofenac increased ELISA phosphorylated p65/total-p65 ratio when compared to control group (Fig. 5). Treatment with vitexin inhibited diclofenac-induced phosphorylated p65/total-p65 ratio (Fig. 5), indicating that vitexin inhibits diclofenac-induced NF-κB activation in the kidney.

4. Discussion

In the present study, we show that treatment with vitexin protects mice against diclofenac-induced nephrotoxicity. Treatment with vitexin reduced diclofenac-induced kidney injury as observed by inhibition of serum urea and creatinine levels and proteinuria. Notably, the

preservation of kidney function seems to be associated with reduction in oxidative stress and modulation of cytokine production and NF-κB activation.

Kidney injury and disease are characterized by the generation of oxidant species (36). In diclofenac-induced AKI, elevated levels of ROS, followed by DNA damage and apoptosis of kidney cells, depicts the role of redox imbalance in renal damage in this model (9, 10, 19). In regard to cell death mechanisms, diclofenac induces apoptosis as observed by increased c-Myc protein (19), which is linked to ROS-, NF-κB-, and p53-related apoptotic mechanisms (37-39). Additionally, in diclofenac nephrotoxicity, antioxidant defenses are depleted and the kidney tissue is highly susceptible to oxidative-mediated damage (10). As such, strategies aimed at controlling oxidative stress may represent promising therapeutic approaches given that ROS can activate NF-κB signaling pathway (40) and an increase of ROS levels are linked with GFR impairment (41). Vitexin possesses *in vitro* and *in vivo* antioxidant activity (42-45). *In vitro* evidence shows that vitexin possesses an IC_{50} of 84 μg/mL for DPPH radical scavenger ability (42) and ABTS radical scavenger ability at 16 μg/mL (reduction of 46%) (43). Moreover, vitexin possesses superoxide anion scavenger ability at a varied range of concentrations (42, 44) and reduces Fe(II)-induced lipid peroxidation with an IC_{50} of 2313 μM (45). These findings corroborate the *in vivo* antioxidant activity of vitexin previously described in myocardial ischemia/reperfusion injury (25), doxorubicin cardiotoxicity (27), and carrageenan-induced inflammatory pain (31). Furthermore, it is in line with the vitexin reduction of diclofenac-induced superoxide anion production and lipid peroxidation. Therefore, this set of data explains the increase in antioxidant defense (i.e. depletion in GSH levels, FRAP, and ABTS) in the blood and kidney by vitexin. Considering that increased levels of ROS is prevalent during the progression of kidney injury (36), vitexin presents itself as a promising therapeutic for oxidative mediated damage in diclofenac AKI.

In addition to oxidative stress, numerous studies have shown that a strong association between the inflammatory response and AKI exists (46-48). The generation of inflammatory mediators such as cytokines by vascular endothelial cells and/or in tubular epithelium plays an important role in the pathophysiology of AKI and renal failure (4, 48-51). In fact, diclofenac intoxication induces the production of IL-1β, TNF-α, IL-6, and IFN-γ in the kidney (19). In the present study, diclofenac increased the production of IL-1β, TNF-α, IL-6, and IFN-γ and decreased IL-10 levels in the kidney. Treatment with vitexin inhibited both the production of IL-1β, TNF-α, IL-6, and IFN-γ and reduction in IL-10 levels. Inflammatory cytokines are important in the initiation and extension of inflammation in the kidney (47). IL-6, for example, mediates injurious inflammatory response in both nephrotoxic and ischemic AKI in mice (51, 52). TNF-α, on the other hand, is a potent mediator of apoptosis and tissue damage (53). Cisplatin and endotoxin-induced AKI is mediated in-part by TNF-α and the inhibition of the release or action of TNF-α protects the kidney from nephrotoxicity (54). In contrast, IL-10 is a

potent anti-inflammatory cytokine that inhibits inflammatory and cytotoxic pathways implicated in AKI (55). Therefore, it is conceivable that vitexin reduces kidney inflammation by inhibiting the production of inflammatory cytokines and preventing the decrease in IL-10. Moreover, vitexin also inhibited diclofenac-induced increase in IL-6 levels in the serum. Higher levels of cytokines in the blood are associated with increased risk of mortality in patients diagnosed with acute renal failure (56). In this sense, the modulation of cytokine production by vitexin may be a protective mechanism in diclofenac-induced nephrotoxicity.

Over the years, data showing the role of the transcription factor NF-κB in the pathophysiology of AKI has surfaced. NF-κB has been ascribed to various forms of human and experimental kidney injury, including diclofenac-induced AKI (46, 57, 58). In human renal disease, there is evidence of NF-κB activation in the kidney in diabetic nephropathy, glomerular disease, and AKI (57-59). In agreement with our previous study (19), herein diclofenac also enhanced NF-κB activation in the kidney. Diclofenac-induced increase in NF-κB activation has also been observed in other cell types, such as HCT116 cells (60), astrocytes (61), and microglia (62). Corroborating the role of NF-κB activation in diclofenac-induced AKI, treatment with vinpocetine [an inhibitor of IKK (IκB kinases)] [19] or PDTC (pyrrolidine dithiocarbamate ammonium, a widely-used NF-κB inhibitor molecule) [Borghi et al. in preparation] reduce diclofenac-induced oxidative stress, cytokine production, and NF-κB activation in the kidney. Therefore, targeting this signaling pathway is a promising therapeutic approach for the treatment of AKI. Furthermore, i*n vitro* evidence demonstrates that the NF-κB inhibitor PDTC, but not the antioxidant molecule N-acetylcysteine, reduces LPS-induced NF-κB activation in kidney tubular epithelial cells (63) suggesting that at least in this cell type, molecules with the ability to target this signaling pathway are more important than molecules with antioxidant activity. However, mechanistic studies are necessary to determine whether or not direct targeting of NF-κB and/or antioxidant reduction of NF-κB activation is observed in a sterile model of inflammation such as a drug-induced kidney injury. Importantly, treatment with vitexin inhibited this response, which is consistent with previous reports of inhibition of NF-κB activation by this flavonoid in other settings (25, 27). NF-κB regulates the expression of various inflammatory mediators, among them cytokines (64), thus the decrease in proinflammatory cytokines by vitexin may be secondary to the inhibition of NF-κB activation. It is noteworthy that the mechanism by which vitexin modulates NF-κB activation may be by inhibiting the decrease in IL-10 levels in the kidney, given that vitexin increases IL-10 levels (31), as we also observed herein. It has been shown that IL-10 signaling can block NF-κB activation by suppressing IKK activity, thus inhibiting degradation of IκB and subsequent NF-κB nuclear translocation. Moreover, IL-10 signaling can also block NF-κB binding to DNA (65). Oxidative stress and inflammation are closely linked to disease affliction in renal tissue (46). The inhibition of NF-κB activation by PDTC renders protection against

oxidative stress and early restoration of renal function in folic acid-induced AKI (46). Therefore, it is conceivable that inhibition of NF-κB by vitexin contributes to the decrease in oxidative stress. However, the inverse is also plausible, given that NF-κB, and downstream cytokine production, can be activated by stimuli such as ROS (64).

5. Conclusions

Herein we demonstrate that vitexin reduces diclofenac-induced AKI in mice. Vitexin reduces kidney damage by inhibiting oxidative stress and modulating NF-κB activation and downstream cytokine production. Therefore, the present work contributes to better understanding of the mechanisms of action of vitexin and points to the potential therapeutic use of vitexin in diclofenac-induced AKI. To the best of our knowledge, this is the first report demonstrating the protective potential of vitexin in diclofenac-induced nephrotoxicity.

Acknowledgements

This study was supported by Brazilian grants from Coordenadoria de Aperfeiçoamento de Pessoal de Nível Superior (CAPES), Conselho Nacional de Desenvolvimento Científico e Tecnológico (CNPq), Ministério da Ciência, Tecnologia e Inovação (MCTI), Secretaria da Ciência, Tecnologia e Inovação (SETI), Fundação Araucária, and Governo do Estado do Paraná.

Conflict of interests

The authors declare no conflict of interests.

References

1. Coca SG, Singanamala S, Parikh CR. Chronic kidney disease after acute kidney injury: a systematic review and meta-analysis. *Kidney Int* 2012; 81: 442-448.
2. Murugan R, Kellum JA. Acute kidney injury: what's the prognosis? *Nat Rev Nephrol* 2011; 7: 209-217.
3. Liano F, Pascual J. Epidemiology of acute renal failure: a prospective, multicenter, community-based study. Madrid Acute Renal Failure Study Group. *Kidney Int* 1996; 50: 811-818.
4. Bonventre JV. Mechanisms of Acute Kidney Injury and Repair. In: Jörres A, Ronco C, Kellum JA, editors. Management of Acute Kidney Problems: Springer; 2010. p. 13-20.
5. Schmeltzer PA, Kosinski AS, Kleiner DE, Hoofnagle JH, Stolz A, Fontana RJ, Russo MW, Drug-Induced Liver Injury N. Liver injury from nonsteroidal anti-inflammatory drugs in the United States. *Liver Int* 2016; 36: 603-609.
6. Brogden RN, Heel RC, Pakes GE, Speight TM, Avery GS. Diclofenac sodium: a review of its pharmacological properties and therapeutic use in rheumatic diseases and pain of varying origin. *Drugs* 1980; 20: 24-48.
7. Boelsterli UA. Diclofenac-induced liver injury: a paradigm of idiosyncratic drug toxicity. *Toxicol Appl Pharmacol* 2003; 192: 307-322.
8. Harirforoosh S, Asghar W, Jamali F. Adverse effects of nonsteroidal antiinflammatory drugs: an update of gastrointestinal, cardiovascular and renal complications. *J Pharm Pharm Sci* 2013; 16: 821-847.
9. Ng LE, Vincent AS, Halliwell B, Wong KP. Action of diclofenac on kidney mitochondria and cells. *Biochem Biophys Res Commun* 2006; 348: 494-500.
10. Hickey EJ, Raje RR, Reid VE, Gross SM, Ray SD. Diclofenac induced in vivo nephrotoxicity may involve oxidative stress-mediated massive genomic DNA fragmentation and apoptotic cell death. *Free Radic Biol Med* 2001; 31: 139-152.
11. Ting A, Freund J. Nonsteroidal antiinflammatory-induced acute renal failure detected on bone scintigraphy. *Clin Nucl Med* 2004; 29: 318-319.
12. Ungprasert P, Cheungpasitporn W, Crowson CS, Matteson EL. Individual non-steroidal anti-inflammatory drugs and risk of acute kidney injury: A systematic review and meta-analysis of observational studies. *Eur J Intern Med* 2015; 26: 285-291.
13. Mowry JB, Spyker DA, Brooks DE, McMillan N, Schauben JL. 2014 Annual Report of the American Association of Poison Control Centers' National Poison Data System (NPDS): 32nd Annual Report. *Clinical toxicology* 2015; 53: 962-1147.
14. Perazella MA, Markowitz GS. Drug-induced acute interstitial nephritis. *Nat Rev Nephrol* 2010; 6: 461-470.
15. Kim GH. Renal effects of prostaglandins and cyclooxygenase-2 inhibitors. *Electrolyte Blood Press* 2008; 6: 35-41.
16. Peterson K, McDonagh M, Thakurta S, Dana T, Roberts C, Chou R, Helfand M. Drug Class Review: Nonsteroidal Antiinflammatory Drugs (NSAIDs): Final Update 4 Report. Portland (OR); 2010.
17. Oaks JL, Gilbert M, Virani MZ, Watson RT, Meteyer CU, Rideout BA, Shivaprasad HL, Ahmed S, Chaudhry MJ, Arshad M, Mahmood S, Ali A, Khan AA. Diclofenac residues as the cause of vulture population decline in Pakistan. *Nature* 2004; 427: 630-633.

18. Mingatto FE, Santos AC, Uyemura SA, Jordani MC, Curti C. In vitro interaction of nonsteroidal anti-inflammatory drugs on oxidative phosphorylation of rat kidney mitochondria: respiration and ATP synthesis. *Arch Biochem Biophys* 1996; 334: 303-308.
19. Fattori V, Borghi SM, Guazelli CF, Giroldo AC, Crespigio J, Bussmann AJ, Coelho-Silva L, Ludwig NG, Mazzuco TL, Casagrande R, Verri WA, Jr. Vinpocetine reduces diclofenac-induced acute kidney injury through inhibition of oxidative stress, apoptosis, cytokine production, and NF-kappaB activation in mice. *Pharmacol Res* 2017; 120: 10-22.
20. Verri WA, Jr , Vicentini FTMC, Baracat MM, DGeorgetti SR, Cardosos RD, Cunha TM, Ferreira SH, Cunha FQ, Fonseca MJ, Casagrande R. Flavonoids as Anti-Inflammatory and Analgesic Drugs: Mechanisms of Action and Perspectives in the Development of Pharmaceutical Forms. In: Atta-ur-Rahman, editor. Studies in Natural Products Chemistry, 1st ed: Elsevier; 2012.
21. Kang I, Choi S, Ha TJ, Choi M, Wi HR, Lee BW, Lee M. Effects of Mung Bean (Vigna radiata L.) Ethanol Extracts Decrease Proinflammatory Cytokine-Induced Lipogenesis in the KK-Ay Diabese Mouse Model. *J Med Food* 2015; 18: 841-849.
22. Edwards JE, Brown PN, Talent N, Dickinson TA, Shipley PR. A review of the chemistry of the genus Crataegus. *Phytochemistry* 2012; 79: 5-26.
23. Pereira CA, Yariwake JH, McCullagh M. Distinction of the C-glycosylflavone isomer pairs orientin/isoorientin and vitexin/isovitexin using HPLC-MS exact mass measurement and in-source CID. *Phytochem Anal* 2005; 16: 295-301.
24. Zhang J, Yuan K, Zhou WL, Zhou J, Yang P. Studies on the active components and antioxidant activities of the extracts of Mimosa pudica Linn. from southern China. *Pharmacogn Mag* 2011; 7: 35-39.
25. Dong LY, Li S, Zhen YL, Wang YN, Shao X, Luo ZG. Cardioprotection of vitexin on myocardial ischemia/reperfusion injury in rat via regulating inflammatory cytokines and MAPK pathway. *Am J Chin Med* 2013; 41: 1251-1266.
26. He JD, Wang Z, Li SP, Xu YJ, Yu Y, Ding YJ, Yu WL, Zhang RX, Zhang HM, Du HY. Vitexin suppresses autophagy to induce apoptosis in hepatocellular carcinoma via activation of the JNK signaling pathway. *Oncotarget* 2016; 7: 84520-84532.
27. Sun Z, Yan B, Yu WY, Yao X, Ma X, Sheng G, Ma Q. Vitexin attenuates acute doxorubicin cardiotoxicity in rats via the suppression of oxidative stress, inflammation and apoptosis and the activation of FOXO3a. *Exp Ther Med* 2016; 12: 1879-1884.
28. An F, Yang G, Tian J, Wang S. Antioxidant effects of the orientin and vitexin in Trollius chinensis Bunge in D-galactose-aged mice. *Neural Regen Res* 2012; 7: 2565-2575.
29. Che X, Wang X, Zhang J, Peng C, Zhen Y, Shao X, Zhang G, Dong L. Vitexin exerts cardioprotective effect on chronic myocardial ischemia/reperfusion injury in rats via inhibiting myocardial apoptosis and lipid peroxidation. *Am J Transl Res* 2016; 8: 3319-3328.
30. Gupta SC, Tyagi AK, Deshmukh-Taskar P, Hinojosa M, Prasad S, Aggarwal BB. Downregulation of tumor necrosis factor and other proinflammatory biomarkers by polyphenols. *Arch Biochem Biophys* 2014; 559: 91-99.
31. Borghi SM, Carvalho TT, Staurengo-Ferrari L, Hohmann MS, Pinge-Filho P, Casagrande R, Verri WA, Jr. Vitexin inhibits inflammatory pain in mice by targeting TRPV1, oxidative stress, and cytokines. *J Nat Prod* 2013; 76: 1141-1149.
32. Hohmann MS, Cardoso RD, Pinho-Ribeiro FA, Crespigio J, Cunha TM, Alves-Filho JC, da Silva RV, Pinge-Filho P, Ferreira SH, Cunha FQ, Casagrande R, Verri WA, Jr. 5-

lipoxygenase deficiency reduces acetaminophen-induced hepatotoxicity and lethality. *Biomed Res Int* 2013; 2013: 627046.
33. Katalinic V, Modun D, Music I, Boban M. Gender differences in antioxidant capacity of rat tissues determined by 2,2'-azinobis (3-ethylbenzothiazoline 6-sulfonate; ABTS) and ferric reducing antioxidant power (FRAP) assays. *Comp Biochem Physiol C Toxicol Pharmacol* 2005; 140: 47-52.
34. Fattori V, Pinho-Ribeiro FA, Borghi SM, Alves-Filho JC, Cunha TM, Cunha FQ, Casagrande R, Verri WA, Jr. Curcumin inhibits superoxide anion-induced pain-like behavior and leukocyte recruitment by increasing Nrf2 expression and reducing NF-kappaB activation. *Inflamm Res* 2015; 64: 993-1003.
35. Oliveira FJ, Cecchini R. Oxidative stress of liver in hamsters infected with Leishmania (L.) chagasi. *J Parasitol* 2000; 86: 1067-1072.
36. Ratliff BB, Abdulmahdi W, Pawar R, Wolin MS. Oxidant Mechanisms in Renal Injury and Disease. *Antioxid Redox Signal* 2016; 25: 119-146.
37. Vafa O, Wade M, Kern S, Beeche M, Pandita TK, Hampton GM, Wahl GM. c-Myc can induce DNA damage, increase reactive oxygen species, and mitigate p53 function: a mechanism for oncogene-induced genetic instability. *Molecular cell* 2002; 9: 1031-1044.
38. Qin ZH, Chen RW, Wang Y, Nakai M, Chuang DM, Chase TN. Nuclear factor kappaB nuclear translocation upregulates c-Myc and p53 expression during NMDA receptor-mediated apoptosis in rat striatum. *The Journal of neuroscience : the official journal of the Society for Neuroscience* 1999; 19: 4023-4033.
39. Hoffman B, Liebermann DA. Apoptotic signaling by c-MYC. *Oncogene* 2008; 27: 6462-6472.
40. Ghosh S, Hayden MS. New regulators of NF-kappaB in inflammation. *Nat Rev Immunol* 2008; 8: 837-848.
41. Sverrisson K, Axelsson J, Rippe A, Asgeirsson D, Rippe B. Acute reactive oxygen species (ROS)-dependent effects of IL-1beta, TNF-alpha, and IL-6 on the glomerular filtration barrier (GFB) in vivo. *Am J Physiol Renal Physiol* 2015; 309: F800-806.
42. Kim JH, Lee BC, Kim JH, Sim GS, Lee DH, Lee KE, Yun YP, Pyo HB. The isolation and antioxidative effects of vitexin from Acer palmatum. *Archives of pharmacal research* 2005; 28: 195-202.
43. Li HM, Hwang SH, Kang BG, Hong JS, Lim SS. Inhibitory effects of Colocasia esculenta (L.) Schott constituents on aldose reductase. *Molecules* 2014; 19: 13212-13224.
44. Shibano M, Kakutani K, Taniguchi M, Yasuda M, Baba K. Antioxidant constituents in the dayflower (Commelina communis L.) and their alpha-glucosidase-inhibitory activity. *Journal of natural medicines* 2008; 62: 349-353.
45. Snijman PW, Joubert E, Ferreira D, Li XC, Ding Y, Green IR, Gelderblom WC. Antioxidant activity of the dihydrochalcones Aspalathin and Nothofagin and their corresponding flavones in relation to other Rooibos (Aspalathus linearis) Flavonoids, Epigallocatechin Gallate, and Trolox. *Journal of agricultural and food chemistry* 2009; 57: 6678-6684.
46. Kumar D, Singla SK, Puri V, Puri S. The restrained expression of NF-kB in renal tissue ameliorates folic acid induced acute kidney injury in mice. *PLoS One* 2015; 10: e115947.
47. Akcay A, Nguyen Q, Edelstein CL. Mediators of inflammation in acute kidney injury. *Mediators of inflammation* 2009; 2009: 137072.

48. Bonventre JV, Zuk A. Ischemic acute renal failure: an inflammatory disease? *Kidney Int* 2004; 66: 480-485.
49. Daha MR, van Kooten C. Is the proximal tubular cell a proinflammatory cell? *Nephrol Dial Transplant* 2000; 15 Suppl 6: 41-43.
50. Goes N, Urmson J, Ramassar V, Halloran PF. Ischemic acute tubular necrosis induces an
extensive local cytokine response: evidence for induction of interferon-c, transforming growth factor-b 1, granulocyte-macrophage colony-stimulating factor, interleukin-2, andinterleukin-10. . *Transplantation* 1995; 59: 565–572.
51. Kielar ML, John R, Bennett M, Richardson JA, Shelton JM, Chen L, Jeyarajah DR, Zhou XJ, Zhou H, Chiquett B, Nagami GT, Lu CY. Maladaptive role of IL-6 in ischemic acute renal failure. *J Am Soc Nephrol* 2005; 16: 3315-3325.
52. Nechemia-Arbely Y, Barkan D, Pizov G, Shriki A, Rose-John S, Galun E, Axelrod JH. IL-6/IL-6R axis plays a critical role in acute kidney injury. *J Am Soc Nephrol* 2008; 19: 1106-1115.
53. Rath PC, Aggarwal BB. TNF-induced signaling in apoptosis. *J Clin Immunol* 1999; 19: 350-364.
54. Ramesh G, Reeves WB. TNF-alpha mediates chemokine and cytokine expression and renal injury in cisplatin nephrotoxicity. *J Clin Invest* 2002; 110: 835-842.
55. Deng J, Kohda Y, Chiao H, Wang Y, Hu X, Hewitt SM, Miyaji T, McLeroy P, Nibhanupudy B, Li S, Star RA. Interleukin-10 inhibits ischemic and cisplatin-induced acute renal injury. *Kidney Int* 2001; 60: 2118-2128.
56. Simmons EM, Himmelfarb J, Sezer MT, Chertow GM, Mehta RL, Paganini EP, Soroko S, Freedman S, Becker K, Spratt D, Shyr Y, Ikizler TA, Group PS. Plasma cytokine levels predict mortality in patients with acute renal failure. *Kidney international* 2004; 65: 1357-1365.
57. Zheng L, Sinniah R, Hsu SI. In situ glomerular expression of activated NF-kappaB in human lupus nephritis and other non-proliferative proteinuric glomerulopathy. *Virchows Arch* 2006; 448: 172-183.
58. Mezzano SA, Barria M, Droguett MA, Burgos ME, Ardiles LG, Flores C, Egido J. Tubular NF-kappaB and AP-1 activation in human proteinuric renal disease. *Kidney Int* 2001; 60: 1366-1377.
59. Mezzano S, Aros C, Droguett A, Burgos ME, Ardiles L, Flores C, Schneider H, Ruiz-Ortega M, Egido J. NF-kappaB activation and overexpression of regulated genes in human diabetic nephropathy. *Nephrol Dial Transplant* 2004; 19: 2505-2512.
60. Cho M, Gwak J, Park S, Won J, Kim DE, Yea SS, Cha IJ, Kim TK, Shin JG, Oh S. Diclofenac attenuates Wnt/beta-catenin signaling in colon cancer cells by activation of NF-kappaB. *FEBS letters* 2005; 579: 4213-4218.
61. Kakita H, Aoyama M, Hussein MH, Kato S, Suzuki S, Ito T, Togari H, Asai K. Diclofenac enhances proinflammatory cytokine-induced nitric oxide production through NF-kappaB signaling in cultured astrocytes. *Toxicology and applied pharmacology* 2009; 238: 56-63.
62. Kakita H, Aoyama M, Nagaya Y, Asai H, Hussein MH, Suzuki M, Kato S, Saitoh S, Asai K. Diclofenac enhances proinflammatory cytokine-induced phagocytosis of cultured microglia via nitric oxide production. *Toxicology and applied pharmacology* 2013; 268: 99-105.
63. Woods JS, Ellis ME, Dieguez-Acuna FJ, Corral J. Activation of NF-kappaB in normal rat kidney epithelial (NRK52E) cells is mediated via a redox-insensitive, calcium-dependent pathway. *Toxicology and applied pharmacology* 1999; 154: 219-227.

64. Tak PP, Firestein GS. NF-kappaB: a key role in inflammatory diseases. *J Clin Invest* 2001; 107: 7-11.
65. Schottelius AJ, Mayo MW, Sartor RB, Baldwin AS, Jr. Interleukin-10 signaling blocks inhibitor of kappaB kinase activity and nuclear factor kappaB DNA binding. *J Biol Chem* 1999; 274: 31868-31874.

Figure Legends

Fig. 1. Vitexin reduces diclofenac-induced increase in serum urea and creatinine and proteinuria

Mice were treated with vitexin (1, 3, or 10 mg/kg, i.p.) 30 min before the administration of diclofenac (200 mg/kg, p.o.). Blood and urine samples were collected 24 hours after the stimulus for the determination of urea (A) and creatinine (B) serum levels and proteinuria (C). Results are expressed as mean ± SEM, n = 6 mice per group per experiment, two independent experiments. **$p < 0.01$ and ***$p < 0.001$ compared to saline control; #$p < 0.05$ and ##$p < 0.01$ compared to 0 mg/kg of vitexin group. One-way ANOVA followed by Tukey's post hoc.

Fig. 2. Vitexin inhibits diclofenac-induced oxidative stress in the kidney

Mice were treated with vitexin (10 mg/kg, i.p.) 30 min before the stimulus with diclofenac (200 mg/kg, p.o.) and kidney samples were collected after 24 hours for the determination of reduced glutathione (GSH) levels (A), Ferric-reducing antioxidant power (FRAP) (B), free-radical scavenging ability (ABTS) (C), superoxide anion production [nitro blue tetrazolium (NBT) reduction] (D), and lipid peroxidation (E). Results are expressed as mean ± SEM, n = 6 mice per group per experiment, two independent experiments. *$p < 0.05$ and **$p < 0.01$ compared to saline control; # $p < 0.05$, ##$p < 0.01$, and ###$p < 0.001$ compared to 0 mg/kg of vitexin group. One-way ANOVA followed by Tukey's post hoc.

Fig. 3. Vitexin inhibits diclofenac-induced oxidative stress in the blood

Mice were treated with vitexin (10 mg/kg, i.p.) 30 min before the stimulus with diclofenac (200 mg/kg, p.o.) and blood samples were collected after 24 hours for the determination of Ferric-reducing antioxidant power (FRAP) (A), free-radical scavenging ability (ABTS) (B), superoxide anion production [nitro blue tetrazolium (NBT) reduction] (C), and lipid peroxidation (D). Results are expressed as mean ± SEM, n = 6 mice per group per experiment, two independent experiments. *$p < 0.05$ compared to saline control; #$p < 0.05$ and ####$p < 0.0001$ compared to 0 mg/kg of vitexin group. One-way ANOVA followed by Tukey's post hoc.

Fig. 4. Vitexin modulates diclofenac-induced cytokine production in the kidney and blood

Mice were treated with vitexin (10 mg/kg, i.p.) 30 min before the stimulus with diclofenac (200 mg/kg, p.o.) and kidney and blood samples were collected after 24 hours for the

determination of IL-1β (A), TNF-α (B), IL-6 (C), IFN-γ (D), and IL-10 (E) levels in the kidney and IL-6 (F) levels in the serum. Results are expressed as mean ± SEM, n = 6 mice per group per experiment, two independent experiments. ** $p < 0.01$ and **** $p < 0.0001$ compared to saline control; # $p < 0.05$, ## $p < 0.01$, and #### $p < 0.0001$ compared to 0 mg/kg of vitexin group. One-way ANOVA followed by Tukey's post hoc.

Fig. 5. Vitexin inhibits diclofenac-induced NF-κB activation in the kidney

Mice were treated with vitexin (10 mg/kg, i.p.) 30 min before the stimulus with diclofenac (200 mg/kg, p.o.) and, after 24 hours, kidney samples were collected and NF-κB activation was determined by measuring tissue levels of total and phospho-NF-κB p65 subunits. Results are expressed as mean ± SEM, n = 6 mice per group per experiment, two independent experiments. ** $p < 0.01$ compared to saline control; # $p < 0.05$ compared to 0 mg/kg of vitexin group. One-way ANOVA followed by Tukey's post hoc.

Figure 1

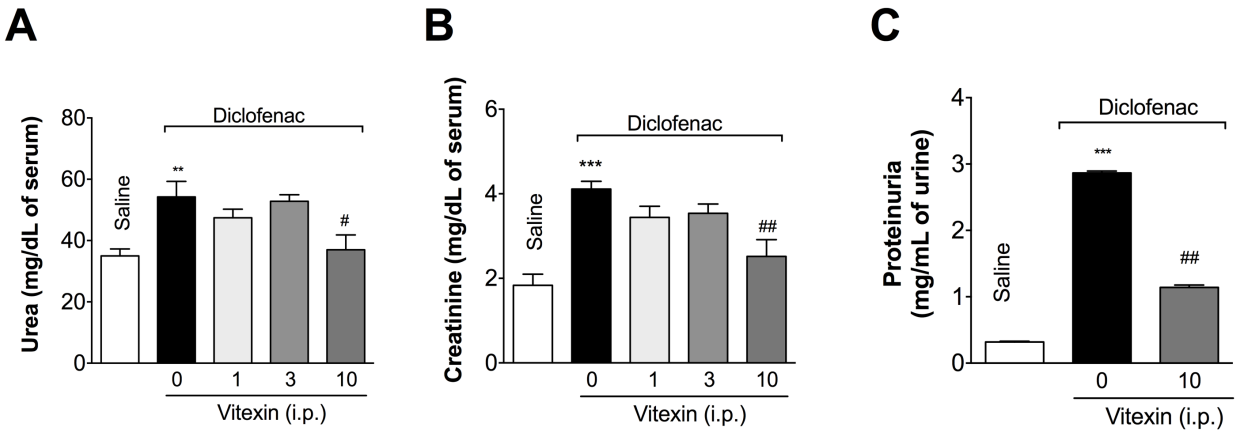
A
Urea (mg/dL of serum)
80
60
40
20
0
Saline
Diclofenac
**
#
0
1
3
10
Vitexin (i.p.)
B
Creatinine (mg/dL of serum)
6
4
2
0
Saline
Diclofenac
***
##
0
1
3
10
Vitexin (i.p.)
C
Proteinuria (mg/mL of urine)
4
3
2
1
0
Saline
Diclofenac
***
##
0
10
Vitexin (i.p.)

Figure 2

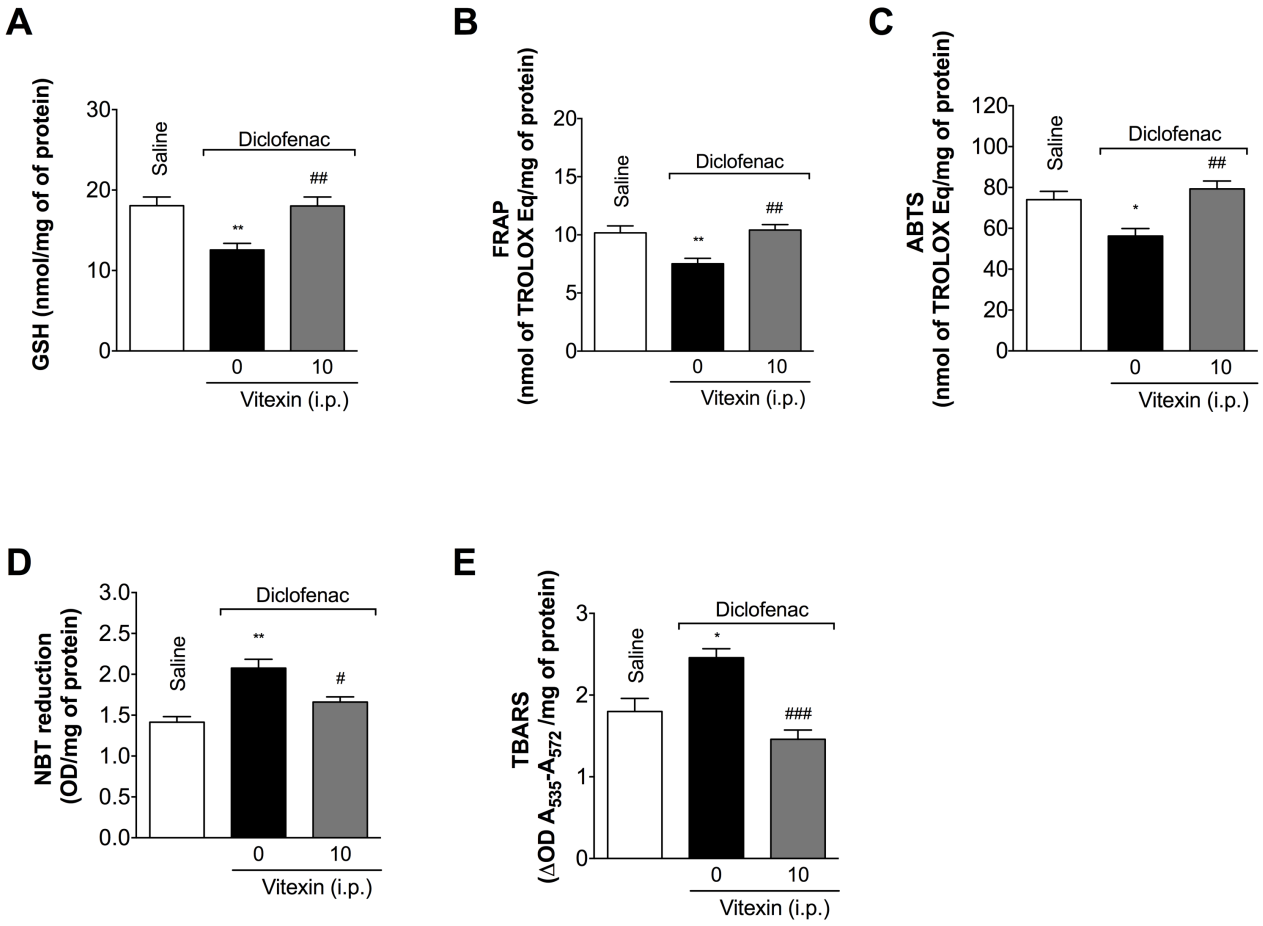
A
GSH (nmol/mg of of protein)
30
20
10
0
Saline
Diclofenac
**
##
0
10
Vitexin (i.p.)
B
FRAP
(nmol of TROLOX Eq/mg of protein)
20
15
10
5
0
Saline
Diclofenac
**
##
0
10
Vitexin (i.p.)
C
ABTS
(nmol of TROLOX Eq/mg of protein)
120
100
80
60
40
20
0
Saline
Diclofenac
*
##
0
10
Vitexin (i.p.)
D
NBT reduction
(OD/mg of protein)
3.0
2.5
2.0
1.5
1.0
0.5
0.0
Saline
Diclofenac
**
#
0
10
Vitexin (i.p.)
E
TBARS
(ΔOD A535-A572 /mg of protein)
3
2
1
0
Saline
Diclofenac
*
###
0
10
Vitexin (i.p.)

Figure 3

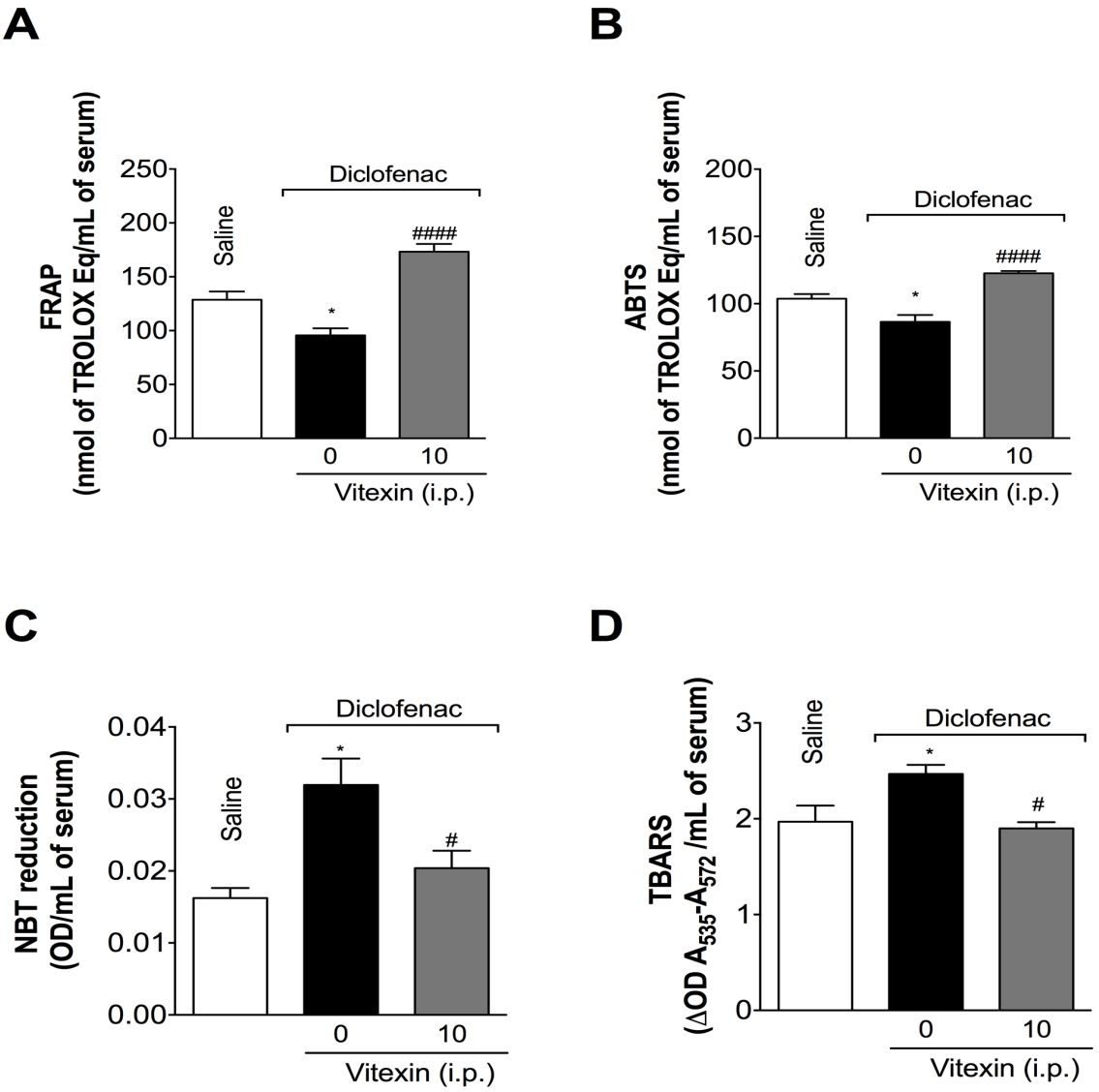
A
FRAP
(nmol of TROLOX Eq/mL of serum)
250
200
150
100
50
0
Saline
Diclofenac
*
####
0
10
Vitexin (i.p.)
B
ABTS
(nmol of TROLOX Eq/mL of serum)
200
150
100
50
0
Saline
Diclofenac
*
####
0
10
Vitexin (i.p.)
C
NBT reduction
(OD/mL of serum)
0.04
0.03
0.02
0.01
0.00
Saline
Diclofenac
*
#
0
10
Vitexin (i.p.)
D
TBARS
(ΔOD A535-A572 /mL of serum)
3
2
1
0
Saline
Diclofenac
*
#
0
10
Vitexin (i.p.)

Figure 4

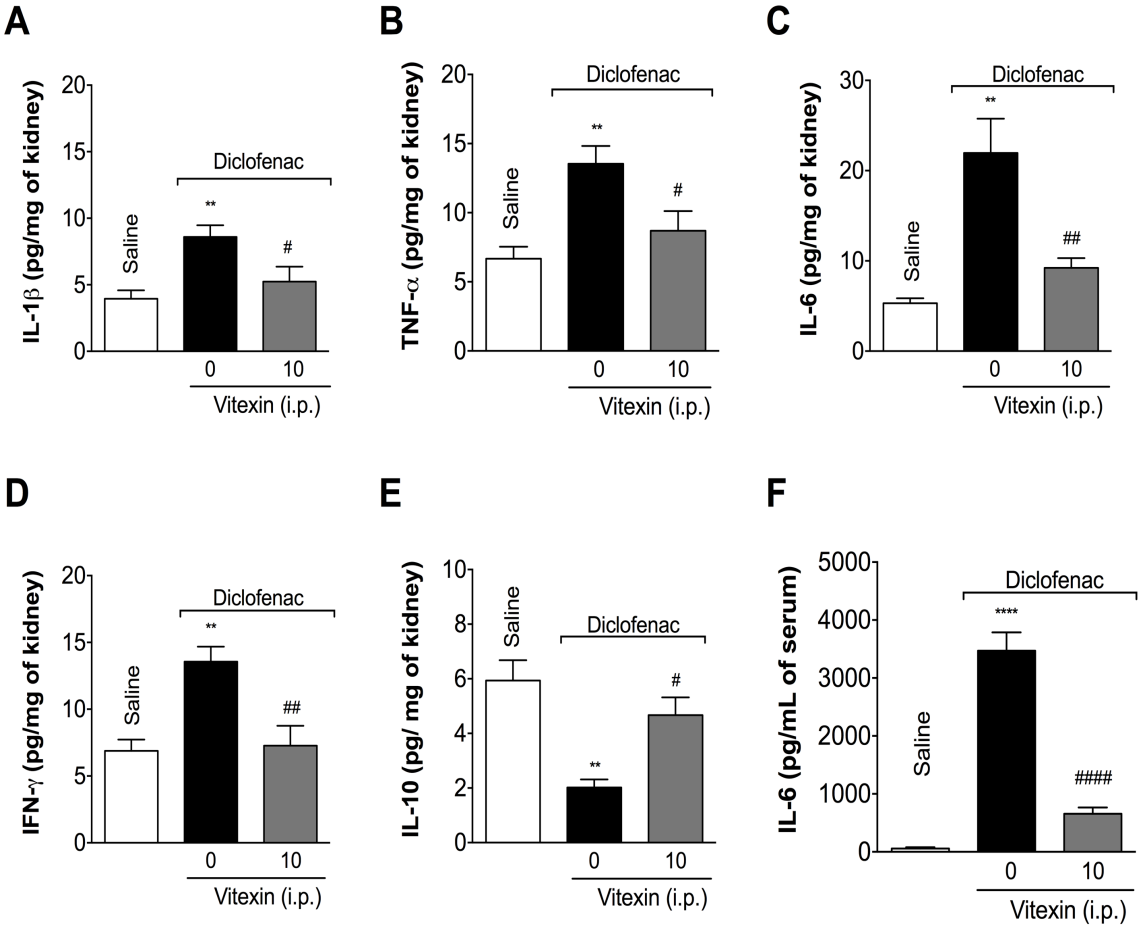
A
IL-1β (pg/mg of kidney)
Saline
Diclofenac
**
#
0
10
Vitexin (i.p.)
B
TNF-α (pg/mg of kidney)
Saline
Diclofenac
**
#
0
10
Vitexin (i.p.)
C
IL-6 (pg/mg of kidney)
Saline
Diclofenac
**
##
0
10
Vitexin (i.p.)
D
IFN-γ (pg/mg of kidney)
Saline
Diclofenac
**
##
0
10
Vitexin (i.p.)
E
IL-10 (pg/ mg of kidney)
Saline
Diclofenac
**
#
0
10
Vitexin (i.p.)
F
IL-6 (pg/mL of serum)
Saline
Diclofenac
****
####
0
10
Vitexin (i.p.)

Figure 5

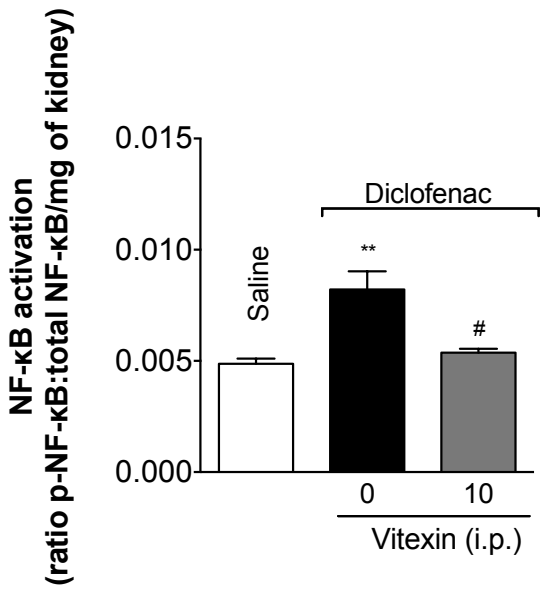
NF-κB activation
(ratio p-NF-κB:total NF-κB/mg of kidney)
0.015
0.010
0.005
0.000
Saline
Diclofenac
**
#
0
10
Vitexin (i.p.)

4.3 Artigo científico 3: “Quercetin enhances ligand-induced apoptosis in senescent idiopathic pulmonary fibrosis fibroblasts”. Este artigo será submetido ao periódico científico American Journal of Respiratory and Critical Care Medicine.

Normas do periódico: http://www.atsjournals.org/page/ajrccm/instructions

Quercetin Enhances Ligand-induced Apoptosis in Senescent Idiopathic Pulmonary Fibrosis Fibroblasts.

Miriam S. Hohmann[1], David M. Habiel[2], Ana L. Coelho[2], Waldiceu A. Verri, Jr[1], Cory M. Hogaboam[2].

[1]Departmento de Ciências Patológicas, Universidade Estadual de Londrina, Londrina, Paraná, Brasil; [2] Department of Medicine, Cedars-Sinai Medical Center, Los Angeles, California, USA

Corresponding Author: Cory M. Hogaboam, Ph.D., Women's Guild Lung Institute, Department of Medicine, Cedars-Sinai Medical Center, Los Angeles, California, USA. E-mail: cory.hogaboam@cshs.org

Author contribution: conception and design M.S.H., D.M.H., C.M.H.; Acquisition of data M.S.H., A.L.C.; Analysis and interpretation of data M.S.H., D.M.H., C.M.H.; Drafting the manuscript and intellectual content M.S.H., D.M.H., W.A.V., C.M.H.

Supported by: A Coordenação de Aperfeiçoamento de Pessoal de Nível Superior (CAPES) scholarship (MSH), a Conselho Nacional de Desenvolvimento Científico e Tecnológico (CNPq) fellowship (308052/2013-7; WAV), funding from Cedars Sinai Medical Center (CMH), and a National Institutes of Health R01 grant (HL123899; CMH).

A short running head: **Quercetin enhances apoptotic ligand responsiveness**

Descriptor number: 3.25

Word count body of the manuscript: 3500 words

At a Glance Commentary

Scientific Knowledge on the Subject:

While cellular senescence may be a protective mechanism in modulating proliferative capacity, fibroblast senescence is now recognized as a key pathogenic mechanism in IPF. In bleomycin-induced pulmonary fibrosis in mice, senescent fibroblasts play a central in non-resolving lung fibrosis and the persistence of these cells seems to be related to apoptosis-resistant phenotype.

What This Study Adds to the Field:

The present study demonstrates that the flavonoid quercetin renders senescent primary human IPF fibroblasts exhibiting apoptosis-resistant phenotype susceptible to pro-apoptotic ligands such as Fas ligand (FasL) and tumor necrosis factor (TNF)-related apoptosis-inducing ligand (TRAIL). Quercetin mediates these effects in senescent IPF fibroblasts via increased caveolin-1 and FasL receptor expression, and the inhibition of AKT activation.

The present study corroborates fibroblast senescence and apoptosis resistance in IPF. We show that quercetin can render senescent primary human IPF fibroblasts exhibiting an apoptosis-resistant phenotype susceptible to pro-apoptotic ligands. Fibroblast senescence is now recognized as an important pathogenic mechanism in IPF and apoptosis-resistance seems to have a central role in non-resolving lung fibrosis, thus the results provided in this study may contribute to future therapeutic strategies for IPF and other fibrotic disorder that progress with the accumulation of senescent fibroblasts.

This article has an online data supplement, which is accessible from this issue's table of content online at www.atsjournals.org"

Abstract

Rationale: IPF is characterized by senescent fibroblasts but until recently few studies addressed therapeutic strategies directed at these cells.

Objectives: Investigate whether quercetin restores the susceptibility of senescent IPF fibroblasts to pro-apoptotic stimuli and the mechanisms involved.

Methods: NL and IPF fibroblasts derived from patients with stable and rapidly progressing disease were serially passaged until senescence. Senescent NL and IPF fibroblasts were compared for the expression of FasL and TRAIL agonist receptor expression and susceptibility to apoptosis by these ligands. The effect of quercetin on the susceptibility to apoptosis and the mechanisms that may be involved in the restored susceptibility to apoptosis by quercetin was also explored.

Measurements and Main Results: Unlike senescent NL fibroblasts, IPF fibroblasts were highly resistant to FasL- or TRAIL-induced apoptosis. Senescent IPF fibroblasts exhibited decreased expression of FasL and TRAIL agonist receptors and caveolin-1 and increased AKT activation compared with senescent NL fibroblasts. Resistance to FasL- or TRAIL-induced apoptosis in senescent IPF fibroblasts was abolished with the co-addition of quercetin and either ligand. Mechanistically, quercetin up regulated Fas and caveolin-1 expression, and modulated AKT activation.

Conclusion: Unlike senescent NL fibroblasts, IPF fibroblasts exhibit a resistance to death ligand induced apoptosis. Quercetin reversed this property in IPF fibroblasts by promoting FasL receptor and caveolin-1 expression, and inhibiting AKT activation.

Word count: 213 words

Keywords: flavonoid, cellular senescence, lung fibrosis.

Introduction

Idiopathic pulmonary fibrosis (IPF) is the most common and lethal form of idiopathic interstitial pneumonia, despite the advent of therapeutic interventions. It is characterized histologically by the presence of usual interstitial pneumonia (UIP) and fibroblastic foci, which are speculated to be the site of active tissue remodeling (1). The disease course of IPF patients is highly variable, with a subset of patients exhibiting disease stability for prolonged periods of time (stable IPF), while other patients exhibit rapid disease progression and deterioration (rapid IPF) (2, 3). Although progression is a key feature of IPF, little is known about what dictates clinical progression of this disease.

Cellular senescence is a state of permanent growth arrest combined with stereotyped phenotypic changes and it has an important role in maintaining physiological homeostasis (4). However, accumulating evidence indicates that senescent cells may also have causal and/or contributing role in tissue remodeling and age-related diseases, including IPF and chronic obstructive pulmonary disease (COPD) (4-7). In fact, it was recently shown that fibroblastic foci are predominantly comprised of senescent myofibroblasts. Further, senescent fibroblasts are detected in the lungs of aged mice and, the persistence of these cells prevents resolution of bleomycin-induced pulmonary fibrosis (8).

Senescent cells secrete pro-inflammatory cytokines, chemokines, and extracellular matrix proteases, which collectively constitute the senescence-associated secretory phenotype (SASP). The SASP and increased reactive oxygen species (ROS) levels in senescent cells can chronically sustain inflammation and tissue damage, which explains the correlation between the build up of these cells and progressive fibrosis (9-11). Consequently, therapeutic interventions that target and reduce the burden of senescent cells pose as promising strategies to modulate the progression of IPF and other age-related diseases.

Recently, Zhu et al. showed that the flavonoid quercetin had direct senolytic effects on senescent cells and this effect was linked to quercetin's effect on the sensitivity of senescent cells to apoptosis (12). Although, quercetin showed a potent capacity to reduce the viability and number of senescent cells *in vitro* and *in vivo*, these previous studies were conducted in mice (12) leading us in the present study to query whether quercetin had any effects on the apoptotic responses of senescent human lung fibroblasts. Thus, considering, i) the deleterious effects of senescent cells in the progression of fibrosis, ii) that apoptosis-resistant phenotype of senescent fibroblasts is responsible for the accumulation of these cells in the lungs (8), and iii) recent evidence that quercetin can regulate apoptosis resistance, we

assessed the pro-apoptotic and modulatory effects of quercetin on apoptosis-resistant, senescent IPF fibroblasts.

Methods

(Additional details are provided in the online supplement)

Culture of primary pulmonary fibroblast

This study was approved by an IRB at Cedars Sinai Medical Center **(**Approval number: Pro34067). Pulmonary fibroblast cell lines from normal patients and patients with stable and rapidly progressing IPF were cultured in complete media (DMEM (Lonza) containing 15% FBS (Cell Generation), 100 IU penicillin and 100 µg/ml streptomycin (Lonza), 292 µg/ml L-Glutamine (Lonza) and 100 µg/ml of Primocin (Invivogen) at 37 ºC in a 10% CO_2 incubator. All the experiments in this study were performed under comparable conditions.

Generating senescent fibroblasts

Proliferating normal and IPF lung fibroblasts were serially passaged in culture until the cells acquired a clear senescent phenotype (flattened morphology, permanent arrest of cell proliferation, altered pattern of gene expression (upregulation of *CDKN1A, CDKN2A, IL6,* and *IL8* genes), and senescence-associated ß-galactosidase activity (β-Galactosidase Staining Kit, BioVision).

Apoptosis studies

Senescent lung fibroblasts (5 x 10^4 cells per well) were treated with quercetin (50 µM) (Sigma-Aldrich), cross-linked recombinant human (rh) FasL (75 or 150 ng/mL) (R&D Systems), cross-linked rhTRAIL (100 or 200 ng/mL) (R&D Systems), and/or vehicle (0.05% DMSO in complete media) for 24 hours. rhFasL and rhTRAIL were cross-linked by mouse anti-polyHistidine monoclonal antibody (R&D Systems). Apoptosis was assessed by measuring caspase-3 activity, cell viability, and LDH release. Phase-contrast images of fibroblast cultures were collected using IncuCyte ZOOM® Live Cell Imaging (Essen Bioscience).

qPCR

Expression levels of genes of interest were quantitated by a real-time quantitative PCR (ViiA™ 7 Real-Time PCR System, Life Technologies) using predesigned primers (Integrated DNA Technologies) and primers and probe sets (Life Technologies). The full primers sequence and IDs for primers and probes are listed in Table 1 in the online supplement. Transcript levels were normalized to 18S mRNA and the fold change in gene expression was calculated using Data Assist software (Life Technologies). Heat map was generated manually using the relative expression values between quercetin and vehicle (control)-treated cells.

Western blot analysis

Cells were lysed lysis buffer (Cell Signaling Technology) containing protease inhibitor cocktail (Roche, Germany). Equal amount of total protein was loaded into a Bolt 4-12% Bis-Tris Plus gel (Life Technologies). Samples were transferred onto a nitrocellulose membrane and blotted using antibodies to the following: p-AKT (Ser473) and AKT (pan) (Cell Signaling Technology), Caveolin-1 (ThermoScientific), and β-actin (Santa Cruz Biotechnology).

Statistical analysis

Analyses were performed using GraphPad Prism (GraphPad Software). Data were expressed as means ± SEM and assessed for significance by one-way ANOVA followed by Tukey's multiple comparisons test. Values of $P < 0.05$ were considered significant.

Results

Senescent IPF fibroblasts are resistant to apoptosis

Lung fibroblasts were derived from diagnostic biopsies removed from patients who subsequently exhibited slow or rapidly progressing IPF (slow IPF and rapid IPF, respectively) over the first year after diagnosis. Primary normal fibroblasts (NL) were also derived from non-fibrotic lung samples lacking any evidence of disease. In the present study, lung fibroblasts derived from stable and rapid IPF patients exhibited a strikingly slower growth rate

at the same passage (i.e. passages 7 – 8; Figure 1A). Further, regardless of clinical progression, IPF fibroblasts senesced after significantly fewer serial passage rounds compared with NL fibroblasts (See Figure E1A in online data supplement). Stable and rapid IPF fibroblasts expressed 2-fold or higher expression of *CDKN1A* and *CDKN2A* genes (Figure 1B), which encode cycle inhibitor proteins p21 and p16, respectively. Up regulation of p21 and/or p16 proteins are widely used markers of cellular senescence (4). A notably higher number of senescence-associated β-galactosidase (SA-β-gal)-positive cells were observed in IPF fibroblast cultures compared with cultures of NL fibroblasts at the same passage number (Figure 1C). Together, these findings suggested that unlike NL fibroblasts, IPF lung fibroblasts are much more prone to senesce in culture.

To undertake further study of senescent NL and IPF fibroblasts (n=3 of each), we first serially passaged fibroblast lines until all cells in these cultures ceased to proliferate and acquired flattened morphology (Figure 1D, Figures E1B and E1C). Replicative senescence was further confirmed in NL and IPF lines by up regulation of *CDKN1A*, *CDKN2A*, *IL6*, and *IL8* expression and positive SA-β-gal staining in NL, stable IPF, and rapid IPF fibroblasts (Figure E1D and Figure 1D, respectively). We next determined the susceptibility of senescent human fibroblasts to pro-apoptotic ligands. Senescent NL and IPF fibroblasts were exposed to FasL (75 or 150 ng/mL) or TRAIL (100 or 200 ng/mL) for 24 hours and caspase-3 activity was measured. Senescent NL fibroblasts exhibited a dose-dependent increase in casapse-3 activity following exposure to FasL or TRAIL (Figure 1E and F). In contrast, neither stable nor rapid senescent IPF fibroblasts exhibited equivalent responsiveness to FasL- or TRAIL-induced apoptosis (i.e. caspase-3 activity; Figure 1E and F). Thus, these findings demonstrate that senescent IPF fibroblasts are markedly less susceptible to FasL- and TRAIL-induced apoptosis.

Expression of Fas, DR4, and DR5 is decreased in senescent IPF fibroblasts

To determine why senescent IPF fibroblasts are resistant to FasL and TRAIL-induced apoptosis, we next assessed the expression of Fas (i.e. FasL receptor) and death receptors (DR) 4 and 5 by quantitative PCR. Both rapid and stable senescent IPF fibroblasts showed significantly decreased expression of *FAS* and *DR5* compared with NL fibroblasts (Figure 1G and 1I). Senescent rapid IPF fibroblasts also showed decreased expression of *DR4* compared to NL and stable IPF fibroblasts (Figure 1H). Interestingly, *FAS* and *DR4* expression was approximately 2-fold lower in rapid IPF fibroblasts compared with stable IPF fibroblasts. Decreased death receptor expression is implicated in apoptosis resistance (13,

14), thus the resistance of senescent IPF fibroblast to apoptotic signals might be attributed to decreased expression of FasL and TRAIL receptors by these cells.

Quercetin induces Fas expression in senescent IPF lung fibroblasts

Recently, it was shown that quercetin selectively killed senescent cells via induction of apoptosis (12). To determine whether quercetin modulated apoptosis in senescent IPF fibroblasts, cells were treated with quercetin (at 50 μM) or vehicle (i.e. 0.05% DMSO) for 24 hours and *FAS*, *DR4*, and *DR5* mRNA expression was quantified. Quercetin induced an approximate 2-fold increase in *FAS* mRNA expression in NL, stable IPF, and rapid IPF fibroblasts compared with vehicle-treated groups (Figure 2A). In contrast, no difference was observed in *DR4* or *DR5* mRNA expression in NL or IPF fibroblasts treated with quercetin compared with the vehicle groups (Figure 2B and C). A qPCR array revealed that quercetin had modest effects on fibrosis-associated transcripts but markedly up-regulated *FAS* in all fibroblast groups (Figure 2D). In contrast, Nintedanib (also referred to as Bibf-1120) markedly down-regulated the expression of genes involved in fibrosis, but did not alter *FAS* or *FasL* compared with vehicle-treated senescent fibroblasts (Figure 2D). These data demonstrate that quercetin up regulates the expression of Fas in senescent NL and IPF fibroblasts.

Quercetin increases the susceptibility of senescent lung fibroblasts to FasL- and TRAIL-induced apoptosis

We examined whether quercetin had a direct pro-apoptotic effect on senescent lung fibroblasts. NL and IPF fibroblasts were treated with quercetin (50 or 100 μM) or vehicle for 24 hours, and caspase-3 activity, cell viability, and lactate dehydrogenase (LDH) release were measured. Compared with the vehicle-treated groups, neither 50 nor 100 μM of quercetin changed caspase-3 (Figure E2A), cell viability (Figure E2B), and LDH release (Figure E2C) in senescent NL or IPF fibroblasts, indicating that quercetin alone did not induce apoptosis in senescent lung fibroblasts.

Given these findings, we next examined whether quercetin rendered senescent IPF fibroblasts susceptible to pro-apoptotic stimuli. NL and IPF fibroblasts were treated with FasL (75 ng/mL) for 24 hours with DMSO or quercetin (50 μM) and apoptosis was assessed using the three parameters indicated above. Neither quercetin nor FasL alone induced significant changes in caspase-3 (Figure 3A, 3D, and 3G), cell viability (Figure 3B, 3E, and 3H), or LDH release (Figure 3C, 3F, and 3I) in any of the senescent fibroblast groups. In contrast, the combination of quercetin + FasL significantly induced caspase-3 activity, reduced cell

viability, and increased LDH release in NL and IPF senescent fibroblast cultures compared with fibroblasts given DMSO alone (Figure 3A-I). Microscopically, a marked decrease in the number of viable cells was also observed in cultures of senescent fibroblasts treated with quercetin + FasL (Figure 4A-L), confirming that quercetin increased the susceptibility of both NL and IPF senescent fibroblasts to FasL-induced apoptosis.

Although we observed negligible effects of quercetin on *DR4* and *DR5* (see Figure 2B-C), we next assessed whether quercetin altered the responsiveness of senescent IPF fibroblasts to TRAIL. Fibroblasts were treated with TRAIL (100 ng/mL) for 24 hours in the presence of DMSO or quercetin (50 μM) and changes in apoptosis parameters were assessed. Unlike mono treatment with quercetin or TRAIL, the addition of quercetin + TRAIL (100 ng/mL) significantly induced caspase-3 activity, reduced cell viability, and increased LDH release in senescent NL and IPF fibroblast cultures compared with DMSO vehicle-treated controls (Figure E3). A microscopically evident decrease in the number of cells was also observed in NL and IPF senescent fibroblast cultures treated with the combination of quercetin + TRAIL (Figure E4A-L). Collectively, these data demonstrate that quercetin renders both senescent NL and IPF fibroblasts susceptible to FasL- and TRAIL-induced apoptosis.

Quercetin up regulates caveolin-1 expression

Low caveolin-1 expression in proliferating IPF fibroblasts appears to account, in part, for the reduced susceptibility of these cells to pro-apoptotic stimuli (15). In the present study, both stable and rapid senescent IPF fibroblasts exhibited markedly lower caveolin-1 protein expression compared with senescent NL fibroblasts (Figure 5A), suggesting that the association between loss of caveolin-1 and increased resistance to apoptosis is also present in senescent lung fibroblasts in IPF. We examined the effect of quercetin on caveolin-1 by measuring *CAV1* mRNA by qPCR and protein expression by Western blot. Quercetin induced an approximate 1.5-fold in *CAV1* mRNA expression in stable and rapid IPF fibroblasts, but not in NL fibroblast cultures (Figure 5B). In line with this observation, caveolin-1 protein expression was significantly increased in stable and rapid IPF fibroblasts treated with quercetin (Figure 5C). It is noteworthy that, although caveolin-1 protein expression was increased, quercetin did not completely restore caveolin-1 protein expression in stable or rapid IPF fibroblasts to levels observed in NL fibroblast cultures (Figure 5C). Thus, these findings suggest that the increased susceptibility of senescent IPF fibroblasts to pro-apoptotic ligands might be due, in part, to increased caveolin-1 levels in these cells.

Increased susceptibility to apoptosis by quercetin is independent of cellular redox homeostasis

Stable and rapid IPF fibroblasts showed increased *NOX4* mRNA expression (Figure E5A), hydrogen peroxide (H_2O_2) release (Figure E5B), and reactive oxygen species (ROS) (Figure E5C) levels compared to NL fibroblasts. Since previous studies have shown that increased ROS levels can induce the degradation of caveolin-1 and quercetin can preserve caveolin-1 in stromal fibroblasts by reducing oxidative imbalance (16, 17), we hypothesized that quercetin might increase caveolin-1 expression in senescent IPF fibroblasts by modulating the oxidative imbalance. Although quercetin is well known for having antioxidant properties, quercetin did not reduce *NOX4* mRNA expression, H_2O_2 release, or ROS levels in NL or IPF fibroblasts. Further, quercetin showed no modulatory effect on *NRF2* (Figure E5D), or *NRF2*-responsive target gene, *HO1* (Figure E5E), mRNA expression, which suggests that quercetin increased caveolin-1 via a mechanism that is independent of restoring the oxidative balance in IPF fibroblasts.

Quercetin modulates AKT activation

AKT is a central component of PI 3-kinase/AKT cell survival pathway (18) and AKT activation has been implicated in low caveolin-1 expression in IPF fibroblasts (19). To address whether quercetin modulates AKT activation in senescent IPF fibroblasts, we measured basal phosphorylated-AKT (p-AKT) expression in NL and IPF fibroblasts. In agreement with previous reports (15), p-AKT expression was significantly higher in stable and rapid IPF fibroblasts (Figure 6A and B). Treatment with quercetin resulted in ~2 fold decrease in the expression of p-AKT in both NL and IPF fibroblasts (Figure 6A and C). Thus, it appears that quercetin increases caveolin-1 expression and the susceptibility to apoptosis by modulating AKT activation in senescent NL and IPF fibroblasts.

Discussion

Although IPF is a fibroproliferative disease, there is growing evidence of increased fibroblast senescence (20) particularly within the fibroblastic foci of IPF lung biopsies (8). During bleomycin-induced pulmonary fibrosis in aged mice, an apoptosis-resistant phenotype favors the persistence of senescent myofibroblasts and these cells contribute to a non-resolving, progressive lung fibrosis (8). The SASP, appears to directly affect lung tissue remodeling and promote senescence of the surrounding cells (11). Herein, we provide evidence that primary lung fibroblasts derived from patients with IPF (regardless of the pace

of disease progression) exhibited a senescent state. Specifically, lung fibroblasts from patients with slow or rapid IPF exhibited: 1) a limited replicative capacity *in vitro*; 2) the up regulation of genes that encode for cell cycle inhibitor proteins; and 3) senescence-associated β-galactosidase staining. More notably, we observed that unlike senescent NL fibroblasts, senescent IPF fibroblasts were highly resistant to FasL- or TRAIL-induced apoptosis. This resistance to ligand-induced apoptosis was abolished with the co-addition of quercetin and either of these ligands to cultures of senescent IPF fibroblasts. Quercetin appeared to target multiple mechanisms in senescent IPF fibroblasts that have been implicated in the resistance of proliferating IPF fibroblasts to apoptosis including FasL receptor and caveolin-1 expression, and AKT activation. Thus, quercetin promoted responsiveness of senescent IPF fibroblasts to pro-apoptotic ligands.

Decreased expression of pro-apoptotic death receptors is a key component in the loss of susceptibility to apoptosis in many cell types (13, 14, 19, 21), thus reduced expression of Fas, DR4, and DR5 might contribute to apoptosis resistance in senescent IPF fibroblasts. Numerous studies have reported lower Fas expression in IPF fibroblasts (19, 21) compared with normal fibroblasts, however, prior to this study the expression levels of DR4 and DR5 in fibroblasts had not been reported in IPF. Likewise, quercetin was known to sensitize leukemia and cancer cell lines to FasL, TRAIL, and other pro-apoptotic stimuli (22, 23) but these types of studies were lacking in the context of cells from IPF patients. Although a recent study demonstrates a direct pro-apoptotic (or senolytic) effect of this compound on various senescent cell types (12), we did not observe a direct pro-apoptotic effect with similar or higher doses of quercetin (50 - 100 μM) on senescent IPF fibroblasts. A plausible explanation for this divergence might be cell, tissue and/or disease specific (12). We observed that senescent IPF fibroblasts showed significantly lower expression of both FasL and agonist TRAIL receptors compared with senescent NL fibroblasts. Quercetin treatment enhanced Fas, but not DR4 or DR5, expression in senescent IPF fibroblasts, suggesting that the increased susceptibility of these cells to FasL-induced apoptosis could be attributed to enhanced Fas expression. In agreement, quercetin was found to increase the expression of genes in the Fas-apoptosis pathway in both senescent NL and IPF fibroblasts. Interestingly, this effect seemed to be specific to quercetin since two other flavonoids tested, namely naringenin and silymarin, did not show similar effects (data not shown). The enhanced responsiveness of quercetin-treated IPF fibroblasts to TRAIL-induced apoptosis appeared to be independent of changes in either DR4 or DR5 presumably indicating that quercetin might be modulating the expression/activation of DcR1 or DcR2, two receptors that antagonize the pro-apoptotic functions of TRAIL (24). Thus, although quercetin alone did not appear to have direct pro-apoptotic effects on senescent NL or IPF fibroblasts, quercetin can render

senescent, apoptosis-resistant IPF fibroblasts susceptible to apoptosis induced by FasL and TRAIL.

Caveolin-1 is a main constituent of cellular membrane structures termed caveolae and low caveolin-1 expression results in reduced Fas membrane expression (19, 25). In line with the previously established role for caveolin-1 deficiency in the apoptosis resistance observed in IPF fibroblasts (19), we observed that caveolin-1 expression was markedly reduced in senescent stable and rapid IPF fibroblasts. Since it was previously shown that the sensitivity to pro-apoptotic stimuli is improved when caveolin-1 levels are increased in fibroblasts (19, 26), we speculated that quercetin might increase caveolin-1 expression in IPF fibroblasts thereby increasing the susceptibility of these cells to pro-apoptotic stimuli. Indeed, treatment with quercetin increased both caveolin-1 mRNA and protein expression in senescent IPF cells. In contrast to previous data showing that quercetin preserves caveolin-1 levels in fibroblasts via the reduction of oxidative stress, quercetin did not alter ROS levels or the expression of Nrf2 or its downstream target HO-1 in senescent IPF fibroblasts. It is therefore unlikely that quercetin is preserving caveolin-1 by modulating the oxidative balance in these cells. These results were counter intuitive due to the remarkable antioxidant properties of quercetin in other systems (27). It is noteworthy that, quercetin may modulate Fas expression via caveolin-1, which coincides with our finding that quercetin increased both caveolin-1 and Fas expression in senescent IPF fibroblasts. Thus, our findings support a role for quercetin in the up regulation of caveolin-1 transcript and protein expression, rather than protecting loss of caveolin-1 levels due to oxidative degradation in senescent IPF fibroblasts.

AKT is a central component of the PI3K/AKT pro-survival pathway and aberrant AKT activation promotes apoptosis resistance (18, 19). In IPF, pathological activation of PI3K/AKT pathway has been attributed to low caveolin-1 expression in fibroblasts. Low caveolin-1 at the plasma membrane creates a membrane microenvironment depleted of PTEN phosphatase activity thereby favoring sustained PI3K/AKT activation (15). Supporting this concept, up regulating caveolin-1 expression results in decreased PI3K/AKT activation, which restores the susceptibility of fibroblasts to apoptosis (19, 26). In the present study, we confirmed that both stable and rapid senescent IPF fibroblasts exhibited increased AKT activation compared with senescent NL fibroblasts. Presently, our data suggest that quercetin might render senescent IPF fibroblasts susceptible to pro-apoptotic stimuli via the caveolin-1-dependent regulation of AKT activation. However, an inverse relation between caveolin-1 and AKT activity cannot be excluded since Nho et al. showed that low caveolin-1 expression is a result of increased activation of PI3K/AKT pathway (19). Thus, although the mechanism whereby quercetin inhibits AKT activation requires further investigation, it is likely that the reduced

activation of this anti-apoptotic signaling pathway following quercetin treatment restores the susceptibility of senescent IPF fibroblasts to apoptosis.

In conclusion, we demonstrate that the flavonoid quercetin renders senescent IPF fibroblasts susceptible to apoptosis induced by FasL and TRAIL, and we provide insight into the mechanisms that are associated with quercetin's effect on senescent IPF fibroblasts. Specifically, quercetin regulates caveolin-1 and Fas expression and modulates AKT activation thereby collectively accounting for the increased susceptibility of senescent fibroblasts to undergo apoptosis. Lastly, we conclude that the *in vitro* data provided in our study are very promising and merit further investigation of the use of quercetin (perhaps in combination with recombinant pro-apoptotic ligands) in aged mice where senescent cells actively participate in the progression of fibrotic lung disease. Ultimately, these studies might culminate in therapeutic strategies for IPF and other fibrotic disorders.

References

1. Habiel DM, Hogaboam C. Heterogeneity in fibroblast proliferation and survival in idiopathic pulmonary fibrosis. *Frontiers in pharmacology* 2014; 5: 2.
2. Trujillo G, Meneghin A, Flaherty KR, Sholl LM, Myers JL, Kazerooni EA, Gross BH, Oak SR, Coelho AL, Evanoff H, Day E, Toews GB, Joshi AD, Schaller MA, Waters B, Jarai G, Westwick J, Kunkel SL, Martinez FJ, Hogaboam CM. TLR9 differentiates rapidly from slowly progressing forms of idiopathic pulmonary fibrosis. *Sci Transl Med* 2010; 2: 57ra82.
3. Martinez FJ, Safrin S, Weycker D, Starko KM, Bradford WZ, King TE, Jr., Flaherty KR, Schwartz DA, Noble PW, Raghu G, Brown KK, Group IPFS. The clinical course of patients with idiopathic pulmonary fibrosis. *Annals of internal medicine* 2005; 142: 963-967.
4. Tominaga K. The emerging role of senescent cells in tissue homeostasis and pathophysiology. *Pathobiology of aging & age related diseases* 2015; 5: 27743.
5. Alder JK, Chen JJ, Lancaster L, Danoff S, Su SC, Cogan JD, Vulto I, Xie M, Qi X, Tuder RM, Phillips JA, 3rd, Lansdorp PM, Loyd JE, Armanios MY. Short telomeres are a risk factor for idiopathic pulmonary fibrosis. *Proc Natl Acad Sci U S A* 2008; 105: 13051-13056.
6. Minagawa S, Araya J, Numata T, Nojiri S, Hara H, Yumino Y, Kawaishi M, Odaka M, Morikawa T, Nishimura SL, Nakayama K, Kuwano K. Accelerated epithelial cell senescence in IPF and the inhibitory role of SIRT6 in TGF-beta-induced senescence of human bronchial epithelial cells. *American journal of physiology Lung cellular and molecular physiology* 2011; 300: L391-401.
7. Dagouassat M, Gagliolo JM, Chrusciel S, Bourin MC, Duprez C, Caramelle P, Boyer L, Hue S, Stern JB, Validire P, Longrois D, Norel X, Dubois-Rande JL, Le Gouvello S, Adnot S, Boczkowski J. The cyclooxygenase-2-prostaglandin E2 pathway maintains senescence of chronic obstructive pulmonary disease fibroblasts. *Am J Respir Crit Care Med* 2013; 187: 703-714.
8. Hecker L, Logsdon NJ, Kurundkar D, Kurundkar A, Bernard K, Hock T, Meldrum E, Sanders YY, Thannickal VJ. Reversal of persistent fibrosis in aging by targeting Nox4-Nrf2 redox imbalance. *Sci Transl Med* 2014; 6: 231ra247.

9. Coppe JP, Patil CK, Rodier F, Sun Y, Munoz DP, Goldstein J, Nelson PS, Desprez PY, Campisi J. Senescence-associated secretory phenotypes reveal cell-nonautonomous functions of oncogenic RAS and the p53 tumor suppressor. *PLoS Biol* 2008; 6: 2853-2868.
10. Kuilman T, Michaloglou C, Vredeveld LC, Douma S, van Doorn R, Desmet CJ, Aarden LA, Mooi WJ, Peeper DS. Oncogene-induced senescence relayed by an interleukin-dependent inflammatory network. *Cell* 2008; 133: 1019-1031.
11. Adnot S, Amsellem V, Boyer L, Marcos E, Saker M, Houssaini A, Kebe K, Dagouassat M, Lipskaia L, Boczkowski J. Telomere Dysfunction and Cell Senescence in Chronic Lung Diseases: Therapeutic Potential. *Pharmacol Ther* 2015; 153: 125-134.
12. Zhu Y, Tchkonia T, Pirtskhalava T, Gower AC, Ding H, Giorgadze N, Palmer AK, Ikeno Y, Hubbard GB, Lenburg M, O'Hara SP, LaRusso NF, Miller JD, Roos CM, Verzosa GC, LeBrasseur NK, Wren JD, Farr JN, Khosla S, Stout MB, McGowan SJ, Fuhrmann-Stroissnigg H, Gurkar AU, Zhao J, Colangelo D, Dorronsoro A, Ling YY, Barghouthy AS, Navarro DC, Sano T, Robbins PD, Niedernhofer LJ, Kirkland JL. The Achilles' heel of senescent cells: from transcriptome to senolytic drugs. *Aging cell* 2015; 14: 644-658.
13. Zhang XD, Nguyen T, Thomas WD, Sanders JE, Hersey P. Mechanisms of resistance of normal cells to TRAIL induced apoptosis vary between different cell types. *FEBS letters* 2000; 482: 193-199.
14. Huang SK, Scruggs AM, Donaghy J, Horowitz JC, Zaslona Z, Przybranowski S, White ES, Peters-Golden M. Histone modifications are responsible for decreased Fas expression and apoptosis resistance in fibrotic lung fibroblasts. *Cell death & disease* 2013; 4: e621.
15. Xia H, Khalil W, Kahm J, Jessurun J, Kleidon J, Henke CA. Pathologic caveolin-1 regulation of PTEN in idiopathic pulmonary fibrosis. *Am J Pathol* 2010; 176: 2626-2637.
16. Mougeolle A, Poussard S, Decossas M, Lamaze C, Lambert O, Dargelos E. Oxidative stress induces caveolin 1 degradation and impairs caveolae functions in skeletal muscle cells. *PLoS One* 2015; 10: e0122654.
17. Martinez-Outschoorn UE, Balliet RM, Rivadeneira DB, Chiavarina B, Pavlides S, Wang C, Whitaker-Menezes D, Daumer KM, Lin Z, Witkiewicz AK, Flomenberg N, Howell A, Pestell RG, Knudsen ES, Sotgia F, Lisanti MP. Oxidative stress in cancer

associated fibroblasts drives tumor-stroma co-evolution: A new paradigm for understanding tumor metabolism, the field effect and genomic instability in cancer cells. *Cell cycle* 2010; 9: 3256-3276.

18. Downward J. PI 3-kinase, Akt and cell survival. *Seminars in cell & developmental biology* 2004; 15: 177-182.
19. Nho RS, Peterson M, Hergert P, Henke CA. FoxO3a (Forkhead Box O3a) deficiency protects Idiopathic Pulmonary Fibrosis (IPF) fibroblasts from type I polymerized collagen matrix-induced apoptosis via caveolin-1 (cav-1) and Fas. *PLoS One* 2013; 8: e61017.
20. Pechkovsky DV, Hogaboam CM, Yao E, Khalil N, Selman M, Knight DA. Fibroblast Senescence In UIP/IPF: A Contributing Factor Or Consequence Of The Disease? [abstract]. *Am J Respir Crit Care Med* 2012; 185: A5282.
21. Wynes MW, Edelman BL, Kostyk AG, Edwards MG, Coldren C, Groshong SD, Cosgrove GP, Redente EF, Bamberg A, Brown KK, Reisdorph N, Keith RC, Frankel SK, Riches DW. Increased cell surface Fas expression is necessary and sufficient to sensitize lung fibroblasts to Fas ligation-induced apoptosis: implications for fibroblast accumulation in idiopathic pulmonary fibrosis. *Journal of immunology* 2011; 187: 527-537.
22. Jacquemin G, Shirley S, Micheau O. Combining naturally occurring polyphenols with TNF-related apoptosis-inducing ligand: a promising approach to kill resistant cancer cells? *Cellular and molecular life sciences : CMLS* 2010; 67: 3115-3130.
23. Russo M, Palumbo R, Mupo A, Tosto M, Iacomino G, Scognamiglio A, Tedesco I, Galano G, Russo GL. Flavonoid quercetin sensitizes a CD95-resistant cell line to apoptosis by activating protein kinase Calpha. *Oncogene* 2003; 22: 3330-3342.
24. LeBlanc HN, Ashkenazi A. Apo2L/TRAIL and its death and decoy receptors. *Cell death and differentiation* 2003; 10: 66-75.
25. Rothberg KG, Heuser JE, Donzell WC, Ying YS, Glenney JR, Anderson RG. Caveolin, a protein component of caveolae membrane coats. *Cell* 1992; 68: 673-682.
26. Liu J, Lee P, Galbiati F, Kitsis RN, Lisanti MP. Caveolin-1 expression sensitizes fibroblastic and epithelial cells to apoptotic stimulation. *Am J Physiol Cell Physiol* 2001; 280: C823-835.
27. Boots AW, Haenen GR, Bast A. Health effects of quercetin: from antioxidant to nutraceutical. *European journal of pharmacology* 2008; 585: 325-337.

Figure legends

Figure 1. Lung fibroblasts isolated from IPF patients exhibit a senescent and an apoptosis-resistant phenotype. (*A*) Number of fibroblasts at 0, 24, 48, and 96 hours, (*B*) *CDKN1A* and *CDKN2A* mRNA expression, and (*C*) senescence associated β-galactosidase (SA-β-gal) staining in fibroblasts at passages 7 - 8. (*D*) Induction of replicative senescence: fibroblasts were serially passaged in culture until cells became senescent late passage. SA-β-gal staining was determined in fibroblasts at early passage (passages 4 - 5) and at late passage (passages 11 – 18). Caspase-3 activity induced by (*E*) FasL (75 or 150 ng/mL) or (*F*) TRAIL (100 or 200 ng/mL) and (G) *FAS*, (H) *DR4*, and (I) *DR5* mRNA expression in senescent fibroblasts. Fibroblasts were isolated from the lungs of normal patients (NL) or patients with stable or rapidly progressing IPF (stable IPF and rapid IPF, respectively). Representative images were taken at 4X magnification. Data are presented as means ± SEM, n = 3-4 per group. **P* ≤ 0.05, ***P* ≤ 0.01, ****P* ≤ 0.001, and *****P* ≤ 0.0001 as indicated by the bars.

Figure 2. Quercetin up regulates FasL receptor expression in senescent human lung fibroblasts. Effect of quercetin on (*A*) *FAS*, (*B*) *DR4*, and (*C*) *DR5* mRNA expression in senescent normal patients (NL) and patients with stable or rapidly progressing IPF (stable IPF and rapid IPF, respectively). (*D*) Heat map of relative expression of inflammatory-, antioxidant-, fibrosis-, and apoptosis-related genes in lung fibroblasts from treated with quercetin (50 μM, 24 hours) or Nintedanib (300 nM). Each gene is represented by a single row of colored bars. Red indicates up regulation of the gene expression and the green color denotes the down regulation of the gene expression compared with vehicle (0.05% DMSO) treated fibroblasts. Data are presented as means ± SEM, n = 3-4 per group. **P* ≤ 0.05, ***P* ≤ 0.01, and ****P* ≤ 0.001 as indicated by the bars.

Figure 3. Quercetin increases the susceptibility to FasL-induced apoptosis in senescent human lung fibroblasts. Caspase-3 activity, cell viability, and lactate dehydrogenase (LDH) release by senescent lung fibroblasts from normal patients (NL) (*A* - *C*) and patients with stable (*D* - *F*) or rapidly progressing IPF (*G* - *I*) (stable IPF and rapid IPF, respectively) following 24 hours treatment with vehicle (0.05%DMSO), quercetin (50 μM), FasL (75 ng/mL), or quercetin + FasL. Caspase-3 activity was expressed as relative fluorescence units (RFU) normalized to β-actin levels, cell viability as OD values at 450 nm, and LDH release as the difference in the absorbance values at 490 and 680 nm. Data are

presented as means ± SEM, n = 3-4 per group. *$P \leq 0.05$, **$P \leq 0.01$, ***$P \leq 0.001$, and ****$P \leq 0.0001$ as indicated by the bars.

Figure 4. Representative phase-contrast images of senescent human lung fibroblasts derived from normal patients (NL) (*A* - *D*) and patients with stable (*E* - *H*) or rapidly progressing (*I* - *L*) IPF (stable IPF and rapid IPF, respectively) treated with: vehicle, quercetin (50 μM), FasL (75 ng/mL), quercetin + FasL for 24 hours. Images were taken at 10x magnification and n = 3 per group.

Figure 5. Quercetin modulates caveolin-1 expression in senescent human lung IPF fibroblasts. (*A*) Basal caveolin-1/β-actin protein expression and effect of quercetin (50 μM, 24 hours) on (*B*) *CAV1* mRNA expression and (*C*) caveolin-1/β-actin protein expression in senescent lung fibroblasts isolated from normal patients (NL) and patients with stable or rapidly progressing IPF (stable IPF and rapid IPF, respectively). Data are presented as means ± SEM, n = 3-4 per group. *$P \leq 0.05$, **$P \leq 0.01$, ***$P \leq 0.001$, and ****$P \leq 0.0001$ as indicated by the bars.

Figure 6. Quercetin modulates AKT activation in senescent human NL and IPF lung fibroblasts. (*A*) Representative western blot of basal p-AKT/AKT protein expression, (*B*) fold change in basal p-AKT/AKT protein expression, and (*C*) effect of quercetin (50 μM, 24 hours) on p-AKT/AKT protein expression in senescent lung fibroblasts isolated from normal patients (NL) and patients with stable or rapidly progressing IPF (stable IPF and rapid IPF, respectively). Data are presented as means ± SEM, n = 3 - 4 per group. ***$P \leq 0.001$, and ****$P \leq 0.0001$ as indicated by the bars.

Figure 7. Schematic illustration of the mechanism by which quercetin renders senescent lung IPF fibroblasts susceptible to apoptosis by Fas ligand (FasL) and TNF-related apoptosis-inducing ligand (TRAIL). (A) Senescent lung fibroblasts derived from patients with IPF (regardless of the pace of disease progression) exhibited a senescent state. Decreased expression of FasL and TRAIL receptors, Fas and death receptor (DR) 4 and DR5, respectively, and caveolin-1 proteins, in addition to increased AKT activation, confer senescent IPF lung fibroblasts with apoptosis resistance to ligands such as FasL and/or TRAIL. The apoptosis-resistant phenotype favors the accumulation of senescent IPF flung fibroblasts and most likely progressive lung fibrosis. (B) Treatment with quercetin produces

notable increases in Fas and caveolin-1 expression and modulates AKT activation in senescent IPF lung fibroblast, thereby restoring susceptibility of senescent fibroblasts to pro-apoptotic FasL and/or TRAIL and favoring the resolution of fibrosis.

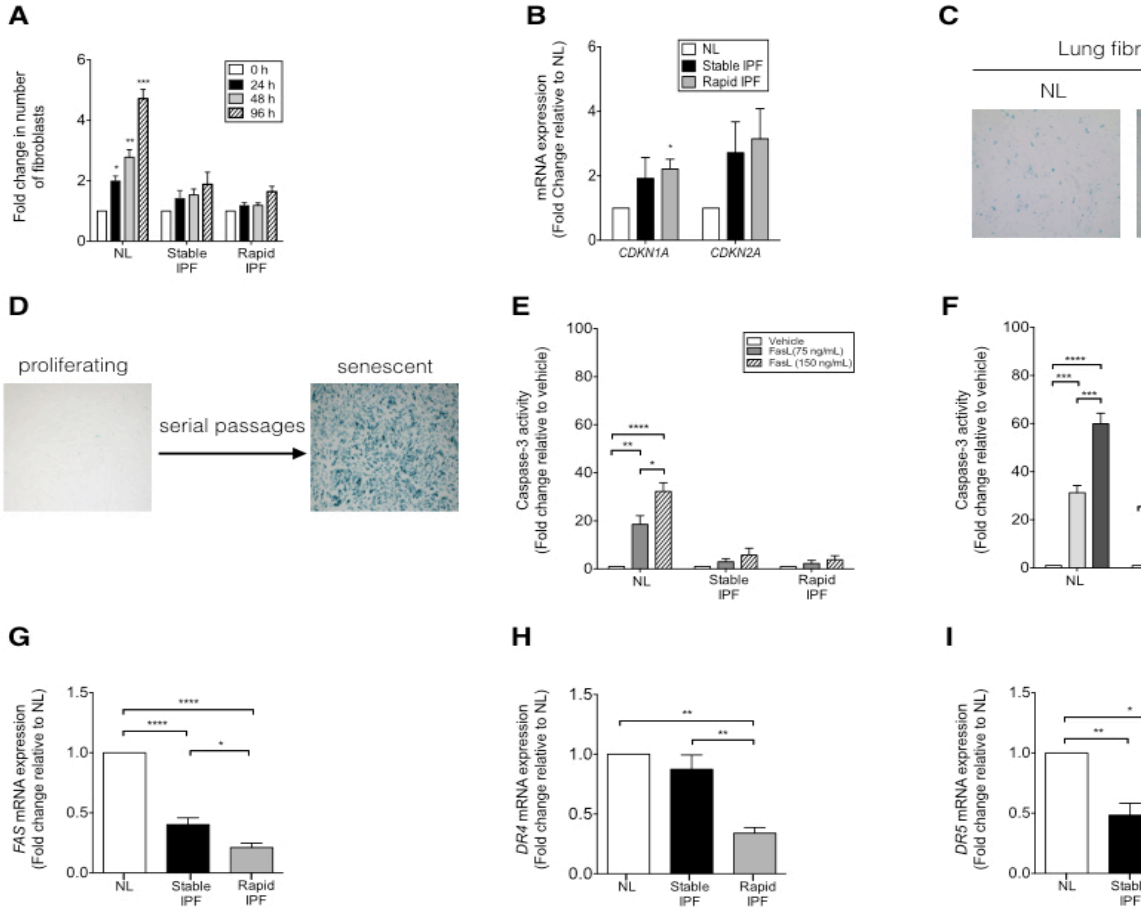
A
Fold change in number of fibroblasts
0 h
24 h
48 h
96 h
NL
Stable IPF
Rapid IPF
B
mRNA expression (Fold Change relative to NL)
NL
Stable IPF
Rapid IPF
CDKN1A
CDKN2A
C
Lung fibr
NL
D
proliferating
serial passages
senescent
E
Caspase-3 activity (Fold change relative to vehicle)
Vehicle
FasL(75 ng/mL)
FasL (150 ng/mL)
NL
Stable IPF
Rapid IPF
F
Caspase-3 activity (Fold change relative to vehicle)
NL
G
FAS mRNA expression (Fold change relative to NL)
NL
Stable IPF
Rapid IPF
H
DR4 mRNA expression (Fold change relative to NL)
NL
Stable IPF
Rapid IPF
I
DR5 mRNA expression (Fold change relative to NL)
NL
Stabl IPF

Figure 1

Figure 2

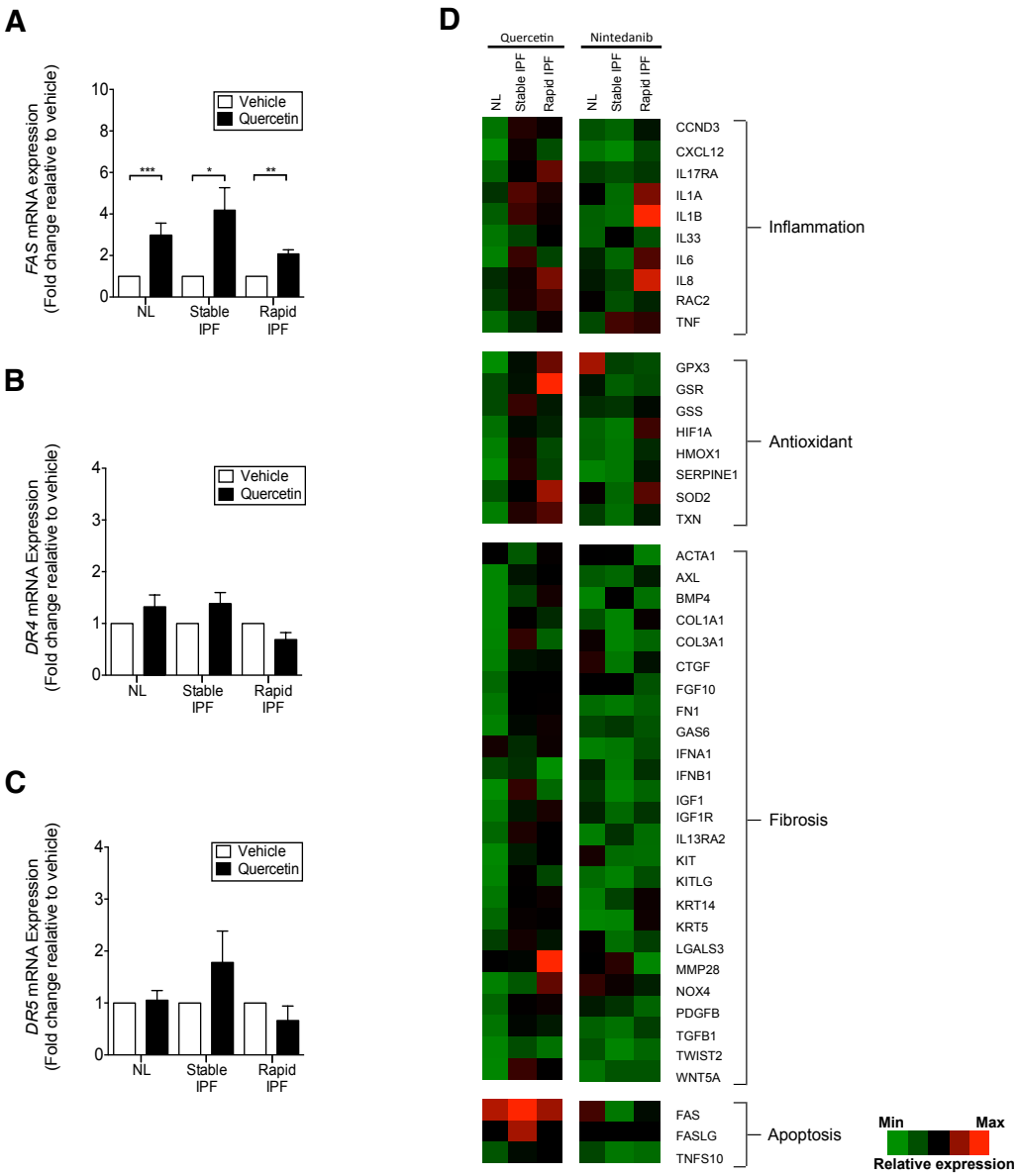
A
FAS mRNA expression
(Fold change realative to vehicle)
Vehicle
Quercetin
***
*
**
NL
Stable IPF
Rapid IPF
B
DR4 mRNA Expression
(Fold change realative to vehicle)
C
DR5 mRNA Expression
(Fold change realative to vehicle)
D
Quercetin
Nintedanib
NL
Stable IPF
Rapid IPF
CCND3
CXCL12
IL17RA
IL1A
IL1B
IL33
IL6
IL8
RAC2
TNF
Inflammation
GPX3
GSR
GSS
HIF1A
HMOX1
SERPINE1
SOD2
TXN
Antioxidant
ACTA1
AXL
BMP4
COL1A1
COL3A1
CTGF
FGF10
FN1
GAS6
IFNA1
IFNB1
IGF1
IGF1R
IL13RA2
KIT
KITLG
KRT14
KRT5
LGALS3
MMP28
NOX4
PDGFB
TGFB1
TWIST2
WNT5A
Fibrosis
FAS
FASLG
TNFS10
Apoptosis
Min
Max
Relative expression

Figure 3

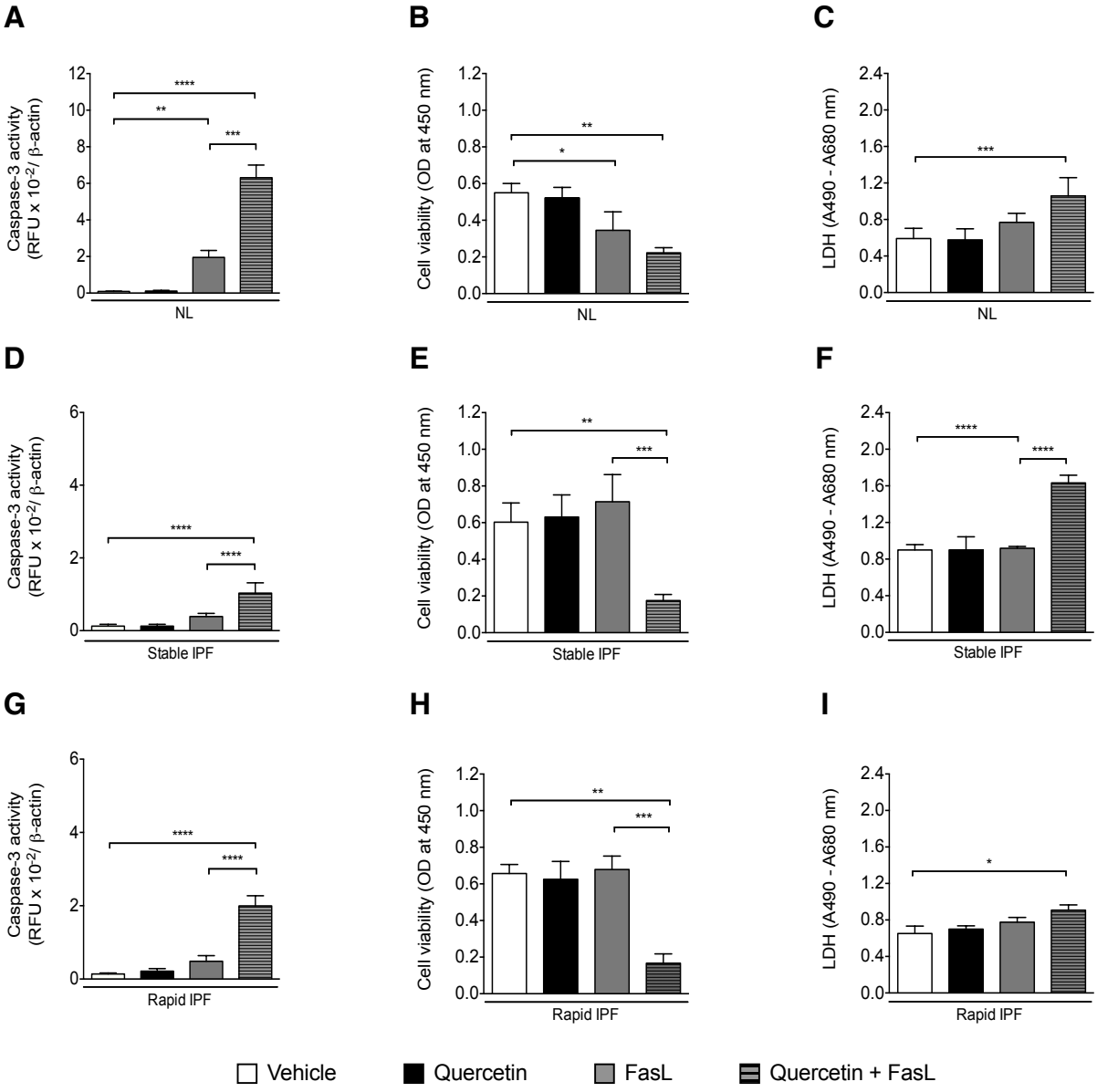
A
B
C
D
E
F
G
H
I
Caspase-3 activity (RFU x 10-2/ β-actin)
Cell viability (OD at 450 nm)
LDH (A490 - A680 nm)
NL
Stable IPF
Rapid IPF
Vehicle
Quercetin
FasL
Quercetin + FasL

Vehicle
Quercetin
Vehicle + FasL
Quercetin + FasL
NL
Stable IPE
Rapid IPE
A
B
C
D
E
F
G
H
I
J
K
L

Figure 4

Figure 5

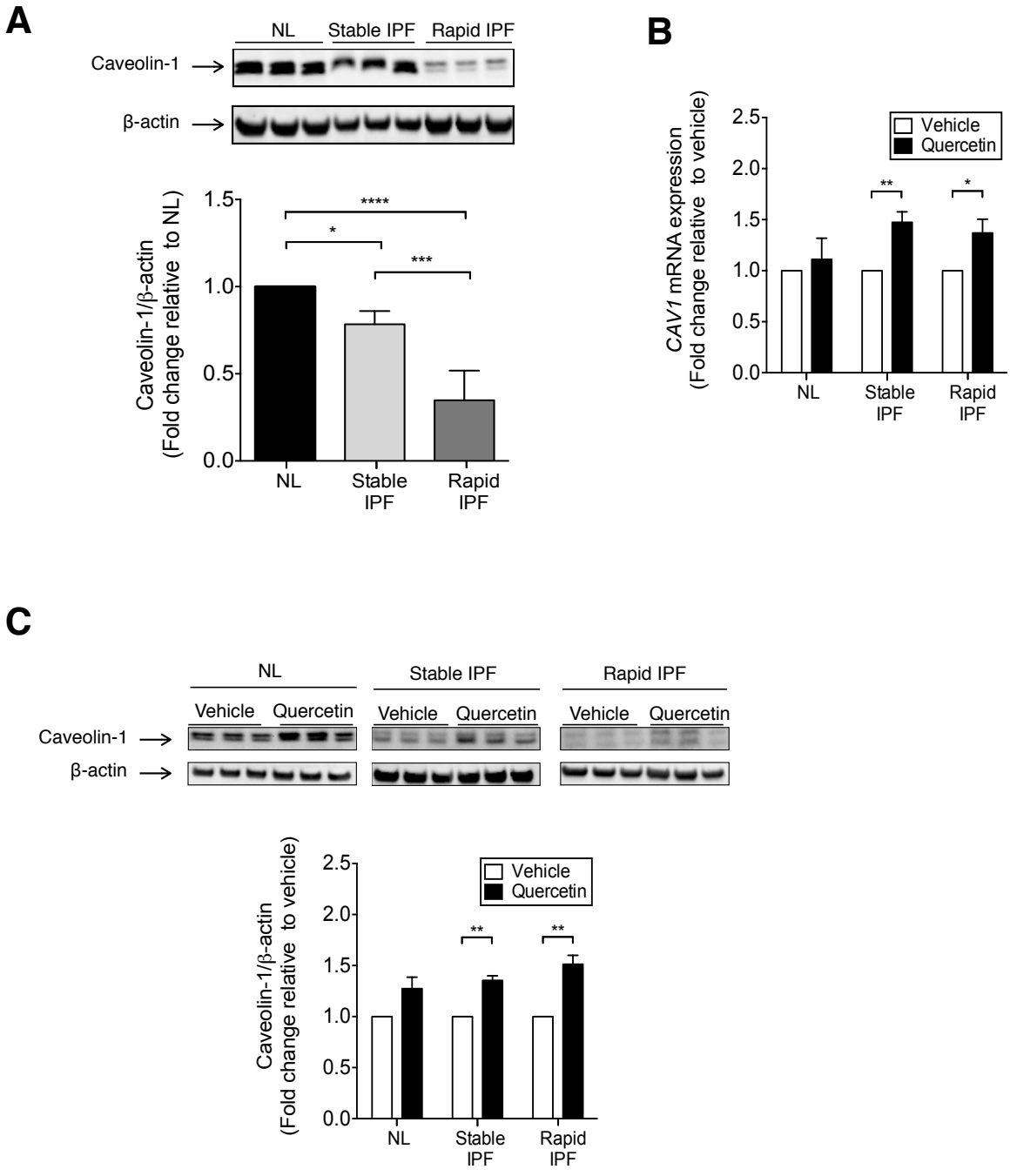
A
NL
Stable IPF
Rapid IPF
Caveolin-1
β-actin
Caveolin-1/β-actin
(Fold change relative to NL)
1.5
1.0
0.5
0.0
****
*
***
NL
Stable IPF
Rapid IPF
B
CAV1 mRNA expression
(Fold change relative to vehicle)
2.5
2.0
1.5
1.0
0.5
0.0
Vehicle
Quercetin
**
*
NL
Stable IPF
Rapid IPF
C
NL
Stable IPF
Rapid IPF
Vehicle
Quercetin
Vehicle
Quercetin
Vehicle
Quercetin
Caveolin-1
β-actin
Caveolin-1/β-actin
(Fold change relative to vehicle)
2.5
2.0
1.5
1.0
0.5
0.0
Vehicle
Quercetin
**
**
NL
Stable IPF
Rapid IPF

Figure 6

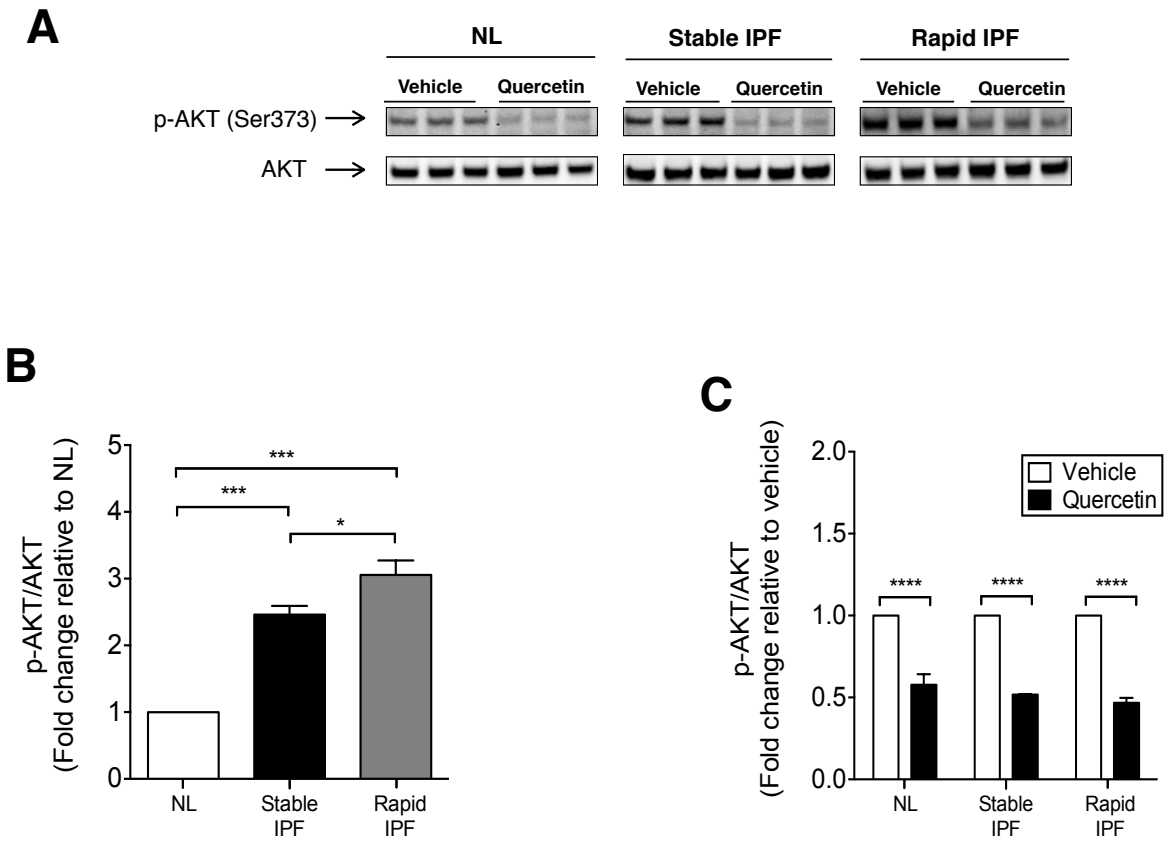
A
NL
Stable IPF
Rapid IPF
Vehicle
Quercetin
Vehicle
Quercetin
Vehicle
Quercetin
p-AKT (Ser373)
AKT
B
p-AKT/AKT
(Fold change relative to NL)
5
4
3
2
1
0
***
***
*
NL
Stable IPF
Rapid IPF
C
p-AKT/AKT
(Fold change relative to vehicle)
2.0
1.5
1.0
0.5
0.0
Vehicle
Quercetin
****
****
****
NL
Stable IPF
Rapid IPF

Figure 7

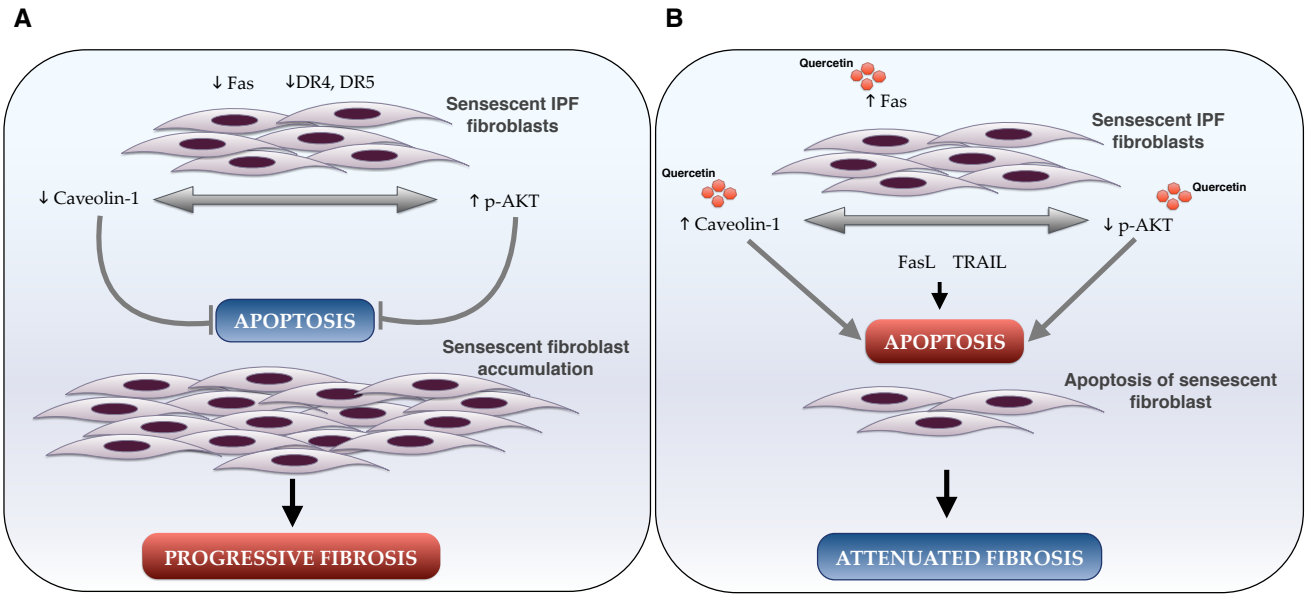
A
↓ Fas
↓DR4, DR5
Sensescent IPF fibroblasts
↓ Caveolin-1
↑ p-AKT
APOPTOSIS
Sensescent fibroblast accumulation
PROGRESSIVE FIBROSIS
B
Quercetin
↑ Fas
Sensescent IPF fibroblasts
Quercetin
Quercetin
↑ Caveolin-1
↓ p-AKT
FasL TRAIL
APOPTOSIS
Apoptosis of sensescent fibroblast
ATTENUATED FIBROSIS

Online Data Supplement

Quercetin Enhances Ligand-induced Apoptosis in Senescent Idiopathic Pulmonary Fibrosis Fibroblasts.

Miriam S. Hohmann, David M. Habiel, Ana L. Coelho, Waldiceu A. Verri, Jr,
Cory M. Hogaboam.

Methods

Isolation of primary pulmonary fibroblast lines

IPF lung fibroblasts were cultured from surgical lung biopsies acquired from clinically classified IPF patients with rapid or stable progressing disease. Normal lung fibroblasts were cultured from lung samples obtained from normal subjects. The lung tissues were finely minced and the dispersed tissue pieces were placed into 150-cm^2 cell culture flasks with complete media. Cells were serially passaged a total of five times to yield pure populations of lung fibroblasts.

Caspase-3 activity

Caspase-3 activity was measured using the Caspase-3 Fluorometric Assay Kit (BioVision). First, the 96-well plates were centrifuged at 400 x *g,* conditioned supernatant was removed from the wells, and the cells were lysed with Cell Lysis Buffer for 30 min on ice. Next, 2x Reaction Buffer containing 10 mM DTT and 50 µM DEVD-AFC substrate were added to lysed samples and incubated at 37°C for 1 h. Samples were read in a fluorometer equipped with a 400 nm excitation filter and 505 nm emission filter and results were expressed as relative fluorescence units (RFU) normalized to β-actin.

Cell viability

For cell viability assay, the supernatant was removed from the wells containing the cultured fibroblasts were washed twice with DPBS. The TetraZ solution provided in the TetraZ Cell Counting Kit (Biolegend) was added to the wells and incubated for 2 h at 37^oC and 10% CO_2. The absorbance at 450 nm was directly proportional to the number of viable cells.

LDH release

The release of LDH by dying cells was assessed in the conditioned supernatant following the manufacturer's instructions (Pierce LDH Cytotoxicity Assay Kit, Life technologies). Briefly, the fibroblast-conditioned supernatant was transferred to a new 96-well plate containing the kit Reaction Mixture. Samples were incubated at room temperature for 30 min and adding Stop Solution stopped reactions. The absorbance at 490 nm and 680 nm was measured using a plate-reading spectrophotometer to determine LDH activity.

Reactive oxygen species (ROS) levels

Lung fibroblasts were treated with quercetin (50 µM) or vehicle (0.05% DMSO) for 24 hours and total intracellular ROS and hydrogen peroxide (H_2O_2) release was determined. Intracellular ROS levels were measured by flow cytometry using the CellROX Green Flow

Cytometry Assay Kit (Life Technologies). Geometric mean fluorescence intensity (GMFI) was acquired using Flowjo (Treestar inc.). H_2O_2 levels were measured using the Amplex Red Hydrogen Peroxide/Peroxidase Assay Kit (ThermoFisher Scientific).

qPCR

TaqMan Primers and probes ID

Genes	**ID**
18S	Hs99999901_s1
ACTA1	Hs00559403_m1
AXL	Hs01064444_m1
BMP4	Hs03676628_s1
CCND3	Hs01017690_g1
CDKN1A	Hs00355782_m1
CDKN2A	Hs00923894_m1
COL1A1	Hs00164004_m1
COL3A1	Hs00943809_m1
CTGF	Hs01026927_g1
CXCL12	Hs03676656_mH
FASLG	Hs00181225_m1
FGF10	Hs00610298_m1
FN1	Hs00365052_m1
GAS6	Hs01090305_m1
GPX3	Hs01078668_m1
GSR	Hs00167317_m1
GSS	Hs01047959_m1
HIF1A	Hs00153153_m1
HMOX1	Hs01110250_m1
IFNA1	Hs00855471_g1
IFNB1	Hs01077958_s1
IGF1	Hs01547656_m1
IGF1R	Hs00609566_m1
IL13RA2	Hs00152924_m1
IL17RA	Hs01064648_m1
IL1A	Hs00174092_m1
IL1B	Hs01555410_m1
IL33	Hs00369211_m1

IL6	Hs00985639_m1
IL8	Hs00174103_m1
KIT	Hs00174029_m1
KITLG	Hs00241497_m1
KRT14	Hs00265033_m1
KRT5	Hs00361185_m1
LGALS3	Hs00173587_m1
MMP28	Hs01020031_m1
NOX4	Hs00418356_m1
PDGFB	Hs00966522_m1
PGF	Hs00182176_m1
RAC2	Hs01036635_s1
SERPINE1	Hs01126606_m1
SOD2	Hs00167309_m1
TGFB1	Hs00998133_m1
TNF	Hs01113624_g1
TNFSF10	Hs00921974_m1
TWIST2	Hs02379973_s1
TXN	Hs01555214_g1
WNT5A	Hs00998537_m1

Primer sequence

Genes	**Sequence**
18S	Forward: 5'-AACCCGTTGAACCCCATT-3' Reverse: 5'-CCATCCAATGCGTAGTAGCG-3'
CAV1	Forward: 5'-CAGGGAAACCTCCTCACAG-3' Reverse: 5'-TGTAGAGATGTCCCTCCGA-3'
DR4	Forward: 5'-CAGAACGTCCTGGAGCCTGTAAC-3' Reverse: 5'-ATGTCCATTGCCTGATTCTTT GTG-3'
DR5	Forward: 5'-GCGAAGAAGATTCTCCTGAGATGTG-3' Reverse: 5'-ACATTGTCCTCAGCCCCAGGTCG -3'
FAS	Forward: 5'-GGTTCTTACGTCTGTTGCT-3' Reverse: 5'-CATGTTCACATCTGGAGGAC-3'
HO1	Forward: 5'-GCCAGGTGCTCAAAAAGATT3'

	Reverse: 5’-CCTGCAACTCCTCAAAAGAGC3’
IL6	Forward: 5'-ATGTAGCCGCACACAGA-3' Reverse: 5'-ATTTGCCGAAGAGCCCCTCAG-3'
IL8	Forward: 5'-AGAGTCATTGAGAGTGGACC-3' Reverse: 5'-ACTTCTCCACAACCCTCTG-3'
NOX4	Forward: 5'-GGAGAGCCAGATGAACAGG-3’ Reverse: 5'-CTCAGTCTTTGACCCTCGG3-’
NRF2	Forward: 5’-GAGAGCCCAGTCTTCATTGC-3’ Reverse: 5’-TTGGCTTCTGGACTTGGAAC-3’

Figure legends

Figure E1. Serial passage leads to replicative senescence in human lung fibroblasts. (*A*) Number of passages necessary for fibroblasts to become senescent, (*B*) representative phase-contrast images of proliferating age and senescent fibroblasts at late passage, (*C*) percent confluence over a period of 96 h, (*D*) *CDKN1A*, *CDKN2A*, *IL6*, and *IL8* mRNA expression in senescent fibroblasts. Images were taken at 10X and 40X magnification. Data are presented as means ± SEM, n = 3 - 4 per group. **P* ≤ 0.05, ***P* ≤ 0.01, and ****P* ≤ 0.001 as indicated by the bars.

Figure E2. Quercetin alone does not induce apoptosis in senescent primary lung fibroblasts. Caspase-3 activity, cell viability, and lactate dehydrogenase (LDH) release by senescent lung fibroblasts from normal patients (NL) and patients with stable (or rapidly progressing IPF (stable IPF and rapid IPF, respectively) following 24 hours treatment with quercetin (50 or 100 μM) or vehicle (0.05%DMSO). Caspase-3 activity was expressed as relative fluorescence units (RFU) normalized to β-actin levels, cell viability as OD values at 450 nm, and LDH release as the difference in the absorbance values at 490 and 680 nm. Data are presented as means ± SEM, n = 3 - 4 per group.

Figure E3. Quercetin increases the susceptibility to TRAIL-induced apoptosis in senescent human lung fibroblasts. Caspase-3 activity, cell viability, and lactate dehydrogenase (LDH) release by senescent fibroblasts from normal lungs (NL) (A-C) and the lungs of patients with stable (D-F) or rapidly progressing (G-I) IPF (stable IPF and rapid IPF, respectively) following 24 hours treatment with vehicle (0.05%DMSO), quercetin (50 μM), TRAIL (100 ng/mL), or quercetin + TRAIL. Caspase-3 activity was expressed as relative fluorescence units (RFU) normalized to β-actin levels, cell viability as OD values at 450 nm, and LDH release as the difference in the absorbance values at 490 and 680 nm. Data are presented as means ± SEM, n = 3-4 per group. **P* ≤ 0.05, ***P* ≤ 0.01, ****P* ≤ 0.001, and *****P* ≤ 0.0001 as indicated by the bars.

Figure E4. Representative phase-contrast images of senescent human lung fibroblasts derived from normal patients (NL) (A – D) and patients with stable (E – H) or rapidly progressing (I – L) IPF (stable IPF and rapid IPF, respectively) treated with: vehicle, quercetin

(50 μM), cross-linked TRAIL (TRAIL) (100 ng/mL), quercetin + TRAIL for 24 hours. Images were taken at 10x magnification and n = 3 per group.

Figure E5. Quercetin's effect is independent of the oxidative status in senescent human lung fibroblasts. Effect of quercetin (50 μM, 24 hours) on (A) total intracellular reactive oxygen species (ROS) levels, (B) hydrogen peroxide levels in the conditioned supernatant, and (C) *NOX4* and (D) *NRF2* mRNA expressional in senescent lung fibroblasts isolated from normal patients (NL) and patients with stable or rapidly progressing IPF (stable IPF and rapid IPF, respectively). Data for ROS levels were expressed as geometric mean fluorescence intensity (GMFI) and hydrogen peroxide levels as relative fluorescence units (RFU). Data are presented as means ± SEM, n = 3-4 per group.

Figure E1

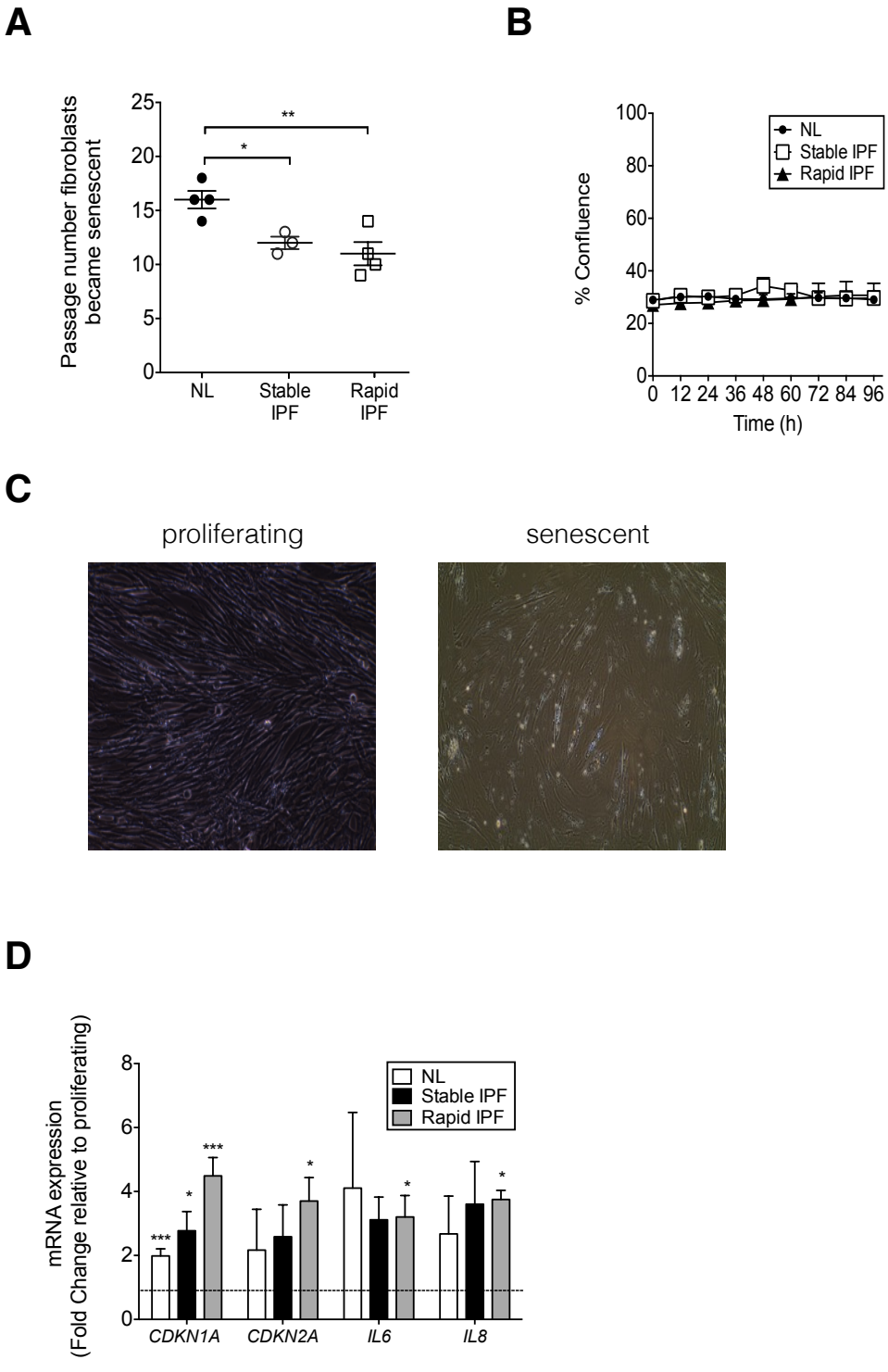
A
B
C
D
Passage number fibroblasts became senescent
25
20
15
10
5
0
**
*
NL
Stable IPF
Rapid IPF
% Confluence
100
80
60
40
20
0
0 12 24 36 48 60 72 84 96
Time (h)
NL
Stable IPF
Rapid IPF
proliferating
senescent
mRNA expression (Fold Change relative to proliferating)
8
6
4
2
0
***
*
***
*
*
*
CDKN1A
CDKN2A
IL6
IL8

Figure E2

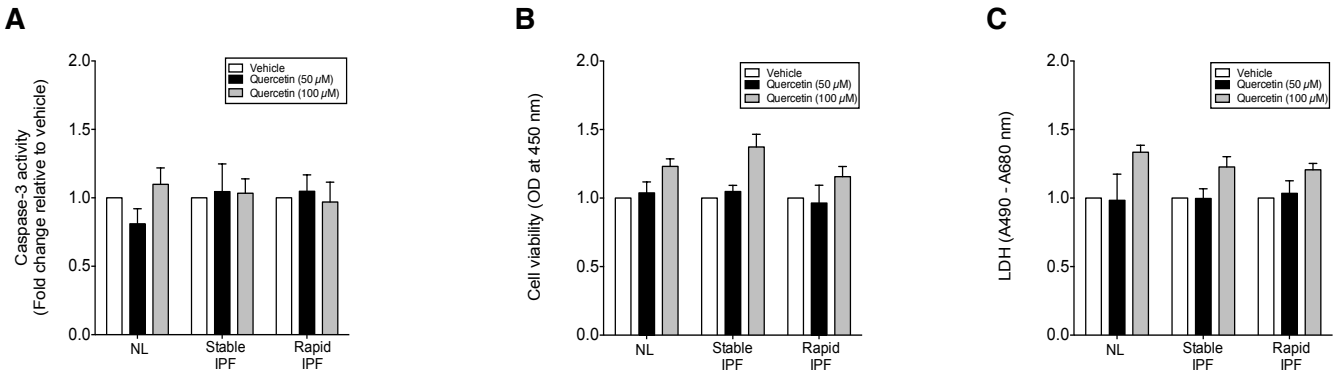
A
Caspase-3 activity
(Fold change relative to vehicle)
Vehicle
Quercetin (50 μM)
Quercetin (100 μM)
2.0
1.5
1.0
0.5
0.0
NL
Stable IPF
Rapid IPF
B
Cell viability (OD at 450 nm)
C
LDH (A490 - A680 nm)

Figure E3

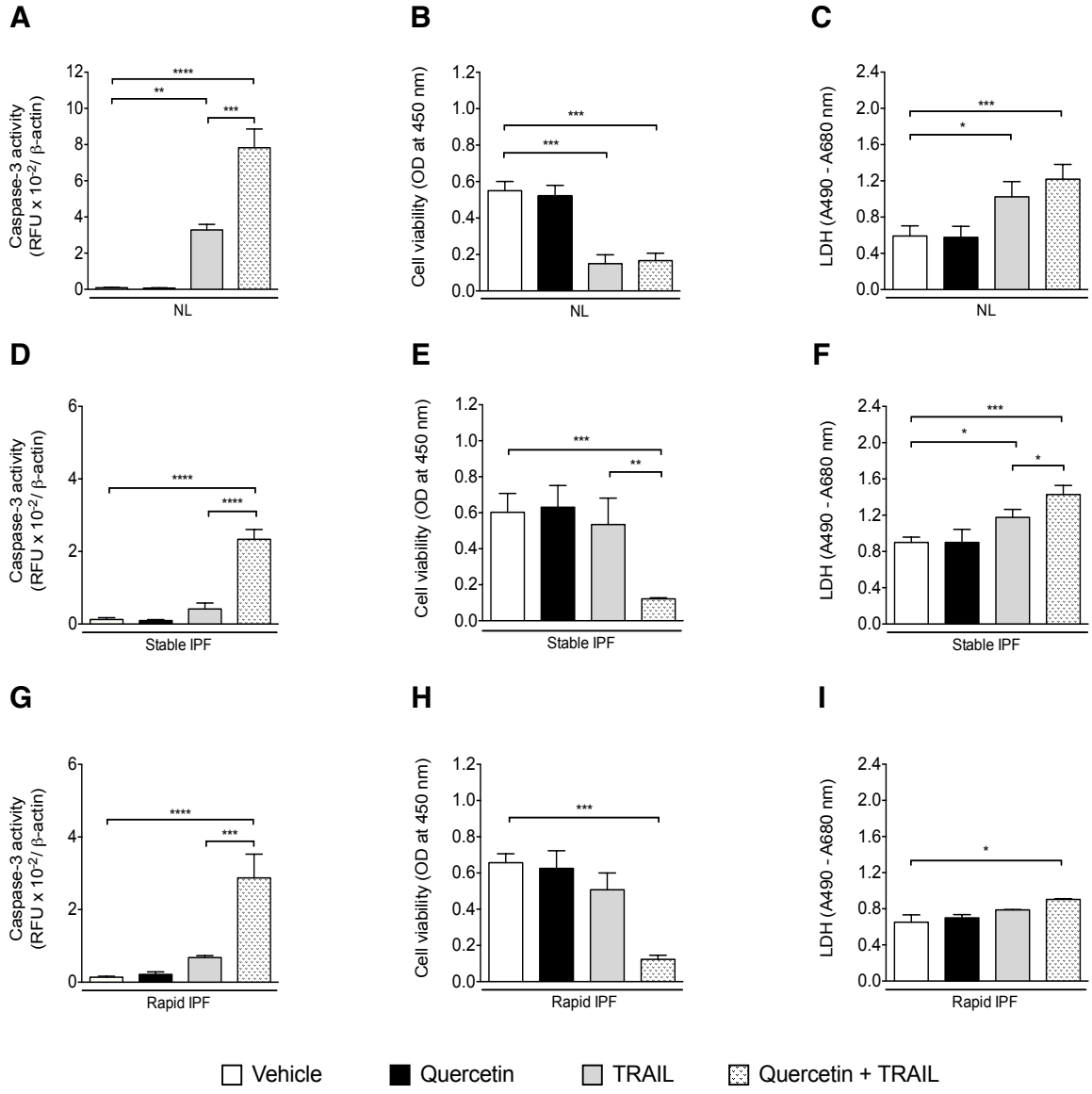
A
B
C
D
E
F
G
H
I
Caspase-3 activity (RFU x 10-2/ β-actin)
Cell viability (OD at 450 nm)
LDH (A490 - A680 nm)
NL
Stable IPF
Rapid IPF
Vehicle
Quercetin
TRAIL
Quercetin + TRAIL

Vehicle
Quercetin
Vehicle + TRAIL
Quercetin + TRAIL
A
B
C
D
E
F
G
H
I
J
K
L
NL
Stable IPF
Rapid IPF

Figure E4

Figure E5

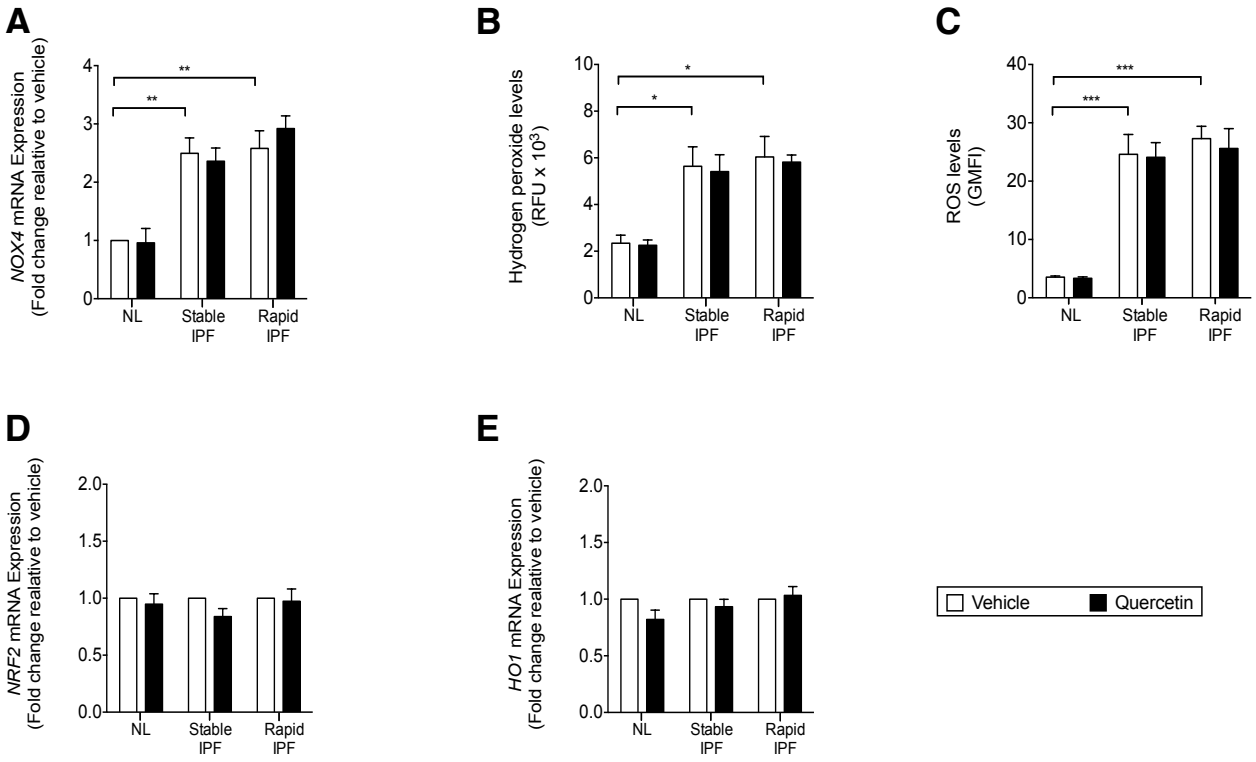
A
NOX4 mRNA Expression
(Fold change realative to vehicle)
B
Hydrogen peroxide levels
(RFU x 10³)
C
ROS levels
(GMFI)
D
NRF2 mRNA Expression
(Fold change realative to vehicle)
E
HO1 mRNA Expression
(Fold change realative to vehicle)
NL
Stable IPF
Rapid IPF
Vehicle
Quercetin

5. CONSIDERAÇÕES FINAIS

Em conjunto os resultados deste trabalho demonstram que o extrato de *H. perforatum* reduz a letalidade e lesão hepática induzidas pelo APAP, bem como inibe o recrutamento de neutrófilos, produção de citocinas e depleção da capacidade antioxidante. Estudos mostram que a inflamação e o estresse oxidativo desempenham papel central na amplificação da lesão hepática iniciada pelo NAPQI. Assim, o efeito protetor do *H. perforatum* parece estar relacionado à inibição destes mecanismos. Considerando que o NAC aumenta a eliminação do NAPQI e o H. perforatum reduz a propagação da lesão hepática induzida por APAP, é possível que o uso concomitante do *H. perforatum* e NAC apresente maiores benefícios no tratamento da hepatotoxicidade por APAP. Portanto, estudos futuros avaliando o efeito do *H. perforatum* e NAC em conjunto podem ser promissores. É importante ressaltar a necessidade de avaliar os efeitos e consequências do uso do *H. Perforatum* por períodos mais longos na prevenção da hepatotoxicidade por APAP. O extrato de *H. Perforatum,* bem como alguns de seus compostos isolados, podem induzir a atividade do CYP2E1, quando utilizados por períodos mais longos (>21 dias) (214, 215). Assim, o uso prolongado do *H. Perforatum* poderia aumentar a toxicidade induzido pelo APAP.

Além disso, os resultados demonstram o efeito protetor da vitexina na nefrotoxicidade induzida pelo diclofenaco. Os mecanismos relacionados a este efeito parecem estar associados à inibição da lesão renal, do estresse oxidativo (i.e. inibição da depleção das defesas antioxidantes, bem como do aumento dos níveis de ânion superóxido e peroxidação lipídica), produção de citocinas inflamatórias, diminuição dos níveis da citocina anti-inflamatória IL-10 e ativação de NF-κB. Considerando que: i) o diclofenaco é um dos AINEs mais utilizados mundialmente, ii) que a utilização desta droga está relacionado a toxicidade e graves reações adversas e iii) que ainda não há terapias específicas para o tratamento da toxicidade e lesão renal induzida pelo diclofenaco, os resultados deste estudo podem beneficiar inúmeros pacientes e contribuir para as abordagens terapêuticas do manejo de quadros de lesão renal induzido pelo diclofenaco, AINES e outros medicamentos.

Por último, os resultados deste estudo demonstram que quercetina restaura a susceptibilidade à apoptose mediada pelo FasL e TRAIL em fibroblastos senescentes de pacientes com FPI. Os mecanismos relacionados a este efeito são a regulação da expressão de caveolina-1 e Fas e modulação da ativação de AKT. A persistência de fibroblastos senescentes no tecido contribui para a fibrose pulmonar progressiva, assim a quercetina mostra-se uma molécula promissora para modular a progressão de fibrose. Nesse sentido, são necessárias futuras investigações avaliando o efeito da quercetina na fibrose pulmonar

em camundongos envelhecidos, um modelo em que as células senescentes resistentes à apoptose participam ativamente na progressão da fibrose pulmonar. Dependendo dos efeitos observados, estas investigações podem servir de base para o desenvolvimento de novas estratégias terapêuticas para o tratamento da FPI e até mesmo outras doenças que têm como fenômeno central a fibrose progressiva.

6. REFERÊNCIAS

1. Medzhitov R. Origin and physiological roles of inflammation. *Nature* 2008; 454: 428-435.
2. Liu Y. Cellular and molecular mechanisms of renal fibrosis. *Nat Rev Nephrol* 2011; 7: 684-696.
3. Nathan C, Ding A. Nonresolving inflammation. *Cell* 2010; 140: 871-882.
4. Kisseleva T, Brenner DA. Fibrogenesis of parenchymal organs. *Proc Am Thorac Soc* 2008; 5: 338-342.
5. Canestaro WJ, Forrester SH, Raghu G, Ho L, Devine BE. Drug Treatment of Idiopathic Pulmonary Fibrosis: Systematic Review and Network Meta-Analysis. *Chest* 2016; 149: 756-766.
6. Smilkstein MJ, Knapp GL, Kulig KW, Rumack BH. Efficacy of oral N-acetylcysteine in the treatment of acetaminophen overdose. Analysis of the national multicenter study (1976 to 1985). *N Engl J Med* 1988; 319: 1557-1562.
7. Nagai J, Uesawa Y, Shimamura R, Kagaya H. Characterization of the Adverse Effects Induced by Acetaminophen and Non-steroidal Anti-Inflammatory Drugs based on the Analysis of the Japanese Adverse Drug Event Report Database. *Clin J Pain* 2016.
8. Clark R, Fisher JE, Sketris IS, Johnston GM. Population prevalence of high dose paracetamol in dispensed paracetamol/opioid prescription combinations: an observational study. *BMC Clin Pharmacol* 2012; 12: 11.
9. Katzung BG. Farmacologia: Básica & Clínica. Rio de Janeiro: Guanabara Koogan; 2005.
10. Larson AM, Polson J, Fontana RJ, Davern TJ, Lalani E, Hynan LS, Reisch JS, Schiodt FV, Ostapowicz G, Shakil AO, Lee WM, Acute Liver Failure Study G. Acetaminophen-induced acute liver failure: results of a United States multicenter, prospective study. *Hepatology* 2005; 42: 1364-1372.
11. Prescott LF. Hepatotoxicity of mild analgesics. *Br J Clin Pharmacol* 1980; 10 Suppl 2: 373S-379S.
12. Mitchell JR, Jollow DJ, Potter WZ, Davis DC, Gillette JR, Brodie BB. Acetaminophen-induced hepatic necrosis. I. Role of drug metabolism. *J Pharmacol Exp Ther* 1973; 187: 185-194.
13. Lee WM. Acute liver failure. *Semin Respir Crit Care Med* 2012; 33: 36-45.
14. Andrade Filho DAC, Campolina D, Dias MB. Toxicologia na prática clínica. Belo Horizonte: Folium 2013.
15. Schuh DC. Intoxicações e exposições por paracetamol: Análise de seis anos de registros do Centro de Informações Toxicológicas de Santa Catarina – CIT/SC. 2007. . Florianópolis, SC: Universidade Federal de Santa Catarina; 2007.
16. Nesi RS. Estudo clínico-epidemiológico das intoxicações por paracetamol regsitradas no Centro de Informações Toxicológicas de Santa Catarina no Período de Janeiro de 2003 a dezembro de 2010. Florianópolis, SC: Universidade Federal de Santa Catarina; 2012.
17. Patten CJ, Thomas PE, Guy RL, Lee M, Gonzalez FJ, Guengerich FP, Yang CS. Cytochrome P450 enzymes involved in acetaminophen activation by rat and human liver microsomes and their kinetics. *Chem Res Toxicol* 1993; 6: 511-518.
18. Mitchell JR, Jollow DJ, Potter WZ, Gillette JR, Brodie BB. Acetaminophen-induced hepatic necrosis. IV. Protective role of glutathione. *J Pharmacol Exp Ther* 1973; 187: 211-217.

19. Jollow DJ, Mitchell JR, Potter WZ, Davis DC, Gillette JR, Brodie BB. Acetaminophen-induced hepatic necrosis. II. Role of covalent binding in vivo. *J Pharmacol Exp Ther* 1973; 187: 195-202.
20. Jaeschke H, Williams CD, Ramachandran A, Bajt ML. Acetaminophen hepatotoxicity and repair: the role of sterile inflammation and innate immunity. *Liver Int* 2012; 32: 8-20.
21. Qiu Y, Benet LZ, Burlingame AL. Identification of hepatic protein targets of the reactive metabolites of the non-hepatotoxic regioisomer of acetaminophen, 3'-hydroxyacetanilide, in the mouse in vivo using two-dimensional gel electrophoresis and mass spectrometry. *Adv Exp Med Biol* 2001; 500: 663-673.
22. Cover C, Mansouri A, Knight TR, Bajt ML, Lemasters JJ, Pessayre D, Jaeschke H. Peroxynitrite-induced mitochondrial and endonuclease-mediated nuclear DNA damage in acetaminophen hepatotoxicity. *J Pharmacol Exp Ther* 2005; 315: 879-887.
23. Knight TR, Kurtz A, Bajt ML, Hinson JA, Jaeschke H. Vascular and hepatocellular peroxynitrite formation during acetaminophen toxicity: role of mitochondrial oxidant stress. *Toxicol Sci* 2001; 62: 212-220.
24. Han D, Dara L, Win S, Than TA, Yuan L, Abbasi SQ, Liu ZX, Kaplowitz N. Regulation of drug-induced liver injury by signal transduction pathways: critical role of mitochondria. *Trends Pharmacol Sci* 2013; 34: 243-253.
25. Saito C, Lemasters JJ, Jaeschke H. c-Jun N-terminal kinase modulates oxidant stress and peroxynitrite formation independent of inducible nitric oxide synthase in acetaminophen hepatotoxicity. *Toxicol Appl Pharmacol* 2010; 246: 8-17.
26. Kon K, Kim JS, Jaeschke H, Lemasters JJ. Mitochondrial permeability transition in acetaminophen-induced necrosis and apoptosis of cultured mouse hepatocytes. *Hepatology* 2004; 40: 1170-1179.
27. Bajt ML, Farhood A, Lemasters JJ, Jaeschke H. Mitochondrial bax translocation accelerates DNA fragmentation and cell necrosis in a murine model of acetaminophen hepatotoxicity. *J Pharmacol Exp Ther* 2008; 324: 8-14.
28. Bajt ML, Cover C, Lemasters JJ, Jaeschke H. Nuclear translocation of endonuclease G and apoptosis-inducing factor during acetaminophen-induced liver cell injury. *Toxicol Sci* 2006; 94: 217-225.
29. Martin-Murphy BV, Holt MP, Ju C. The role of damage associated molecular pattern molecules in acetaminophen-induced liver injury in mice. *Toxicol Lett* 2010; 192: 387-394.
30. Gujral JS, Knight TR, Farhood A, Bajt ML, Jaeschke H. Mode of cell death after acetaminophen overdose in mice: apoptosis or oncotic necrosis? *Toxicol Sci* 2002; 67: 322-328.
31. Blazka ME, Wilmer JL, Holladay SD, Wilson RE, Luster MI. Role of proinflammatory cytokines in acetaminophen hepatotoxicity. *Toxicol Appl Pharmacol* 1995; 133: 43-52.
32. Michael SL, Pumford NR, Mayeux PR, Niesman MR, Hinson JA. Pretreatment of mice with macrophage inactivators decreases acetaminophen hepatotoxicity and the formation of reactive oxygen and nitrogen species. *Hepatology* 1999; 30: 186-195.
33. Blazka ME, Elwell MR, Holladay SD, Wilson RE, Luster MI. Histopathology of acetaminophen-induced liver changes: role of interleukin 1 alpha and tumor necrosis factor alpha. *Toxicol Pathol* 1996; 24: 181-189.

34. Knight TR, Ho YS, Farhood A, Jaeschke H. Peroxynitrite is a critical mediator of acetaminophen hepatotoxicity in murine livers: protection by glutathione. *J Pharmacol Exp Ther* 2002; 303: 468-475.
35. Lawson JA, Farhood A, Hopper RD, Bajt ML, Jaeschke H. The hepatic inflammatory response after acetaminophen overdose: role of neutrophils. *Toxicol Sci* 2000; 54: 509-516.
36. Jaeschke H, Hasegawa T. Role of neutrophils in acute inflammatory liver injury. *Liver Int* 2006; 26: 912-919.
37. Liu ZX, Han D, Gunawan B, Kaplowitz N. Neutrophil depletion protects against murine acetaminophen hepatotoxicity. *Hepatology* 2006; 43: 1220-1230.
38. Jaeschke H, Smith CW. Mechanisms of neutrophil-induced parenchymal cell injury. *J Leukoc Biol* 1997; 61: 647-653.
39. Hasegawa T, Malle E, Farhood A, Jaeschke H. Generation of hypochlorite-modified proteins by neutrophils during ischemia-reperfusion injury in rat liver: attenuation by ischemic preconditioning. *Am J Physiol Gastrointest Liver Physiol* 2005; 289: G760-767.
40. Jaeschke H, Ho YS, Fisher MA, Lawson JA, Farhood A. Glutathione peroxidase-deficient mice are more susceptible to neutrophil-mediated hepatic parenchymal cell injury during endotoxemia: importance of an intracellular oxidant stress. *Hepatology* 1999; 29: 443-450.
41. Cover C, Liu J, Farhood A, Malle E, Waalkes MP, Bajt ML, Jaeschke H. Pathophysiological role of the acute inflammatory response during acetaminophen hepatotoxicity. *Toxicol Appl Pharmacol* 2006; 216: 98-107.
42. Bilzer M, Roggel F, Gerbes AL. Role of Kupffer cells in host defense and liver disease. *Liver Int* 2006; 26: 1175-1186.
43. Roberts RA, Ganey PE, Ju C, Kamendulis LM, Rusyn I, Klaunig JE. Role of the Kupffer cell in mediating hepatic toxicity and carcinogenesis. *Toxicol Sci* 2007; 96: 2-15.
44. Larrick JW, Wright SC. Cytotoxic mechanism of tumor necrosis factor-alpha. *FASEB J* 1990; 4: 3215-3223.
45. Ishida Y, Kondo T, Ohshima T, Fujiwara H, Iwakura Y, Mukaida N. A pivotal involvement of IFN-gamma in the pathogenesis of acetaminophen-induced acute liver injury. *FASEB J* 2002; 16: 1227-1236.
46. Du K, Ramachandran A, Jaeschke H. Oxidative stress during acetaminophen hepatotoxicity: Sources, pathophysiological role and therapeutic potential. *Redox Biol* 2016; 10: 148-156.
47. Jaeschke H, Knight TR, Bajt ML. The role of oxidant stress and reactive nitrogen species in acetaminophen hepatotoxicity. *Toxicol Lett* 2003; 144: 279-288.
48. Reid AB, Kurten RC, McCullough SS, Brock RW, Hinson JA. Mechanisms of acetaminophen-induced hepatotoxicity: role of oxidative stress and mitochondrial permeability transition in freshly isolated mouse hepatocytes. *J Pharmacol Exp Ther* 2005; 312: 509-516.
49. Alric L, Orfila C, Carrere N, Beraud M, Carrera G, Lepert JC, Duffaut M, Pipy B, Vinel JP. Reactive oxygen intermediates and eicosanoid production by kupffer cells and infiltrated macrophages in acute and chronic liver injury induced in rats by CCl4. *Inflamm Res* 2000; 49: 700-707.
50. Grattagliano I, Bonfrate L, Diogo CV, Wang HH, Wang DQ, Portincasa P. Biochemical mechanisms in drug-induced liver injury: certainties and doubts. *World J Gastroenterol* 2009; 15: 4865-4876.

51. James LP, Mayeux PR, Hinson JA. Acetaminophen-induced hepatotoxicity. *Drug Metab Dispos* 2003; 31: 1499-1506.
52. Radi R, Beckman JS, Bush KM, Freeman BA. Peroxynitrite oxidation of sulfhydryls. The cytotoxic potential of superoxide and nitric oxide. *J Biol Chem* 1991; 266: 4244-4250.
53. Ahmad ST, Arjumand W, Nafees S, Seth A, Ali N, Rashid S, Sultana S. Hesperidin alleviates acetaminophen induced toxicity in Wistar rats by abrogation of oxidative stress, apoptosis and inflammation. *Toxicol Lett* 2012; 208: 149-161.
54. Huber PC, Almeida WP, Fátima A. Glutathione and related enzymes: biological roles and importance in pathological processes. *Química Nova* 2008; 31.
55. Haddad JJ. Antioxidant and prooxidant mechanisms in the regulation of redox(y)-sensitive transcription factors. *Cell Signal* 2002; 14: 879-897.
56. Sarada S, Himadri P, Mishra C, Geetali P, Ram MS, Ilavazhagan G. Role of oxidative stress and NFkB in hypoxia-induced pulmonary edema. *Exp Biol Med (Maywood)* 2008; 233: 1088-1098.
57. Valerio DA, Georgetti SR, Magro DA, Casagrande R, Cunha TM, Vicentini FT, Vieira SM, Fonseca MJ, Ferreira SH, Cunha FQ, Verri WA, Jr. Quercetin reduces inflammatory pain: inhibition of oxidative stress and cytokine production. *J Nat Prod* 2009; 72: 1975-1979.
58. Larson AM. Acetaminophen hepatotoxicity. *Clin Liver Dis* 2007; 11: 525-548, vi.
59. Russo E, Scicchitano F, Whalley BJ, Mazzitello C, Ciriaco M, Esposito S, Patane M, Upton R, Pugliese M, Chimirri S, Mammi M, Palleria C, De Sarro G. Hypericum perforatum: pharmacokinetic, mechanism of action, tolerability, and clinical drug-drug interactions. *Phytother Res* 2014; 28: 643-655.
60. Nahrstedt A, Butterweck V. Biologically active and other chemical constituents of the herb of Hypericum perforatum L. *Pharmacopsychiatry* 1997; 30 Suppl 2: 129-134.
61. Karioti A, Bilia AR. Hypericins as potential leads for new therapeutics. *Int J Mol Sci* 2010; 11: 562-594.
62. Cellarova E, Daxnerova Z, Kimakova K, Haluskova J. The variability of the hypericin content in the regenerants of Hypericum perforatum
. *Acta Biotechnologica* 1994; 14: 267–274.
63. Panossian AG, Gabrielian E, Manvelian V, Jurcic K, Wagner H. Immunosuppressive effects of hypericin on stimulated human leukocytes: inhibition of the arachidonic acid release, leukotriene B(4) and Interleukin-Ialpha production, and activation of nitric oxide formation. *Phytomedicine* 1996; 3: 19-28.
64. Hammer KD, Hillwig ML, Solco AK, Dixon PM, Delate K, Murphy PA, Wurtele ES, Birt DF. Inhibition of prostaglandin E(2) production by anti-inflammatory hypericum perforatum extracts and constituents in RAW264.7 Mouse Macrophage Cells. *J Agric Food Chem* 2007; 55: 7323-7331.
65. Feisst C, Pergola C, Rakonjac M, Rossi A, Koeberle A, Dodt G, Hoffmann M, Hoernig C, Fischer L, Steinhilber D, Franke L, Schneider G, Radmark O, Sautebin L, Werz O. Hyperforin is a novel type of 5-lipoxygenase inhibitor with high efficacy in vivo. *Cellular and molecular life sciences : CMLS* 2009; 66: 2759-2771.
66. Sosa S, Pace R, Bornancin A, Morazzoni P, Riva A, Tubaro A, Della Loggia R. Topical anti-inflammatory activity of extracts and compounds from Hypericum perforatum L. *J Pharm Pharmacol* 2007; 59: 703-709.
67. Kurth H, Spreemann R. Phytochemical characterization of various St. John's Wort extracts. *Adv Ther* 1998; 15: 117-128.

68. Hansen SH, Jensen AG, Cornett C, Bjørnsdottir I, Wright B, Wilson ID. High-Performance Liquid Chromatography On-Line Coupled to High-Field NMR and Mass Spectrometry for Structure Elucidation of Constituents of Hypericum perforatum L. *Analytical Chemistry, 1999, 71 (22), pp 5235–5241* 1999; 71: 5235-5241.
69. Boadi WY, Amartey PK, Lo A. Effect of quercetin, genistein and kaempferol on glutathione and glutathione-redox cycle enzymes in 3T3-L1 preadipocytes. *Drug Chem Toxicol* 2016; 39: 239-247.
70. Suchal K, Malik S, Gamad N, Malhotra RK, Goyal SN, Chaudhary U, Bhatia J, Ojha S, Arya DS. Kaempferol Attenuates Myocardial Ischemic Injury via Inhibition of MAPK Signaling Pathway in Experimental Model of Myocardial Ischemia-Reperfusion Injury. *Oxid Med Cell Longev* 2016; 2016: 7580731.
71. Guo YF, Xu NN, Sun W, Zhao Y, Li CY, Guo MY. Luteolin reduces inflammation in Staphylococcus aureus-induced mastitis by inhibiting NF-kB activation and MMPs expression. *Oncotarget* 2017.
72. Chen S, Fan B. Myricetin protects cardiomyocytes from LPS-induced injury. *Herz* 2017.
73. Piao MJ, Kang KA, Zhang R, Ko DO, Wang ZH, You HJ, Kim HS, Kim JS, Kang SS, Hyun JW. Hyperoside prevents oxidative damage induced by hydrogen peroxide in lung fibroblast cells via an antioxidant effect. *Biochim Biophys Acta* 2008; 1780: 1448-1457.
74. Kim SJ, Um JY, Lee JY. Anti-inflammatory activity of hyperoside through the suppression of nuclear factor-kappaB activation in mouse peritoneal macrophages. *Am J Chin Med* 2011; 39: 171-181.
75. Chen WY, Huang YC, Yang ML, Lee CY, Chen CJ, Yeh CH, Pan PH, Horng CT, Kuo WH, Kuan YH. Protective effect of rutin on LPS-induced acute lung injury via down-regulation of MIP-2 expression and MMP-9 activation through inhibition of Akt phosphorylation. *Int Immunopharmacol* 2014; 22: 409-413.
76. Nikfarjam BA, Adineh M, Hajiali F, Nassiri-Asl M. Treatment with Rutin - A Therapeutic Strategy for Neutrophil-Mediated Inflammatory and Autoimmune Diseases: - Anti-inflammatory Effects of Rutin on Neutrophils. *J Pharmacopuncture* 2017; 20: 52-56.
77. Sanchez de Medina F, Vera B, Galvez J, Zarzuelo A. Effect of quercitrin on the early stages of hapten induced colonic inflammation in the rat. *Life Sci* 2002; 70: 3097-3108.
78. Sanchez de Medina F, Galvez J, Romero JA, Zarzuelo A. Effect of quercitrin on acute and chronic experimental colitis in the rat. *J Pharmacol Exp Ther* 1996; 278: 771-779.
79. Xie W, Wang M, Chen C, Zhang X, Melzig MF. Hepatoprotective effect of isoquercitrin against acetaminophen-induced liver injury. *Life Sci* 2016; 152: 180-189.
80. Berghofer R, Holzl J. solation of I3',II 8-biapigenin (amentoflavone) from Hypericum perforatum *Planta Medica* 1989; 55.
81. Berghofer R, Holzl J. Biflavonoids in Hypericum perforatum1; Part 1. Isolation of I3, II8-Biapigenin. *Planta Med* 1987; 53: 216-217.
82. Melzer R, Fricke U, Holzl J. Vasoactive properties of procyanidins from Hypericum perforatum L. in isolated porcine coronary arteries. *Arzneimittelforschung* 1991; 41: 481-483.

83. Terra X, Palozza P, Fernandez-Larrea J, Ardevol A, Blade C, Pujadas G, Salvado J, Arola L, Blay MT. Procyanidin dimer B1 and trimer C1 impair inflammatory response signalling in human monocytes. *Free Radic Res* 2011; 45: 611-619.
84. Saddiqe Z, Naeem I, Maimoona A. A review of the antibacterial activity of Hypericum perforatum L. *J Ethnopharmacol* 2010; 131: 511-521.
85. Paterniti I, Briguglio E, Mazzon E, Galuppo M, Oteri G, Cordasco G, Cuzzocrea S. Effects of Hypericum Perforatum, in a rodent model of periodontitis. *BMC Complement Altern Med* 2010; 10: 73.
86. Spelman K, Aldag R, Hamman A, Kwasnik EM, Mahendra MA, Obasi TM, Morse J, Williams EJ. Traditional herbal remedies that influence cell adhesion molecule activity. *Phytother Res* 2011; 25: 473-483.
87. Herold A, Cremer L, Calugaru A, Tamas V, Ionescu F, Manea S, Szegli G. Hydroalcoholic plant extracts with anti-inflammatory activity. *Roum Arch Microbiol Immunol* 2003; 62: 117-129.
88. Hohmann MS, Cardoso RD, Pinho-Ribeiro FA, Crespigio J, Cunha TM, Alves-Filho JC, da Silva RV, Pinge-Filho P, Ferreira SH, Cunha FQ, Casagrande R, Verri WA, Jr. 5-lipoxygenase deficiency reduces acetaminophen-induced hepatotoxicity and lethality. *Biomed Res Int* 2013; 2013: 627046.
89. De Paola R, Muia C, Mazzon E, Genovese T, Crisafulli C, Menegazzi M, Caputi AP, Suzuki H, Cuzzocrea S. Effects of Hypericum perforatum extract in a rat model of ischemia and reperfusion injury. *Shock* 2005; 24: 255-263.
90. Sloley BD, Urichuk LJ, Ling L, Gu LD, Coutts RT, Pang PK, Shan JJ. Chemical and pharmacological evaluation of Hypericum perforatum extracts. *Acta Pharmacol Sin* 2000; 21: 1145-1152.
91. Romeo C, Antonuccio P, Esposito M, Marini H, Impellizzeri P, Turiaco N, Altavilla D, Bitto A, Zuccarello B, Squadrito F. Raxofelast, a hydrophilic vitamin E-like antioxidant, reduces testicular ischemia-reperfusion injury. *Urol Res* 2004; 32: 367-371.
92. Cuzzocrea S, Costantino G, Mazzon E, Micali A, De Sarro A, Caputi AP. Beneficial effects of melatonin in a rat model of splanchnic artery occlusion and reperfusion. *J Pineal Res* 2000; 28: 52-63.
93. Hunt EJ, Lester CE, Lester EA, Tackett RL. Effect of St. John's wort on free radical production. *Life Sci* 2001; 69: 181-190.
94. Saija A, Scalese M, Lanza M, Marzullo D, Bonina F, Castelli F. Flavonoids as antioxidant agents: importance of their interaction with biomembranes. *Free Radic Biol Med* 1995; 19: 481-486.
95. Verri WA, Jr , Vicentini FTMC, Baracat MM, DGeorgetti SR, Cardosos RD, Cunha TM, Ferreira SH, Cunha FQ, Fonseca MJ, Casagrande R. Flavonoids as Anti-Inflammatory and Analgesic Drugs: Mechanisms of Action and Perspectives in the Development of Pharmaceutical Forms. In: Atta-ur-Rahman, editor. Studies in Natural Products Chemistry, 1st ed: Elsevier; 2012.
96. Di Paola R, Mazzon E, Muia C, Crisafulli C, Genovese T, Di Bella P, Esposito E, Menegazzi M, Meli R, Suzuki H, Cuzzocrea S. Protective effect of Hypericum perforatum in zymosan-induced multiple organ dysfunction syndrome: relationship to its inhibitory effect on nitric oxide production and its peroxynitrite scavenging activity. *Nitric Oxide* 2007; 16: 118-130.
97. Curhan GC, Bullock AJ, Hankinson SE, Willett WC, Speizer FE, Stampfer MJ. Frequency of use of acetaminophen, nonsteroidal anti-inflammatory drugs, and aspirin in US women. *Pharmacoepidemiol Drug Saf* 2002; 11: 687-693.

98. Peterson K, McDonagh M, Thakurta S, Dana T, Roberts C, Chou R, Helfand M. Drug Class Review: Nonsteroidal Antiinflammatory Drugs (NSAIDs): Final Update 4 Report. Portland (OR); 2010.
99. Vane JR, Bakhle YS, Botting RM. Cyclooxygenases 1 and 2. *Annu Rev Pharmacol Toxicol* 1998; 38: 97-120.
100. Kirkby NS, Chan MV, Zaiss AK, Garcia-Vaz E, Jiao J, Berglund LM, Verdu EF, Ahmetaj-Shala B, Wallace JL, Herschman HR, Gomez MF, Mitchell JA. Systematic study of constitutive cyclooxygenase-2 expression: Role of NF-kappaB and NFAT transcriptional pathways. *Proc Natl Acad Sci U S A* 2016; 113: 434-439.
101. Fry AC, Farrington K. Management of acute renal failure. *Postgrad Med J* 2006; 82: 106-116.
102. Derry S, Wiffen PJ, Moore RA. Single dose oral diclofenac for acute postoperative pain in adults. *Cochrane Database Syst Rev* 2015: CD004768.
103. Brogden RN, Heel RC, Pakes GE, Speight TM, Avery GS. Diclofenac sodium: a review of its pharmacological properties and therapeutic use in rheumatic diseases and pain of varying origin. *Drugs* 1980; 20: 24-48.
104. Todd PA, Sorkin EM. Diclofenac sodium. A reappraisal of its pharmacodynamic and pharmacokinetic properties, and therapeutic efficacy. *Drugs* 1988; 35: 244-285.
105. Boelsterli UA. Diclofenac-induced liver injury: a paradigm of idiosyncratic drug toxicity. *Toxicol Appl Pharmacol* 2003; 192: 307-322.
106. Harirforoosh S, Asghar W, Jamali F. Adverse effects of nonsteroidal antiinflammatory drugs: an update of gastrointestinal, cardiovascular and renal complications. *J Pharm Pharm Sci* 2013; 16: 821-847.
107. Ng LE, Vincent AS, Halliwell B, Wong KP. Action of diclofenac on kidney mitochondria and cells. *Biochem Biophys Res Commun* 2006; 348: 494-500.
108. Hickey EJ, Raje RR, Reid VE, Gross SM, Ray SD. Diclofenac induced in vivo nephrotoxicity may involve oxidative stress-mediated massive genomic DNA fragmentation and apoptotic cell death. *Free Radic Biol Med* 2001; 31: 139-152.
109. Ting A, Freund J. Nonsteroidal antiinflammatory-induced acute renal failure detected on bone scintigraphy. *Clin Nucl Med* 2004; 29: 318-319.
110. Kulling PE, Backman EA, Skagius AS, Beckman EA. Renal impairment after acute diclofenac, naproxen, and sulindac overdoses. *J Toxicol Clin Toxicol* 1995; 33: 173-177.
111. Ungprasert P, Cheungpasitporn W, Crowson CS, Matteson EL. Individual non-steroidal anti-inflammatory drugs and risk of acute kidney injury: A systematic review and meta-analysis of observational studies. *Eur J Intern Med* 2015; 26: 285-291.
112. Belayev LY, Palevsky PM. The link between acute kidney injury and chronic kidney disease. *Current opinion in nephrology and hypertension* 2014; 23: 149-154.
113. Mowry JB, Spyker DA, Brooks DE, McMillan N, Schauben JL. 2014 Annual Report of the American Association of Poison Control Centers' National Poison Data System (NPDS): 32nd Annual Report. *Clinical toxicology* 2015; 53: 962-1147.
114. Perazella MA, Markowitz GS. Drug-induced acute interstitial nephritis. *Nat Rev Nephrol* 2010; 6: 461-470.
115. Kim GH. Renal effects of prostaglandins and cyclooxygenase-2 inhibitors. *Electrolyte Blood Press* 2008; 6: 35-41.
116. Oaks JL, Gilbert M, Virani MZ, Watson RT, Meteyer CU, Rideout BA, Shivaprasad HL, Ahmed S, Chaudhry MJ, Arshad M, Mahmood S, Ali A, Khan AA. Diclofenac

residues as the cause of vulture population decline in Pakistan. *Nature* 2004; 427: 630-633.
117. Mingatto FE, Santos AC, Uyemura SA, Jordani MC, Curti C. In vitro interaction of nonsteroidal anti-inflammatory drugs on oxidative phosphorylation of rat kidney mitochondria: respiration and ATP synthesis. *Arch Biochem Biophys* 1996; 334: 303-308.
118. Fattori V, Borghi SM, Guazelli CF, Giroldo AC, Crespigio J, Bussmann AJ, Coelho-Silva L, Ludwig NG, Mazzuco TL, Casagrande R, Verri WA, Jr. Vinpocetine reduces diclofenac-induced acute kidney injury through inhibition of oxidative stress, apoptosis, cytokine production, and NF-kappaB activation in mice. *Pharmacol Res* 2017; 120: 10-22.
119. Bonventre JV, Zuk A. Ischemic acute renal failure: an inflammatory disease? *Kidney Int* 2004; 66: 480-485.
120. Akcay A, Nguyen Q, Edelstein CL. Mediators of inflammation in acute kidney injury. *Mediators of inflammation* 2009; 2009: 137072.
121. Kielar ML, John R, Bennett M, Richardson JA, Shelton JM, Chen L, Jeyarajah DR, Zhou XJ, Zhou H, Chiquett B, Nagami GT, Lu CY. Maladaptive role of IL-6 in ischemic acute renal failure. *J Am Soc Nephrol* 2005; 16: 3315-3325.
122. Nechemia-Arbely Y, Barkan D, Pizov G, Shriki A, Rose-John S, Galun E, Axelrod JH. IL-6/IL-6R axis plays a critical role in acute kidney injury. *J Am Soc Nephrol* 2008; 19: 1106-1115.
123. Rath PC, Aggarwal BB. TNF-induced signaling in apoptosis. *J Clin Immunol* 1999; 19: 350-364.
124. Simmons EM, Himmelfarb J, Sezer MT, Chertow GM, Mehta RL, Paganini EP, Soroko S, Freedman S, Becker K, Spratt D, Shyr Y, Ikizler TA, Group PS. Plasma cytokine levels predict mortality in patients with acute renal failure. *Kidney international* 2004; 65: 1357-1365.
125. Mezzano S, Aros C, Droguett A, Burgos ME, Ardiles L, Flores C, Schneider H, Ruiz-Ortega M, Egido J. NF-kappaB activation and overexpression of regulated genes in human diabetic nephropathy. *Nephrol Dial Transplant* 2004; 19: 2505-2512.
126. Mezzano SA, Barria M, Droguett MA, Burgos ME, Ardiles LG, Flores C, Egido J. Tubular NF-kappaB and AP-1 activation in human proteinuric renal disease. *Kidney Int* 2001; 60: 1366-1377.
127. Zheng L, Sinniah R, Hsu SI. In situ glomerular expression of activated NF-kappaB in human lupus nephritis and other non-proliferative proteinuric glomerulopathy. *Virchows Arch* 2006; 448: 172-183.
128. Kumar D, Singla SK, Puri V, Puri S. The restrained expression of NF-kB in renal tissue ameliorates folic acid induced acute kidney injury in mice. *PLoS One* 2015; 10: e115947.
129. Buysen JG, Houthoff HJ, Krediet RT, Arisz L. Acute interstitial nephritis: a clinical and morphological study in 27 patients. *Nephrol Dial Transplant* 1990; 5: 94-99.
130. Galpin JE, Shinaberger JH, Stanley TM, Blumenkrantz MJ, Bayer AS, Friedman GS, Montgomerie JZ, Guze LB, Coburn JW, Glassock RJ. Acute interstitial nephritis due to methicillin. *Am J Med* 1978; 65: 756-765.
131. Gonzalez E, Gutierrez E, Galeano C, Chevia C, de Sequera P, Bernis C, Parra EG, Delgado R, Sanz M, Ortiz M, Goicoechea M, Quereda C, Olea T, Bouarich H, Hernandez Y, Segovia B, Praga M, Grupo Madrileno De Nefritis I. Early steroid treatment improves the recovery of renal function in patients with drug-induced acute interstitial nephritis. *Kidney Int* 2008; 73: 940-946.

132. Koselj M, Kveder R, Bren AF, Rott T. Acute renal failure in patients with drug-induced acute interstitial nephritis. *Ren Fail* 1993; 15: 69-72.
133. Clarkson MR, Giblin L, O'Connell FP, O'Kelly P, Walshe JJ, Conlon P, O'Meara Y, Dormon A, Campbell E, Donohoe J. Acute interstitial nephritis: clinical features and response to corticosteroid therapy. *Nephrol Dial Transplant* 2004; 19: 2778-2783.
134. Bhaumik SK, Kher V, Arora P, Rai PK, Singhal M, Gupta A, Pandey R, Sharma RK. Evaluation of clinical and histological prognostic markers in drug-induced acute interstitial nephritis. *Ren Fail* 1996; 18: 97-104.
135. Kang I, Choi S, Ha TJ, Choi M, Wi HR, Lee BW, Lee M. Effects of Mung Bean (Vigna radiata L.) Ethanol Extracts Decrease Proinflammatory Cytokine-Induced Lipogenesis in the KK-Ay Diabese Mouse Model. *J Med Food* 2015; 18: 841-849.
136. Edwards JE, Brown PN, Talent N, Dickinson TA, Shipley PR. A review of the chemistry of the genus Crataegus. *Phytochemistry* 2012; 79: 5-26.
137. Pereira CA, Yariwake JH, McCullagh M. Distinction of the C-glycosylflavone isomer pairs orientin/isoorientin and vitexin/isovitexin using HPLC-MS exact mass measurement and in-source CID. *Phytochem Anal* 2005; 16: 295-301.
138. Zhang J, Yuan K, Zhou WL, Zhou J, Yang P. Studies on the active components and antioxidant activities of the extracts of Mimosa pudica Linn. from southern China. *Pharmacogn Mag* 2011; 7: 35-39.
139. Dong LY, Li S, Zhen YL, Wang YN, Shao X, Luo ZG. Cardioprotection of vitexin on myocardial ischemia/reperfusion injury in rat via regulating inflammatory cytokines and MAPK pathway. *Am J Chin Med* 2013; 41: 1251-1266.
140. He JD, Wang Z, Li SP, Xu YJ, Yu Y, Ding YJ, Yu WL, Zhang RX, Zhang HM, Du HY. Vitexin suppresses autophagy to induce apoptosis in hepatocellular carcinoma via activation of the JNK signaling pathway. *Oncotarget* 2016; 7: 84520-84532.
141. Sun Z, Yan B, Yu WY, Yao X, Ma X, Sheng G, Ma Q. Vitexin attenuates acute doxorubicin cardiotoxicity in rats via the suppression of oxidative stress, inflammation and apoptosis and the activation of FOXO3a. *Exp Ther Med* 2016; 12: 1879-1884.
142. Kim JH, Lee BC, Kim JH, Sim GS, Lee DH, Lee KE, Yun YP, Pyo HB. The isolation and antioxidative effects of vitexin from Acer palmatum. *Archives of pharmacal research* 2005; 28: 195-202.
143. Li HM, Hwang SH, Kang BG, Hong JS, Lim SS. Inhibitory effects of Colocasia esculenta (L.) Schott constituents on aldose reductase. *Molecules* 2014; 19: 13212-13224.
144. Shibano M, Kakutani K, Taniguchi M, Yasuda M, Baba K. Antioxidant constituents in the dayflower (Commelina communis L.) and their alpha-glucosidase-inhibitory activity. *Journal of natural medicines* 2008; 62: 349-353.
145. Snijman PW, Joubert E, Ferreira D, Li XC, Ding Y, Green IR, Gelderblom WC. Antioxidant activity of the dihydrochalcones Aspalathin and Nothofagin and their corresponding flavones in relation to other Rooibos (Aspalathus linearis) Flavonoids, Epigallocatechin Gallate, and Trolox. *Journal of agricultural and food chemistry* 2009; 57: 6678-6684.
146. An F, Yang G, Tian J, Wang S. Antioxidant effects of the orientin and vitexin in Trollius chinensis Bunge in D-galactose-aged mice. *Neural Regen Res* 2012; 7: 2565-2575.
147. Borghi SM, Carvalho TT, Staurengo-Ferrari L, Hohmann MS, Pinge-Filho P, Casagrande R, Verri WA, Jr. Vitexin inhibits inflammatory pain in mice by targeting TRPV1, oxidative stress, and cytokines. *J Nat Prod* 2013; 76: 1141-1149.

148. Che X, Wang X, Zhang J, Peng C, Zhen Y, Shao X, Zhang G, Dong L. Vitexin exerts cardioprotective effect on chronic myocardial ischemia/reperfusion injury in rats via inhibiting myocardial apoptosis and lipid peroxidation. *Am J Transl Res* 2016; 8: 3319-3328.
149. Gupta SC, Tyagi AK, Deshmukh-Taskar P, Hinojosa M, Prasad S, Aggarwal BB. Downregulation of tumor necrosis factor and other proinflammatory biomarkers by polyphenols. *Arch Biochem Biophys* 2014; 559: 91-99.
150. Rosa SI, Rios-Santos F, Balogun SO, Martins DT. Vitexin reduces neutrophil migration to inflammatory focus by down-regulating pro-inflammatory mediators via inhibition of p38, ERK1/2 and JNK pathway. *Phytomedicine* 2016; 23: 9-17.
151. Kumar V, Abbas A, Aster JC. Inflammation and repair. In: Kumar, V.; Abbas, AK.; Aster, J.C., editors. Pathologic Basis of Disease. 9th edition. Elsevier Saunders; Philadelphia, PA. 2015: 69-113.
152. Wynn TA. Common and unique mechanisms regulate fibrosis in various fibroproliferative diseases. *J Clin Invest* 2007; 117: 524-529.
153. Friedman SL. Mechanisms of disease: Mechanisms of hepatic fibrosis and therapeutic implications. *Nat Clin Pract Gastroenterol Hepatol* 2004; 1: 98-105.
154. Wynn TA. Cellular and molecular mechanisms of fibrosis. *J Pathol* 2008; 214: 199-210.
155. Borensztajn K, Crestani B, Kolb M. Idiopathic pulmonary fibrosis: from epithelial injury to biomarkers--insights from the bench side. *Respiration* 2013; 86: 441-452.
156. Fernandez Perez ER, Daniels CE, Schroeder DR, St Sauver J, Hartman TE, Bartholmai BJ, Yi ES, Ryu JH. Incidence, prevalence, and clinical course of idiopathic pulmonary fibrosis: a population-based study. *Chest* 2010; 137: 129-137.
157. Kim DS, Collard HR, King TE, Jr. Classification and natural history of the idiopathic interstitial pneumonias. *Proc Am Thorac Soc* 2006; 3: 285-292.
158. King TE, Jr., Tooze JA, Schwarz MI, Brown KR, Cherniack RM. Predicting survival in idiopathic pulmonary fibrosis: scoring system and survival model. *American journal of respiratory and critical care medicine* 2001; 164: 1171-1181.
159. Martinez FJ, Safrin S, Weycker D, Starko KM, Bradford WZ, King TE, Jr., Flaherty KR, Schwartz DA, Noble PW, Raghu G, Brown KK, Group IPFS. The clinical course of patients with idiopathic pulmonary fibrosis. *Annals of internal medicine* 2005; 142: 963-967.
160. Baumgartner KB, Samet JM, Coultas DB, Stidley CA, Hunt WC, Colby TV, Waldron JA. Occupational and environmental risk factors for idiopathic pulmonary fibrosis: a multicenter case-control study. Collaborating Centers. *Am J Epidemiol* 2000; 152: 307-315.
161. Baumgartner KB, Samet JM, Stidley CA, Colby TV, Waldron JA. Cigarette smoking: a risk factor for idiopathic pulmonary fibrosis. *Am J Respir Crit Care Med* 1997; 155: 242-248.
162. Alder JK, Chen JJ, Lancaster L, Danoff S, Su SC, Cogan JD, Vulto I, Xie M, Qi X, Tuder RM, Phillips JA, 3rd, Lansdorp PM, Loyd JE, Armanios MY. Short telomeres are a risk factor for idiopathic pulmonary fibrosis. *Proceedings of the National Academy of Sciences of the United States of America* 2008; 105: 13051-13056.
163. Wolters PJ, Collard HR, Jones KD. Pathogenesis of idiopathic pulmonary fibrosis. *Annu Rev Pathol* 2014; 9: 157-179.

164. Hecker L, Thannickal VJ. Nonresolving fibrotic disorders: idiopathic pulmonary fibrosis as a paradigm of impaired tissue regeneration. *Am J Med Sci* 2011; 341: 431-434.
165. Moore MW, Herzog EL. Regulation and Relevance of Myofibroblast Responses in Idiopathic Pulmonary Fibrosis. *Curr Pathobiol Rep* 2013; 1: 199-208.
166. Pechkovsky DV, Hogaboam CM, Yao E, Khalil N, Selman M, Knight DA. Fibroblast Senescence In UIP/IPF: A Contributing Factor Or Consequence Of The Disease? [abstract]. *Am J Respir Crit Care Med* 2012; 185: A5282.
167. Hecker L, Logsdon NJ, Kurundkar D, Kurundkar A, Bernard K, Hock T, Meldrum E, Sanders YY, Thannickal VJ. Reversal of persistent fibrosis in aging by targeting Nox4-Nrf2 redox imbalance. *Sci Transl Med* 2014; 6: 231ra247.
168. Tominaga K. The emerging role of senescent cells in tissue homeostasis and pathophysiology. *Pathobiology of aging & age related diseases* 2015; 5: 27743.
169. Dagouassat M, Gagliolo JM, Chrusciel S, Bourin MC, Duprez C, Caramelle P, Boyer L, Hue S, Stern JB, Validire P, Longrois D, Norel X, Dubois-Rande JL, Le Gouvello S, Adnot S, Boczkowski J. The cyclooxygenase-2-prostaglandin E2 pathway maintains senescence of chronic obstructive pulmonary disease fibroblasts. *Am J Respir Crit Care Med* 2013; 187: 703-714.
170. Minagawa S, Araya J, Numata T, Nojiri S, Hara H, Yumino Y, Kawaishi M, Odaka M, Morikawa T, Nishimura SL, Nakayama K, Kuwano K. Accelerated epithelial cell senescence in IPF and the inhibitory role of SIRT6 in TGF-beta-induced senescence of human bronchial epithelial cells. *American journal of physiology Lung cellular and molecular physiology* 2011; 300: L391-401.
171. Adnot S, Amsellem V, Boyer L, Marcos E, Saker M, Houssaini A, Kebe K, Dagouassat M, Lipskaia L, Boczkowski J. Telomere Dysfunction and Cell Senescence in Chronic Lung Diseases: Therapeutic Potential. *Pharmacology & therapeutics* 2015; 153: 125-134.
172. Coppe JP, Patil CK, Rodier F, Sun Y, Munoz DP, Goldstein J, Nelson PS, Desprez PY, Campisi J. Senescence-associated secretory phenotypes reveal cell-nonautonomous functions of oncogenic RAS and the p53 tumor suppressor. *PLoS biology* 2008; 6: 2853-2868.
173. Kuilman T, Michaloglou C, Vredeveld LC, Douma S, van Doorn R, Desmet CJ, Aarden LA, Mooi WJ, Peeper DS. Oncogene-induced senescence relayed by an interleukin-dependent inflammatory network. *Cell* 2008; 133: 1019-1031.
174. Spillare EA, Robles AI, Wang XW, Shen JC, Yu CE, Schellenberg GD, Harris CC. p53-mediated apoptosis is attenuated in Werner syndrome cells. *Genes & development* 1999; 13: 1355-1360.
175. Lu BC, H.D.; Lu, H.G. The relationship between apoptosis and aging. *Advances in bioscience and biotechnology* 2012; 3: 705-711.
176. Marcotte R, Lacelle C, Wang E. Senescent fibroblasts resist apoptosis by downregulating caspase-3. *Mechanisms of ageing and development* 2004; 125: 777-783.
177. Jackson JG, Pereira-Smith OM. p53 is preferentially recruited to the promoters of growth arrest genes p21 and GADD45 during replicative senescence of normal human fibroblasts. *Cancer research* 2006; 66: 8356-8360.
178. Zhu Y, Tchkonia T, Pirtskhalava T, Gower AC, Ding H, Giorgadze N, Palmer AK, Ikeno Y, Hubbard GB, Lenburg M, O'Hara SP, LaRusso NF, Miller JD, Roos CM, Verzosa GC, LeBrasseur NK, Wren JD, Farr JN, Khosla S, Stout MB, McGowan SJ, Fuhrmann-Stroissnigg H, Gurkar AU, Zhao J, Colangelo D, Dorronsoro A, Ling YY, Barghouthy

AS, Navarro DC, Sano T, Robbins PD, Niedernhofer LJ, Kirkland JL. The Achilles' heel of senescent cells: from transcriptome to senolytic drugs. *Aging cell* 2015; 14: 644-658.
179. Downward J. PI 3-kinase, Akt and cell survival. *Seminars in cell & developmental biology* 2004; 15: 177-182.
180. Nho RS, Peterson M, Hergert P, Henke CA. FoxO3a (Forkhead Box O3a) deficiency protects Idiopathic Pulmonary Fibrosis (IPF) fibroblasts from type I polymerized collagen matrix-induced apoptosis via caveolin-1 (cav-1) and Fas. *PLoS One* 2013; 8: e61017.
181. Xia H, Khalil W, Kahm J, Jessurun J, Kleidon J, Henke CA. Pathologic caveolin-1 regulation of PTEN in idiopathic pulmonary fibrosis. *Am J Pathol* 2010; 176: 2626-2637.
182. Knight MJ, Riffkin CD, Muscat AM, Ashley DM, Hawkins CJ. Analysis of FasL and TRAIL induced apoptosis pathways in glioma cells. *Oncogene* 2001; 20: 5789-5798.
183. Rothberg KG, Heuser JE, Donzell WC, Ying YS, Glenney JR, Anderson RG. Caveolin, a protein component of caveolae membrane coats. *Cell* 1992; 68: 673-682.
184. Huang SK, Scruggs AM, Donaghy J, Horowitz JC, Zaslona Z, Przybranowski S, White ES, Peters-Golden M. Histone modifications are responsible for decreased Fas expression and apoptosis resistance in fibrotic lung fibroblasts. *Cell death & disease* 2013; 4: e621.
185. Wynes MW, Edelman BL, Kostyk AG, Edwards MG, Coldren C, Groshong SD, Cosgrove GP, Redente EF, Bamberg A, Brown KK, Reisdorph N, Keith RC, Frankel SK, Riches DW. Increased cell surface Fas expression is necessary and sufficient to sensitize lung fibroblasts to Fas ligation-induced apoptosis: implications for fibroblast accumulation in idiopathic pulmonary fibrosis. *Journal of immunology* 2011; 187: 527-537.
186. Zhang XD, Nguyen T, Thomas WD, Sanders JE, Hersey P. Mechanisms of resistance of normal cells to TRAIL induced apoptosis vary between different cell types. *FEBS letters* 2000; 482: 193-199.
187. Agência Nacional deVigilância Sanitária. <http://portal.anvisa.gov.br/resultado-de-busca?p_p_id=101&p_p_lifecycle=0&p_p_state=maximized&p_p_mode=view&p_p_col_id=column-1&p_p_col_count=1&_101_struts_action=%2Fasset_publisher%2Fview_content&_101_assetEntryId=469573&_101_type=content&_101_groupId=219201&_101_urlTitle=anvisa-concede-o-registro-de-quatro-medicamentos-inovadores&redirect=http%3A%2F%2Fportal.anvisa.gov.br%2Fresultado-de-busca%3Fp_p_id%3D3%26p_p_lifecycle%3D0%26p_p_state%3Dnormal%26p_p_mode%3Dview%26p_p_col_id%3Dcolumn-1%26p_p_col_count%3D. 2016 [cited 2017 7 de fevereiro].
188. Food and Drug Administration. <http://www.fda.gov/newsevents/newsroom/pressannouncements/ucm418991.htm%3E. . 2014 [cited 2017 7 de fevereiro].
189. Food and Drug Administration. <http://www.fda.gov/newsevents/newsroom/pressannouncements/ucm418994.htm> 2014 [cited 2017 7 de fevereiro].
190. Maher TM. Pirfenidone in idiopathic pulmonary fibrosis. *Drugs Today (Barc)* 2010; 46: 473-482.

191. Wollin L, Wex E, Pautsch A, Schnapp G, Hostettler KE, Stowasser S, Kolb M. Mode of action of nintedanib in the treatment of idiopathic pulmonary fibrosis. *Eur Respir J* 2015; 45: 1434-1445.
192. Oku H, Shimizu T, Kawabata T, Nagira M, Hikita I, Ueyama A, Matsushima S, Torii M, Arimura A. Antifibrotic action of pirfenidone and prednisolone: different effects on pulmonary cytokines and growth factors in bleomycin-induced murine pulmonary fibrosis. *Eur J Pharmacol* 2008; 590: 400-408.
193. Iyer SN, Gurujeyalakshmi G, Giri SN. Effects of pirfenidone on transforming growth factor-beta gene expression at the transcriptional level in bleomycin hamster model of lung fibrosis. *J Pharmacol Exp Ther* 1999; 291: 367-373.
194. Gurujeyalakshmi G, Hollinger MA, Giri SN. Pirfenidone inhibits PDGF isoforms in bleomycin hamster model of lung fibrosis at the translational level. *Am J Physiol* 1999; 276: L311-318.
195. Hostettler KE, Zhong J, Papakonstantinou E, Karakiulakis G, Tamm M, Seidel P, Sun Q, Mandal J, Lardinois D, Lambers C, Roth M. Anti-fibrotic effects of nintedanib in lung fibroblasts derived from patients with idiopathic pulmonary fibrosis. *Respiratory research* 2014; 15: 157.
196. Chaudhary NI, Roth GJ, Hilberg F, Muller-Quernheim J, Prasse A, Zissel G, Schnapp A, Park JE. Inhibition of PDGF, VEGF and FGF signalling attenuates fibrosis. *Eur Respir J* 2007; 29: 976-985.
197. Formica JV, Regelson W. Review of the biology of Quercetin and related bioflavonoids. *Food Chem Toxicol* 1995; 33: 1061-1080.
198. Anand David AV, Arulmoli R, Parasuraman S. Overviews of Biological Importance of Quercetin: A Bioactive Flavonoid. *Pharmacogn Rev* 2016; 10: 84-89.
199. Domiciano TP, Wakita D, Jones HD, Crother TR, Verri WA, Jr., Arditi M, Shimada K. Quercetin Inhibits Inflammasome Activation by Interfering with ASC Oligomerization and Prevents Interleukin-1 Mediated Mouse Vasculitis. *Sci Rep* 2017; 7: 41539.
200. Guazelli CF, Fattori V, Colombo BB, Georgetti SR, Vicentini FT, Casagrande R, Baracat MM, Verri WA, Jr. Quercetin-loaded microcapsules ameliorate experimental colitis in mice by anti-inflammatory and antioxidant mechanisms. *J Nat Prod* 2013; 76: 200-208.
201. Gamet-Payrastre L, Manenti S, Gratacap MP, Tulliez J, Chap H, Payrastre B. Flavonoids and the inhibition of PKC and PI 3-kinase. *General pharmacology* 1999; 32: 279-286.
202. Mouria M, Gukovskaya AS, Jung Y, Buechler P, Hines OJ, Reber HA, Pandol SJ. Food-derived polyphenols inhibit pancreatic cancer growth through mitochondrial cytochrome C release and apoptosis. *International journal of cancer* 2002; 98: 761-769.
203. Tanigawa S, Fujii M, Hou DX. Stabilization of p53 is involved in quercetin-induced cell cycle arrest and apoptosis in HepG2 cells. *Bioscience, biotechnology, and biochemistry* 2008; 72: 797-804.
204. Wang IK, Lin-Shiau SY, Lin JK. Induction of apoptosis by apigenin and related flavonoids through cytochrome c release and activation of caspase-9 and caspase-3 in leukaemia HL-60 cells. *European journal of cancer* 1999; 35: 1517-1525.
205. Jacquemin G, Shirley S, Micheau O. Combining naturally occurring polyphenols with TNF-related apoptosis-inducing ligand: a promising approach to kill resistant cancer cells? *Cellular and molecular life sciences : CMLS* 2010; 67: 3115-3130.

206. Russo M, Palumbo R, Mupo A, Tosto M, Iacomino G, Scognamiglio A, Tedesco I, Galano G, Russo GL. Flavonoid quercetin sensitizes a CD95-resistant cell line to apoptosis by activating protein kinase Calpha. *Oncogene* 2003; 22: 3330-3342.
207. Bradley PP, Priebat DA, Christensen RD, Rothstein G. Measurement of cutaneous inflammation: estimation of neutrophil content with an enzyme marker. *J Invest Dermatol* 1982; 78: 206-209.
208. Casagrande R, Georgetti SR, Verri WA, Jr., Dorta DJ, dos Santos AC, Fonseca MJ. Protective effect of topical formulations containing quercetin against UVB-induced oxidative stress in hairless mice. *J Photochem Photobiol B* 2006; 84: 21-27.
209. Sedlak J, Lindsay RH. Estimation of total, protein-bound, and nonprotein sulfhydryl groups in tissue with Ellman's reagent. *Anal Biochem* 1968; 25: 192-205.
210. Lowry OH, Rosebrough NJ, Farr AL, Randall RJ. Protein measurement with the Folin phenol reagent. *J Biol Chem* 1951; 193: 265-275.
211. Katalinic V, Modun D, Music I, Boban M. Gender differences in antioxidant capacity of rat tissues determined by 2,2'-azinobis (3-ethylbenzothiazoline 6-sulfonate; ABTS) and ferric reducing antioxidant power (FRAP) assays. *Comp Biochem Physiol C Toxicol Pharmacol* 2005; 140: 47-52.
212. Oliveira FJ, Cecchini R. Oxidative stress of liver in hamsters infected with Leishmania (L.) chagasi. *J Parasitol* 2000; 86: 1067-1072.
213. Habiel DM, Krepostman N, Lilly M, Cavassani K, Coelho AL, Shibata T, Elenitoba-Johnson K, Hogaboam CM. Senescent stromal cell-induced divergence and therapeutic resistance in T cell acute lymphoblastic leukemia/lymphoma. *Oncotarget* 2016; 7: 83514-83529.
214. Borrelli F, Izzo AA. Herb-drug interactions with St John's wort (Hypericum perforatum): an update on clinical observations. *AAPS J* 2009; 11: 710-727.
215. Bray BJ, Perry NB, Menkes DB, Rosengren RJ. St. John's wort extract induces CYP3A and CYP2E1 in the Swiss Webster mouse. *Toxicol Sci* 2002; 66: 27-33.

Anexo 1

Universidade
Estadual de Londrina

COMISSÃO DE ÉTICA NO USO DE ANIMAIS

OF. CIRC. CEUA Nº 11/11 Londrina, 15 de dezembro de 2011

Prezado Pesquisador

O CEUA/UEL, reunido em 06 de dezembro do ano corrente, avaliou o projeto de pesquisa intitulado **"Avaliação do efeito e mecanismo de ação do *Hypericum perforatum* em modelos de dor inflamatória, dor neuropática, dor no câncer e na toxicidade hepática em camundongos"**, registrado na CEUA sob o processo nº 13280.2011.64, desenvolvido sob sua responsabilidade, julgando-o *aprovado* para execução por entender que os princípios éticos postulados pelo Colégio Brasileiro de Experimentação Animal e do Conselho Nacional de Controle de Experimentação Animal estão respeitados.

Serão utilizados 1240 camundongos Swiss machos de 20-25g. Os camundongos serão divididos em grupos contendo de 5 a 12 indivíduos, na realização de 23 experimentos, por várias metodologias, em um total de 153 grupos. Serão realizadas duas repetições para cada experimento. Tais experimentos serão desenvolvidos visando verificar os mecanismos envolvidos na modulação da dor nos diferentes modelos (subprojetos): 1) modelos de inflamação; 2) modelo de dor no câncer induzido por tumor de Ehrlich; 3) modelo de neuropatia pela constrição crônica do nervo ciático; 4) modelo de intoxicação por acetaminofeno. Trata-se de um projeto que objetiva determinar o efeito do *Hypericum perforatum* como analgésico e anti-inflamatório e, então, os experimentos envolverão administração de agentes químicos e procedimento cirúrgico para constrição do nervo ciático para a avaliação da dor neuropática.. Os experimentos estão previstos para serem desenvolvidos em 36 meses após sua aprovação no CEUA-UEL.

Cumpre orientar que caso pretendam-se quaisquer alterações no protocolo experimental aprovado, deve-se submeter o novo protocolo à apreciação do CEUA/UEL anteriormente à execução das modificações.

Sem mais para o momento, subscrevo-me.

Cordialmente,

Profª. Drª. Miriam Siliane Batista de Souza
Vice-Coordenadora da CEUA/UEL

Ilm. Sr.
Prof. Dr. Waldiceu Aparecido Verri Junior
Coordenador do Projeto
Departamento de Ciências Patológicas
Centro de Ciências Biológicas

Com cópia para Srª Égle Maria de Sousa (Chefe da DCA/PROPPG) e Prof. Luiz Carlos Juliani (Diretor do Biotério Central da UEL).

Campus Universitário: Rodovia Celso Garcia Cid (PR 445), km 380 - Fone (043) 3371-4000 PABX - Fax 3328-4440 - Caixa Postal 6.001 - CEP 86051-990 – Internet http://www.uel.br
Hospital Universitário/Centro de Ciências da Saúde: Av. Robert Koch, 60 - Vila Operária – Fone (043) 381-2000 PABX – Fax 337-4041 e 337-7495 - Caixa Postal 791 - CEP 86038-440
LONDRINA - PARANÁ - BRASIL

Anexo 2

Universidade Estadual de Londrina

COMISSÃO DE ÉTICA NO USO DE ANIMAIS

OF. CIRC. CEUA Nº 163/2016 **Londrina, 01 de Agosto de 2016.**

Prezado Pesquisador,

Certificamos que o projeto intitulado **"Avaliação do efeito flavonoide vitexina em modelo de lesão renal induzida pelo diclofenaco de sódio"**, protocolo CEUA n° **12742.2016.32**, sob a responsabilidade de **Waldiceu Aparecido Verri Junior**, que envolve a produção, manutenção e/ou utilização de animais pertencentes ao filo Chordata, subfilo Vertebrata (exceto o homem), para fins de pesquisa científica (ou ensino), encontra-se de acordo com os preceitos da Lei nº 11.794, de 8 de outubro de 2008, do Decreto nº 6.899, de 15 de julho de 2009, e com as normas editadas pelo Conselho Nacional de Controle da Experimentação Animal (CONCEA), foi **aprovado** pela Comissão de Ética no Uso de Animais da Universidade Estadual de Londrina (CEUA/UEL), em reunião realizada em **26/07/2016**.

O objetivo do projeto é avaliar o efeito terapêutico da vitexina em modelo de lesão renal induzido por diclofenaco de sódio, bem como os mecanismos envolvidos neste efeito. Os animais serão divididos em gaiolas de polipropileno padrão medindo 41 x 34 x 16 cm (Insight®) no biotério de acordo com os grupos experimentais (máximo de 12 animais por gaiola), com livre acesso à água e ração e serão adaptados aos ambientes e condições experimentais com pelo menos 1 hora de antecedência em relação aos experimentos. Os animais serão imobilizados manualmente por curtos períodos, somente para a administração do diclofenaco de sódio (200 mg/kg, via oral, 1 vez por experimento) e tratamento com vitexina (3, 10 e 30mg/Kg, via intraperitoneal, 1 vez por experimento). Ao término dos experimentos os animais serão eutanasiados por inalação de isofluorano (3% em O_2) seguido de decaptação para coleta de amostras. GI 2.

Vigência do Projeto	01/12/2016 a 31/11/2018
Espécie/linhagem	Camundongo heterogênico / Swiss
Nº de animais	168
Peso/Idade	20-25 g / 2 meses
Sexo	Machos
Origem	Biotério Central / UEL
Amostras a serem coletadas	Rim, sangue

Cumpre orientar que caso pretendam-se quaisquer alterações no protocolo experimental aprovado, deve-se submeter o novo protocolo à apreciação da CEUA/UEL anteriormente à execução das modificações.

Coloco-me à disposição para quaisquer esclarecimentos que se fizerem necessária. Sem mais para o momento, subscrevo, cordialmente,

Profa. Dra. Glaura Scantamburlo Alves Fernandes
Coordenadora da CEUA/UEL

Ilmo. Sr.
Prof. Dr. Waldiceu Aparecido Verri Junior
Coordenador do Projeto
Departamento de Ciências Patológicas / Centro de Ciências Biológicas
Com cópia para Coordenação do Biotério Central/UEL; Chefe do Departamento de Ciências Patológicas e Diretor(a) do Centro de Ciências Biológicas

Campus Universitário: Rodovia Celso Garcia Cid (PR 445), km 380 - Fone (043) 3371-4000 PABX - Fax 3328-4440 - Caixa Postal 10.011 - CEP 86057-970 – Internet http://www.uel.br
LONDRINA - PARANÁ - BRASIL